New Experimental and Modeling Approaches to Study the Dynamics of Xylose Fermentation with *Scheffersomyces stipitis*

by

Min Hea Kim

A dissertation submitted to the Graduate Faculty of
Auburn University
in partial fulfillment of the
requirements for the Degree of
Doctor of Philosophy

Auburn, Alabama
August 1, 2015

Key words: *Scheffersomyces stipitis*, *Saccharomyces cerevisiae*, co-culture, bioethanol, co-fermentation, ethanol fermentation, lignocellulosic ethanol, kinetic model

Approved by

Jin Wang, Chair, Associate Professor of Chemical Engineering
Q. Peter He, Associate Professor of Chemical Engineering, Tuskegee University
Yoon Y. Lee, Professor of Chemical Engineering
Thomas Hanley, Professor of Chemical Engineering

Abstract

Ethanol production from lignocellulosic hydrolysates in an economically feasible process requires complete utilization of both glucose and xylose, the main components of cellulose and hemicellulose. *Scheffersomyces stipitis* (formerly known as *Pichia stipitis*) has promising potential for converting lignocellulosic biomass into ethanol since it can ferment both hexose and pentose sugars under microaerophillic conditions (a native yeast strain best capable of utilizing xylose to ethanol). However, this strain has several challenges for lignocellulosic ethanol production from xylose as it has a slower sugar consumption rate than *S. cerevisiae* (hexose fermenting microorganism) and requires oxygen for both growth and maximal ethanol production. In addition, diauxic kinetic is a practical problem associated with mixed sugar utilization by native strains of *S. stipitis* and even with engineered strains of *S. cerevisiae* (Kuyper et al. 2005). Although successful cycles of metabolic engineering have improved xylose utilization in recombinant strain of *S. cerevisiae*, the ethanol production from xylose is still inferior to those of xylose fermentation by native strain of *S. stipitis* (Jeffries and Jin, 2004; Jin *et al.* 2004).

Since *S. stipitis* is a respiratory yeast strain, the xylose fermentation performance depends significantly on the oxygenation level of the culture. High aeration rate results in fast cell growth and acetic acid production, while very low aeration (oxygen-limited) often results in xylitol production, both at the expense of reduced ethanol production. Only optimized microaerobic condition promotes ethanol production by maintaining cell viability and NAD+/NADH balance. Hence, it is critical to determine the optimal oxygen utilization rate (OUR) for ethanol produc-

tion by *S. stipitis*. In order to quantitatively study the effect of OUR on the fermentation performance, accurate control of OUR is essential. Several studies have been reported on the optimum oxygenation conditions for ethanol fermentation by *S. stipitis* (Silva et al., 2012; Slininger et al., 2014; Su et al., 2014; Unrean and Nguyen, 2012). Among these studies, most of the experiments were carried out using batch cultures grown in flasks where the Oxygen Transfer Rate (OTR) and/or Dissolved Oxygen (DO) were not effectively controlled. Different OTR levels have been tested simply by changing volume of media, airflow rate, and agitation speed. However, our research shows that the inaccuracy and inconsistency of controlling OTR/OUR is problematic in these studies.

In order to quantify the metabolic mechanism of OUR on xylose fermentation kinetics by *S. stipitis*, we have developed experimental protocol and equipment to carry out both single culture and co-culture systems under controlled chemostat. The xylose fermentation kinetics of *S. stipitis* data collected from single culture experiment was used to design the co-culture experiment to optimize ethanol yield. For the co-culture system, we have developed a novel co-culture bioreactor for the efficient and simultaneous conversion of mixed glucose and xylose to ethanol by *S. cerevisiae* and *S. stipitis*, which offers a promising alternative to overcome the difficulties of the existing co-culture systems and to study the dynamic properties of co-culture strains. In addition to this, we used a mathematical modeling tool to describe the kinetics of both single culture and co-culture systems, as well as to validate our results. Also, Principal Component Analysis (PCA) was utilized to enable the extraction of correlations between different cellular physiology with respect to carbon uptake and OUR which helped us to understand and quantify the metabolic mechanism of OUR in continuous fermentation.

Acknowledgments

First of all, I would like to express my deepest gratitude to my advisor, Dr. Jin Wang, for her overwhelming guidance, patience and support in this research. I also acknowledge Dr. Q. Peter He for his valuable discussions and guidance. I would like to express my gratitude towards my committee members, Dr. Yoon Y. Lee, Dr. Thomas Henley, Dr. Sangjin Suh (University reader) for their time and assistance in helping me complete this work.

I would like to thank my research group members, Hector Galicia, Zi Xiu Wang, Andrew Damiani, Kyle Stone, Alyson Charles, Tomi Adekoya for their helps and supports along with enjoyable moments. Also special thanks to Meng Laing for his guidance, assistance and support. He has been very instrumental in successful completion of this work. I also thank Brian Schwieker for building several sets of co-culture reactors.

Thanks also goes to Shaima Nahreen, Geyou Ao, Hema Ramsurn, Courtney Ober, Subin Hada and other fellow graduate students who have made my time spent at Auburn University both educational and enjoyable.

Special thanks to my parents, Jongyoun Kim and Heesook Lee, for value my education and for putting my success and happiness before their own. I am also thankful to my elder sister and brother-in-a-law, Minjoo and Todd O'Hara, for their constant love and encouragement throughout the years. I would like to thank my boyfriend Donglee Shin, whose love and support have made this research possible.

Table of Contents

List of Tables

List of Figures

Chapter 1. Introduction

1.1 Sustainable Alternatives

United States has the largest oil consumption in the world about 21.5%. Approximately 71% of this oil consumption is used for transportation fuel and more than 96% of transportation sector is relied on imported oil, which is accountable for one-third of greenhouse gas emissions (EIA, 2011). Hence, finding alternative fuel energy for sustainable transportation is a critical to overcome this dangerous dependence. In order to simultaneously reduce the large dependence on oil and to mitigate climate change in transportation sector, alternative biofuel energy source is necessary. Various types of alternative fuels exist as they offer many advantages as follow. Low cost; wide availability; energy security; and reduction of greenhouse gas emissions. With these advantages, biofuels are emerging as a promising alternative to cope with climate change and a diminishing oil supply (Kim et al., 2010). Lignocellulosic biomass is increasingly recognized as a renewable feed stock for bioethanol production as alternative transportation fuels.

1.1.1 Biomass resources and lignocellulosic biomass

There are four different categories of biomass energy resources. The largest biomass energy source is wood residues and the second largest is municipal solid waste followed by agriculture residues and dedicated energy crops (Monique et al., 2003). Ethanol production by lignocellulosic fermentation is considered as a promising renewable fuel for the transportation sector. First generation bioethanol is produced from first generation of feedstocks such as food crops: cornstarch or sugarcane. *Saccharomyces cerevisiae* is the widely recognized industrial strain, which is often used with commercially available enzyme to achieve high ethanol yields through

maximum substrate conversion. However, those first generation bioethanol cause several concerns as it is produced directly from the food crops. These productions result in food conflicts/competition, land shortages for their feedstock and high energy input required for crop cultivation and conversion (Marris, 2006; Lange, 2007). These limitations are expected to overcome by developing second generation bioethanol. Lignocellulosic biomass has been recognized as an attractive feedstock for second generation bioethanol due to its high content in fermentable sugars and broad availability. Lignocellulosic biomass that can be used as feedstocks to produce bioethanol includes: 1) agricultural residues (leftover material from crops, such as corn stover and wheat straw); 2) forestry wastes (chips and sawdust from lumber mills, dead trees, and tree branches); 3) municipal solid wastes (household garbage and paper products); 4) food processing and other industrial wastes (black liquor, a paper manufacturing by-product); and 5) energy crops (fast-growing trees and grasses, such as switchgrass, poplar and willow) (USDOE, 2006a).

1.1.2 Composition of lignocellulosic biomass

Lignocellulosic biomass can be produced through photosynthesis; plants use solar energy from the sun to convert water and carbon dioxide to sugars that can be stored. Lignocellulosic biomass is composed of complex matrix of carbohydrate polymers contain 40-50% by wt of cellulose, 20-40% by wt of hemicellulose and 10-30% by wt of lignin (Lee et al., 2008). Cellulose is the bundles of fibers which consist of high molecular weight polymers of glucose. Hemicellulose is a cellulose bundle which consists of various sugars in shorter polymers. This hemicellulose consists of D-xylose, D-glucose, D-galactose, D-mannose and L-arabinose (Saha et al., 2003). Lignin is a tri-dimensional polymer that is surrounded in and bound to hemicellulose which can provide a rigidity of the structure. Cellulose can be hydrolyzed to produce hexose sugars like glucose which are readily fermented to ethanol. Hemicellulose is hydrolyzed to pro-

duce a mixture of hexose and pentose sugars, the majority of them are pentose sugars such as xylose and arabinose. Unlike, cellulose and hemicellulose, lignin cannot be fermented in the fermentation process. The composition of cellulose, hemicellulose, and lignin varies with the types of lignocellulosic biomass. Table 1.1 shows the composition of the selected feedstocks.

1.1.3 Lignocellulosic Bioethanol

Lignocellulosic biomass is an attractive raw material for bioethanol production due to its abundancy and low cost. For biochemical route of converting lignocellulosic biomass into bio-ethanol, steps needed are collection of lignocellulosic biomass, pretreatment stage for breaking down of lignocellulosic matrix, and hydrolysis stage to obtain simple sugars from lignocellulosic biomass, and microbial fermentation stage of producing bioethanol. Lignocellulosic ethanol is particularly promising due to the number of advantages over fossil fuels. Firstly, it comes from a renewable resource. Secondly, it is biodegradable, low in toxicity and causes little environmental pollution (Wyman, 1994). Thirdly, relative to fossil fuels, greenhouse gas emissions are reduced about 18% by using corn-based ethanol, but it can be reduced up to 88% by using lignocellulosic ethanol (Service, 2007). In addition, using agricultural wastes in bioprocesses not only provide alternative feedstocks, but also help solve their disposal problem. Hence, with the innovations of biotechnology, mainly in the areas of fermentation technology can open the new avenue for bio-fuel production (Lin and Tanaka, 2006).

Table 1.1 Chemical composition of raw materials and simulated ethanol production (Chandel et al., 2007)

Raw material	Cellulose/ Hexosans (H)	Hemicellulose / Pentosans (P)	Lignin	Ethanol yield /kg dry mass	Reference
Sugarcane baggase	33 (H)	30 (P)	29	0.279	Kuhad and Singh, 1993
Wheat straw	30 (H)	24 (P)	18	0.239	Kuhad and Singh, 1993
Sorghum straw	33 (H)	18 (P)	15	0.240	Kuhad and Singh, 1993
Rice straw	32 (H)	24 (P)	13	0.248	Kuhad and Singh, 1993
Oat straw	41 (H)	16 (P)	11	0.252	Kuhad and Singh, 1993
Corn cob	42 (H)	39 (P)	14	0.358	Kuhad and Singh, 1993
Corn stalks	35 (H)	15 (P)	19	0.221	Kuhad and Singh, 1993
Barley straw	40 (H)	20 (P)	15	0.265	Kuhad and Singh, 1993
Ground nut shell	38 (H)	36 (P)	16	0.327	Kuhad and Singh, 1993
Alfalfa stalks	48.5	6.5	16.6	0.209	Shleser, 1994
Rice hulls	36 (H)	15 (P)	19	0.265	Kuhad and Singh, 1993
Eucalyptus grandis	38	13	37	0.225	Shleser, 1994
Eucalyptus saligna	45	12.0	25.0	0.252	Shleser, 1994
Pine	44.0	26.0	29.0	0.310	Olsson and Hagerdal, 1996
Poplar	47.6	27.4	19.2	0.332	Olsson and Hagerdal, 1996
Saw dust	55.0	14.0	21.0	0.305	Olsson and Hagerdal, 1996
Willow	37.0	23.0	21.0	0.265	Olsson and Hagerdal, 1996
Aspen	51	29.0	16.0	0.354	Olsson and Hagerdal, 1996
Spruce	43.0	26.0	29.0		Olsson and Hagerdal, 1996
Birch	40.0	23.0	21.0	0.305	Olsson and Hagerdal, 1996
Lantana camara	42.50	22.70	22.88	0.288	Chandel (Unpublished work)
Prosopis juliflora	45.5	20.38	24.65	0.291	Chandel (Unpublished work)
Saccharum spontaneum	45.10	22.70	24.56	0.300	Gupta, 2006
Eicchornia crassipis	18.2	48.7	3.50	0.296	Nigam, 2002
Paja brava	32.2	28.1	24.0	0.267	Sanchez et al., 2004
News Paper	61	16	21	0.341	Olsson and Hagerdal, 1996
Processed Paper	47	25	12	0.318	Olsson and Hagerdal, 1996
Paper-based municipal solid waste	43	13	6	0.248	Olsson and Hagerdal, 1996

1.1.4 Environmental, functional and strategic benefits of lignocellulosic bioethanol

Bioethanol is a high octane fuel and can be added into gasoline as an octane enhancer. In the United States, ethanol is blended with gasoline at a 10:90 ethanol-to-gasoline ratio, which allows it to burn more cleanly and reducing urban smog (Service, 2007). A closed carbon dioxide cycle can be formed by using bioethanol as fuels. After combustion of bioethanol, carbon dioxide released from combustion is recycled back into crops or plants as they use carbon dioxide in photosynthesis (Chandel et al., 2007). In addition, blending bioethanol with gasoline will help extend the life of the diminishing fossil oil supplies and ensure greater fuel security, avoiding heavy reliance on oil producing nations that have not always been very stable. Another advantage of encouraging bioethanol use is that the rural economy would receive a boost from growing the necessary crops and creating new employment opportunities (USDOE, 2006b). Fur-

thermore, using agricultural and industrial residues to produce bioethanol can solve the waste disposal problem and provide environmental benefits. Currently the world's largest producer of bioethanol from sugarcane, sugar beet and starch crops is United States, 19.8 billion liters per year using corn as a primary feedstock (Cherubini, 2010). However, the increased demand for bioethanol from corn and wheat will result in serious problems, such as supply scarcity and dramatic increases in the cost of the food. Moreover, even converting all the starch to bioethanol, it can only reduce 10% of the gasoline demand (Service, 2007). Therefore, lignocellulosic bioethanol is thought to be the answer for solving these problems.

1.2 Lignocellulosic Bioethanol Production Process

The conversion of lignocellulosic biomass to ethanol is comprised of four major steps: pretreatment, hydrolysis, fermentation and distillation. The process includes the delignification of cellulose and hemicellulose from their complex matrix, depolymerization of the carbohydrate polymers to produce simple sugars, and fermentation of mixed hexose and pentose sugars to produce ethanol (Lin and Tanaka, 2006).

1.2.1 Pretreatment

Pretreatment is the first and the most expensive processing step in the conversion process of biomass to bioethanol. The aim of this process is to break down of carbohydrates from complex lignin matrix so that the hydrolysis of carbohydrate to monomeric sugars can be achieved easily and rapidly (Mielenz, 2001). There are several pretreatment methods such as mechanical combination, steam explosion, ammonia fiber explosion, acid or alkaline pretreatment and biological treatment (Chandel et al., 2007).

1.2.2 Hydrolysis

After pretreatment, the cellulose and hemicellulose portions form lignocelluloses need to be further broken down into monomeric sugars by enzymes or acids for the fermentation process. There are three major methods of extracting sugars from biomass: dilute acid hydrolysis, concentrated acid hydrolysis and enzymatic hydrolysis.

The dilute acid hydrolysis process is one of the oldest and simplest methods of extracting sugars from biomass. This process is carried out in two stages. Different concentration sulfuric acid and different temperature are applied in the two stages to optimize the process. Limitations associated with dilute acid hydrolysis are follows. With higher temperature, the monomeric sugars derived from hemicellulose will degrade to form fermentative inhibitors, such as furan compounds, weak carboxylic acids and phenolic compounds (Olsson and Hahn-Hägerdal, 1996). In order to remove these fermentation inhibitors, several chemical and biological methods could be used, such as overliming, ion exchange, charcoal adsorption and biological detoxification (Chandel et al., 2007). However, the detoxification method will increase operating cost.

The concentrated acid hydrolysis is more rapid process of converting cellulose and hemicellulose to glucose and xylose, respectively. Approximately, 90% of both cellulose and hemicellulose can be depolymerized into their monomeric sugars with concentrated hydrolysis, so this process has the advantage of high sugar recovery efficiency (Chandel et al., 2007).

The enzymatic hydrolysis of cellulose into glucose is a slow and complex due to the complex embedded structure of cellulose in a matrix of lignin and hemicellulose and the limited availability of biding sites for active enzymes. The factors that affect the enzymatic hydrolysis are cellulose property, substrates, and reaction conditions (temperature, pH, etc.). At the same

time, the process is very expensive compared with acid hydrolysis due to the high enzyme cost (Stephanopoulos, 2007).

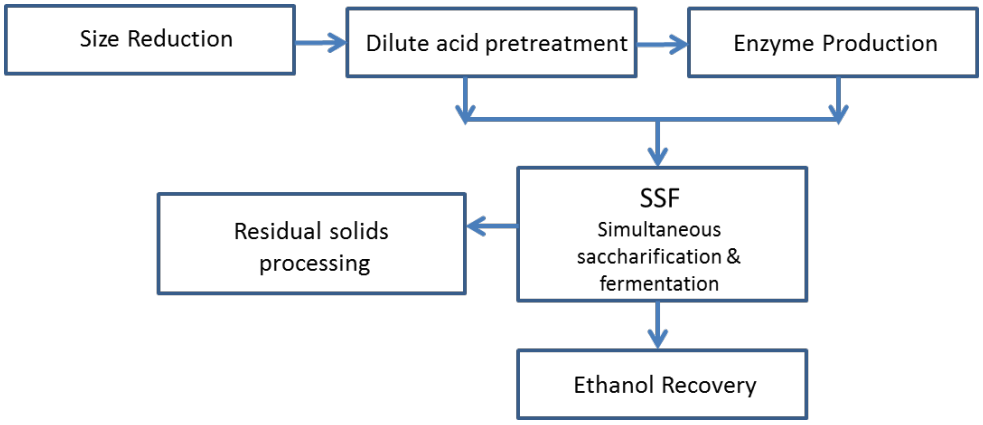

Figure 1.1 Schematic diagram of the conversion of biomass feed stock to ethanol fuel (Lin and Tanaka, 2006)

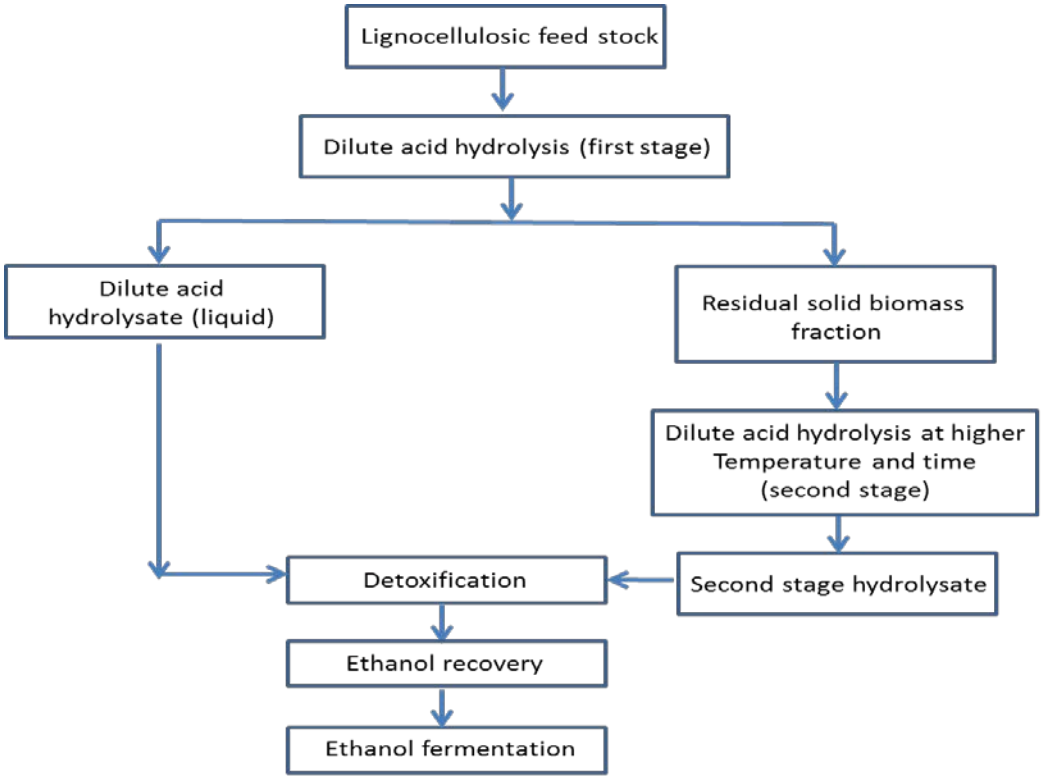

Figure 1.2 Dilute acid hydrolysis and separate fermentation of pentose and hexose sugars (Chandel et al., 2007)

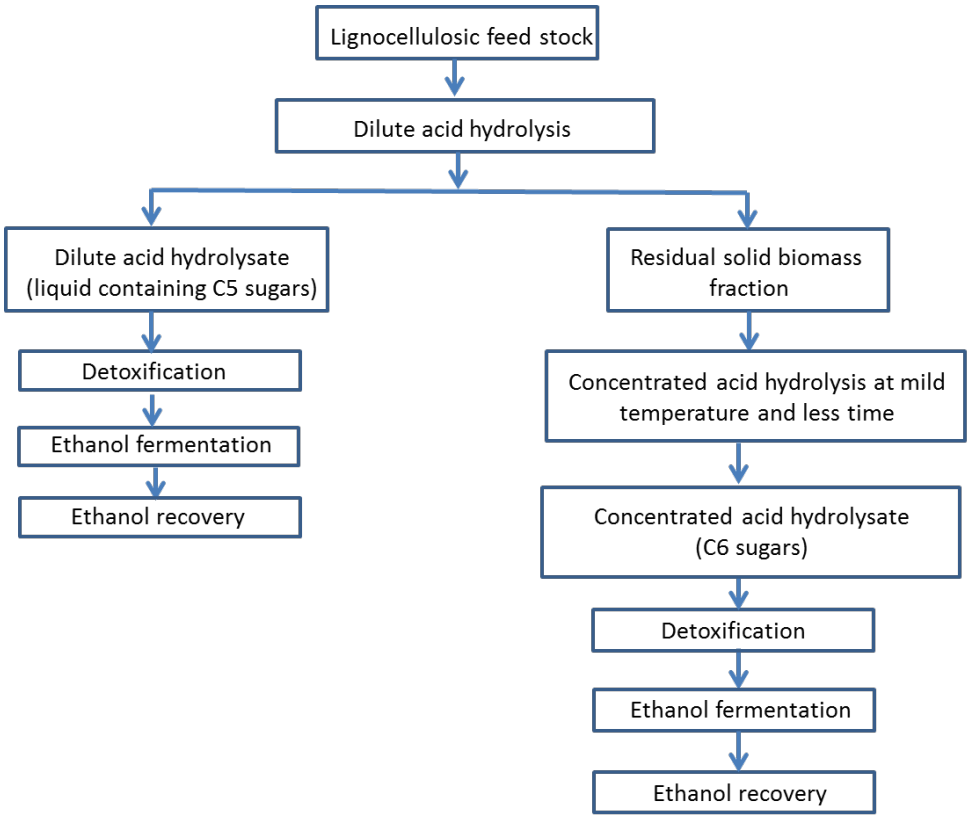

Figure 1.3 Concentrated acid hydrolysis and separate pentose and hexose sugars fermentation (Chandel et al., 2007)

1.2.3 Fermentation

After hydrolysis, the primary fermentable sugars in hydrolysate are pentose and hexose, such as glucose and xylose. Different microorganisms are used to ferment these sugars to produce bioethanol, such as *Saccharomyces cerevisiae*, *Scheffersomyces stipitis*, *Kluyveromyces marxianus*, *Candida shehatae*, *Zymomonas mobilis* and *Escherichia coli*. Currently, the fermentation of a mixture of hexose and pentose is inefficient because no wild organism has been found that can convert all sugars into ethanol at a high yield (Ragauskas et al., 2006). There are several strategies for fermentation process: Consolidated Bio Processing (CBP) (Lynd et al., 2005), Separate Hydrolysis and Fermentation (SHF) (Toon et al., 1997), Simultaneous Saccharification and Fermentation (SSF) (Tomás-Pejó et al., 2008, Eken-Saraçoğlu and Arslan, 2000), and Simulta-

neous Saccharification and Co-Fermentation (SSCF) (Ohgren et al., 2007, Chandel et al., 2007). Fermentation can be performed as a batch, fed-batch or continuous process.

1.2.3.1 Batch fermentation

In industrial ethanol fermentation, most of process uses the batch operation mode. This is because batch operation offers the ease of operation and high initial substrate concentration along with high product concentration due to the complete conversion of substrate (Olsson and Han-Hagerdal, 1996). However, disadvantages associated with this process are the high proportion of unproductive time between batches, low productivity, and high labor costs due to cleaning, sterilization and restarting the process (Shama, 1988).

1.2.3.2 Fed-batch fermentation

For fed-batch fermentation, it offers advantage over batch fermentation as it has higher yield and productivity than batch fermentation. However, fed-batch fermentation performance is limited by the substrate feed rate and cell mass concentration (Lee and Chang, 1987). Hence, proper feed rate with the right component composition is required during process.

1.2.3.3 Continuous fermentation

Continuous fermentation can be carried out using different types of bioreactors such as stirred-tank reactors or plug flow reactors. Continuous fermentation offers advantages over batch fermentation as it provides low labor cost and high productivity by eliminating unproductive time associated with cleaning, recharging, adjustment of media and sterilization. However, major disadvantages of this process are the contamination and the difficulty of obtaining high cell density cultures due to washout. The high cell density of microbes under optimized physiological condition/growth of the organism allows high productivity and short overall processing time compared to batch fermentation. In order to obtain high cell density culture, immobilization of

cells and cell recycling are used to increase productivity and reduce the overall process time. The application of immobilization technique increases fermentation rates with high productivity (Chandel et al., 2007).

1.3 Conversion of Lignocellulosic Biomass to Ethanol by Microorganisms

Lignocellulosic ethanol can be fermented by various microorganisms such as bacteria, yeasts and filamentous fungi. Depending on the overall pretreatment and hydrolysis processes, mixed or separate C5 or C6 sugars can be hydrolyzed. While the lignocellulosic ethanol fermentation of hexose sugars is well established on large scale, the conversion of pentose sugars, such as xylose to ethanol is much difficult (Berg, 2004). However, it was estimated that the bioethanol production cost can be reduced as much as 22% by the complete conversion of pentose sugars to ethanol (Sassner et al., 2008).

1.3.1 Conversion of hexose sugars to ethanol

The commonly used yeast for ethanol fermentation is *Saccharomyces cerevisiae*, which is capable of converting hexose sugars to ethanol. This yeast species has the important features required in fermenting microorganisms such as high ethanol yields and productivities, minimal formation of secondary metabolites and high tolerance to inhibitors during the pretreatment and hydrolysis processes or to ethanol. *S. cerevisiae* catabolizes glucose to ethanol very efficiently by means of the Embden-Meyerhof and Parnas (EMP) pathway followed by alcoholic fermentation under anaerobic conditions. Another microorganism capable of converting glucose into ethanol is *Zymomonas mobilis,* a Gram-negative bacterium which produces ethanol at a high yield (Choi et al., 2008). Nevertheless, both *S. cerevisiae* and *Z. mobilis* cannot ferment pentoses such as xylose present in the hydrolysates of lignocellulosic biomass (Keshwani and Cheng, 2009). Hence, while ethanolic fermentation of hexoses derived from cellulosic biomass, i.e., glucose, mannose

and galactose, using baker's yeast *S. cerevisiae* is well established on large scale, the conversion of the pentoses (e.g., xylose and arabinose) to ethanol is still one of the major barriers to industrializing the production of lignocellulosic ethanol.

1.3.2 Conversion of pentose sugars to ethanol

The inability to ferment xylose limits hexose-fermenting microorganism's usage in lignocellulosic ethanol production. However, there are some microorganisms (bacteria and yeasts) which have the native capacity of utilizing pentoses. The most promising yeasts that have the capability to utilize both hexose and pentose sugars are *Scheffersomyces stipitis*, *Candida shehatae* and *Pachysolan tannophilus*. As shown in Figure 2.1, yeasts metabolize xylose by means of the xylose reductase (XR) that converts xylose to xylitol and xylitol dehydrogenase (XDH) that convert xylitol to xylulose. After phosphorylation, xylulose is metabolized through the pentose phosphate pathway (PPP) to ethanol (Zaldivar et al., 2001). Unlike yeasts, bacteria fermenting xylose directly convert xylose to xylulose through the xylose isomerase (XI), but the wild strains of these bacteria produce much smaller amounts of ethanol compared to yeasts. Among those wild type yeasts fermenting xylose, *S. stipitis* has the highest native capacity for xylose fermentation of any known microorganisms (Agbogbo and Coward-Kelly, 2008).

1.3.2.1 Challenges of pentose (xylose)-fermenting microorganisms

The xylose-fermenting microorganisms have a slower hexose consumption rate compared to glucose-fermenting microorganisms such as *S. cerevisiae*. The ethanol productivity of these strains is at least five to ten-folds lower than that obtained with *S. cerevisiae* during glucose fermentation (Agbogbo et al., 2007). In addition, the use of *S. stipitis* and other wild yeasts for xylose fermentation is limited by the repression of xylose utilization when glucose is also present in the hydrolysates. In fact, a diauxic growth or diauxic kinetic is observed when they are in medi-

um containing mixed sugars, glucose is consumed as first and the other sugars are metabolized after glucose depletion resulting in low ethanol productivity. Furthermore, one of major challenges for ethanol production from xylose by native pentose-fermenting yeasts is controlling the oxygen supply to maximize ethanol production. Too much oxygen leads to aerobic growth and low ethanol yield with the increase accumulation of acetic acid (Rizzi et al., 1989); insufficient oxygen leads to slow fermentation rate with the increase accumulation of xylitol and causes poor ethanol productivity. Under strictly anaerobic condition, *S. stipitis* are only able to grow one doubling before fermentation and cell growth stop (Du Preez, 1994; Slininger et al., 1991). Hence, the fermentation capacity of *S. stipitis* is greatly dependent on the effects of aeration rate for an optimal conversion of sugars to ethanol. Another limited use of *S. stipitis* at an industrial scale is the low tolerance to ethanol and other inhibitors such as acetic acid, furfural and HMF (McMillan, 1993).

1.3.3 Co-fermentation of mixed hydrolysates

In order make economically feasible process of lignocellulosic ethanol production, it is essential to achieve simultaneous complete utilization of both glucose and xylose, the main components of cellulose and hemicellulose. Majority of existing research has been focused on developing genetically modified single recombinant organism, which can ferment both hexose and pentose efficiently into ethanol. In parallel with ongoing development of the genetic recombinant organism strategy, co-culture strategy has been recognized as a promising and cost-effective way to coferment a mixture of glucose and xylose for ethanol production. Recently co-culture approach has drawn increased interest in fermenting lignocellulosic biomass.

1.3.3.1 Recombinant strategy

Due to the inefficient xylose fermentation by xylose-fermenting microorganisms and inability of converting xylose to ethanol by glucose-fermenting microorganisms, development of a single recombinant organism with the application of genetic engineering has been continuously growing. In this regard, different metabolic engineering strategies have been explored. The major part of the engineering strategies is based on the construction of recombinant *S. cerevisiae* organisms due to its robustness and high stress tolerance (Almeida et al, 2007). Xylose metabolism assimilation pathway has been transferred to *S. cerevisiae* through the transfection of the xylose reductase and xylitol dehydrogenase genes from the pentose-utilizing yeast *S. stipitis* (Chu and Lee, 2007; Jeffries, 2006). By introducing multiple changes to the host genome, numerous recombinant strains have been successfully developed to ferment both glucose and xylose, simultaneously. Among them, the representative ones are the recombinant *S. cerevisiae* (424A) (Sedlak and Ho, 2004), engineered *Zymomonas mobilis* (CP4) (Rogers et al., 1982; Zhang et al., 1995) and engineered *Escherichia coli* (KO-11) (Ohta et al., 1991). However, despite the promising results in ethanol production from these recombinant strains, few of them have been realized in industrial applications due to issues related to genetic stabilities, diauxic kinetics or other reasons (Hahn-Hagerdal et al., 2007).

1.3.3.2 Co-culture strategy

While metabolic engineering of developing a single recombinant strain offers the possibility of converting both glucose and xylose simultaneously, alternative approaches have also been emerged. Co-culture consisting of combinations of glucose-fermenting microorganisms and xylose-fermenting microorganisms has been recognized as an effective approach for co-fermentation of both glucose and xylose (Lee et al., 2008). Co-cultures can offer the robustness

over single cultures, as the population of each strain can be adjusted to the different amount of available sugars from lignocelluloses to maximize ethanol productivity (Eiteman et al., 2009). The design of co-cultures offers the great advantage in easy manipulation of combining different microbes to metabolize different pentose and hexose sugars (Alper and Stephanopoulos, 2009). In lignocellulosic ethanol production, many of co-culture processes of hexose-fermenting microbe and pentose-fermenting microbe have been extensively studied with attempts to achieve a simultaneous conversion of glucose and xylose to ethanol (Leschine and Canale-Parola, 1984; Qian et al., 2006; Taniguchi et al., 1997; de Bari et al., 2004; Beck et al., 1990). However, these co-culture processes obtain technical difficulties such as low ethanol yields due to non-compatible optimal oxygen required by each microbe. More detailed review on co-culture systems is described in Chapter 2.

Chapter 2. Review on Co-culture Systems

2.1 Current Co-culture Systems

Co-culture process is not only a promising strategy to lignocellulosic ethanol (bioethanol) production but also a promising strategy to the production of bioenergy such as hydrogen, methane and polyhydroxyalkanoates from renewable resources, which can reduce environmental impacts (Florens et al., 2006; Reis et al., 2003; Rodrguez et al., 2006). The use of controlled co-culture fermentation using *S. cerevisiae* and non *S. cerevisiae* yeasts has been recognized as an effective way to coferment the sugar mixture (hexose and pentose) in lignocellulosic biomass. However, a majority of co-culture studies reported that while the fermentation of glucose can be completely converted with a traditional glucose-fermenting microbe, the fermentation of xylose often resulted in a low efficiency due to the conflicting oxygen requirements between the two microbes along with the catabolite repression on the xylose utilization caused by the glucose (Kordowska-wiater & Targonski, 2002; Lebeau et al., 1997; Grootjen et al., 1991; Laplace et al., 1993). Different approaches in both process engineering and strain engineering have been carried out to circumvent these difficulties and to improve the co-culture processes.

Examples of different co-culture techniques in the process engineering approaches under continuous culture conditions (Grootjen et al., 1991; Laplace et al., 1993b; Delgenes et al., 1996), the immobilization of one of the organisms (Grootjen et al., 1991a), co-immobilization of two organisms (Lebeau et al., 1997; Grootjen et al., 1991a; de Bari et al., 2004), two stage fermentation in one bioreactor (i.e. sequential culture) (Fu & Peiris, 2008) and separate fermentation in two bioreactors (Taniguchi et al., 1997a; Grootjen et al., 1991b) are applied to alleviate

catabolite repression exerted by glucose on xylose consumption by the xylose-fermenting microbes such as *S. stipitis*. For strain engineering approaches, the use of respiratory-deficient mutants of *S. cerevisiae* (Kordowska-wiater & Targonski, 2002; Laplace et al., 1991a; Taniguchi et al., 1997b) and *Saccharomyces diastaticus* (Laplace et al., 1993b; Delgenes et al., 1996; Laplace et al., 1993c), a mutants of *S. stipitis* showing restricted glucose catabolite repression (Kordowska-wiater & Targonski., 2002) and genetically modified organisms are applied to generate an oxygen profile favorable for the xylose-fermenting organisms (Qian et al., 2006).

2.1.1 Co-culture microorganisms

The natural ethanol fermentative microorganisms are categorized as yeasts, fungi, and bacteria. Examples of ethanologenic yeasts are *S. cerevisiae*, *S. stipitis*, *Kluyveromyces marxianus*, *Candida shehatae* and *Pachysolen tannophilus*. Examples of ethanologenic bacteria are *Zymomonas mobilis*, *E. coli*, *Bacillus stearothermophilus* and *Clostridium celluloyticum*. Table 2.1 summarizes the most selected strain combinations used in recent co-culture systems.

2.1.2 Co-culture interactions

In order to select microorganisms for the co-culture system, it is very important to study the interactions and the compatibility of a pair of organisms. Possible interaction between two microbial organisms can be categorized as positive interactions and negative interactions and interactions which are positive for one strain but negative for the other strain (Taniguchi & Tanaka 2004). Laplace et al. (1992) have studied the various microorganisms to test the compabilities of different fermentative conditions. In terms of compatibility, for example, the optimal conditions of pH and temperature for bacterium, *Z. mobilis* to ferment glucose are pH of 7 and 37^{o}C, respectively, but these conditions are not compatible with the optimal conditions of those xylose-fermenting yeasts (*S. stipitis*, *C. shehatae*), which are pH 5 and 30^{o}C, respectively. However, the

optimal fermentative conditions of glucose-fermenting yeasts are compatible with the xylose-fermenting yeasts and hence those strains are widely used in co-culture studies as demonstrated in Table 2.1. Among those organisms, the most commonly used pair of yeasts organisms in current co-culture systems is the combination of *S. stipitis* and *S. cerevisiae* since both are yeasts and have much better compatibility as well as similar fermentation conditions.

Table 2.1 The combinations of two strains used in co-culture systems for ethanol production

Strains	**References**
C. shehatae + *S. cerevisiae*	Hickert et al., 2013
S. stipitis + *S. cerevisiae*	Gutierrez-Rivera et al., 2012
S. stipitis + *S. cerevisiae*	Chandel et al., 2011
S. stipitis + *S. cerevisiae*	Li et al., 2011
S. stipitis + *K. marxianus*	Rouhollah et al., 2007
S. stipitis + *S. cerevisiae*	Rouhollah et al., 2007
Z. mobilis + *P. tannophilus*	Fu and Peiris, 2009
S. cerevisiae + *P. tannophilus*	Qian et al., 2006
Coimmobilized S. stipitis + *S. cerevisiae*	de Bari et al., 2004
Restricted catabolite repressed mutants of *S. stipitis* + *S. cerevisiae*	Kordowska-Waiver and Targonski, 2002
Restricted catabolite repressed mutants of *S. stipitis* + RD mutant of *S. cerevisiae*	Kordowska-Waiver and Targonski, 2002
S. stipitis + RD mutant of *S. cerevisiae*	Kordowska-Waiver and Targonski, 2001
Coimmobilized *S. cerevisiae* + *C. shehatae*	Lebeau et al., 1997
S. stipitis + *S. cerevisiae*	Taniguchi et al., 1997a
S. stipitis + RD mutant *S. cerevisiae*	Taniguchi et al., 1997a
S. stipitis + RD mutant *S. diastaticus*	Laplace et al., 1993a

C. shehatae + *S. cerevisiae*	Laplace et al., 1993b
C. shehatae + RD mutant of *S. cerevisiae*	Laplace et al., 1993b
Coimmobilized *S. stipitis* + *S. cerevisiae*	Grootjen et al., 1991a and 1990a
Immobilized *S. stipitis* + *S. cerevisiae*	Grootjen et al., 1991a

2.2 Challenges of Co-culture Systems

Although the co-culture systems has been recognized as a promising strategy and has drawn increased interest, limited research has been done so far to investigate the dynamic properties of co-culture organisms due to the complexity of the organisms' nature dynamics and the difficulty of controlling the system (Tohyama et al., 2002). In addition, the main difficulty of using two microorganisms for the cofermentation of the two dominating sugars of the lignocellulosic hydrolysates is the inability to provide optimal fermentative conditions for the two organisms simultaneously as well as the limitations existing in the xylose fermentation.

2.2.1 Major limitations in the fermentation of xylose

The rates of ethanol production and the ethanol concentrations attained by the most promising xylose-fermenting yeasts compare poorly with that of ethanol fermentation by glucose-fermenting *S. cerevisiae*. The major limitations of xylose fermentation, including xylose transport mechanisms are described below.

2.2.1.1 Xylose transport system in xylose-fermenting microorganisms

In the conversion of xylose to ethanol by xylose-fermenting microorganisms, xylose is first transported across the cell membrane by a proton symport where xylose is reduced to xylitol via a xylose reductase (XR). Then, xylitol is oxidized to xylulose by a xylitol dehydrogenase (XDH). The xylulose is then phosphorylated to xylulose-5-phosphate before entering the pentose

phosphate pathway (PPP). Thereafter, the xylulose-5-phosphate is metabolized to glyceraldehyde-3-P and fructose-6-P via PPP, and then these compounds are converted to pyruvate where it is finally converted to acetaldehyde, which further reduced to ethanol, as demonstrated in Figure 2.1 (McMillan, 1993). Yeasts and fungi use this two-step oxidoreduction reaction to convert xylose to xylulose. Enzymes used in xylose conversion by different yeasts require different cofactors of NADPH, NADH, NAD+, and NADP+. For *S. stipitis*, it can use either NADPH or NADH as the cofactor, but the affinity (K_m) of NADPH is lower than for NADH (Skoog and Hahn-Hagerdal., 1990). There are two major pathways of converting xylose to xylulose are shown in Figure 2.1. In contrast to yeasts and fungi, most of bacteria use the xylose isomerase pathways (one-step reversible reaction) for catabolism of D-xylose. The enzymes of Mn^{2+}, Co^{2+}, or Mg^{2+} are required for its activity (Chandrakant and Bisaria, 1998).

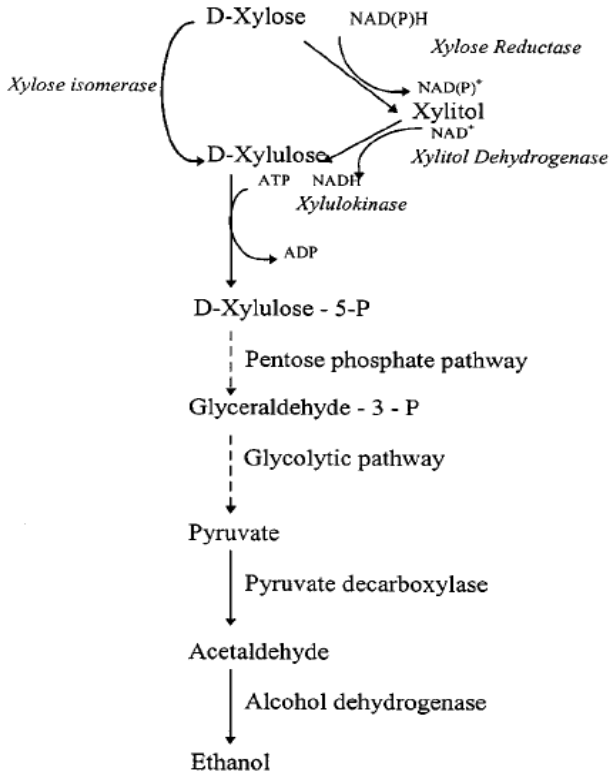

Figure 2.1 Two routes for metabolism of xylose to xylulose and subsequent conversion of xylulose to ethanol (Chandrakant and Bisaria, 1998)

Many xylose conversion pathways are based on chemosmotic proton symport which are strongly pH dependent. Table 2.2 summarizes xylose transport systems for several bacteria and yeasts. Xylose uptake in yeasts can occur by both facilitated diffusion and active transport processes. Active transport systems, in contrast to facilitated diffusion systems, require metabolic energy and can uptake sugars against a concentration gradient (McMillan, 1993). In *S. cerevisiae*, xylose is not metabolized, but xylose is transported by facilitated diffusion (Jeffries, 1983). For *S. stipitis*, no facilitated diffusion system is present and symport system is active in cells (Kilian and van Uden, 1988).

Table 2.2 Xylose transport systems for bacteria and yeasts (Chandrakant and Bisaria, 1998)

Transport System	**Example**	**Reference**
Proton symport	Bacteria: *E. coil* Bacteria: *Staphylococcus xylosus* Yeast: *S. stipitis*	Jeffries (1985) Killian and van Uden (1998) Does and Bisson (1989)
Facilitated diffusion	Yeast: *S. cerevisiae*	Lucas and van Uden (1986)
Aerobic proton symport	Yeast: *Rhodotorula sp.*	Jeffries (1985) Wevvs and Lee (1990)
Proton symport and facilitated diffusion	Yeast: *Candida shehatae*	Lucas and van Uden (1986)

2.2.1.2 Catabolite repression on xylose uptake by glucose

The co-cultures of yeast strains do not always ensure the complete consumption of xylose due to the catabolite repression on the xylose utilization caused by the glucose (Nakamura et al., 2001). During the fermentation of sugars released from hydrolysates, microorganisms tend to selectively utilize a preferred glucose first. Hence, when the glucose is present, the enzymes and sugar transporters of other sugars (pentose sugars) are repressed. According to the studies, they showed that glucose represses the induction of xylose reductase (XR) and xylitol dehydrogenase (XD) activities needed for xylose assimilation in the native xylose fermenting yeasts (Bicho et

al., 1988; Slininger et al., 1987). A possible explanation for this is, in *S. stipitis*, both low-affinity and high-affinity xylose proton symport are simultaneously operated. The low-affinity system is responsible for substrate inhibition when glucose but not when xylose is the substrate. The competition of glucose with the xylose occurs with the low-affinity system and the inhibition of xylose transport occurs by the high-affinity system in non-compatible manner (Kilian and van Uden, 1988). From the study, it confirms that the inhibition of xylose conversion occurs at glucose concentration higher than 2.3g/L (Grootjen et al., 1991b). Once the glucose is consumed by xylose-fermenting organisms, their growth and fermentation cease until the enzymes required for metabolizing xylose can be prepared. This preferential consumption of sugar (glucose) makes it challenging to design and efficiently control the fermentation processes using lignocellulosic biomass (Kim et al., 2010). Therefore, this diauxic kinetic is a practical problem in the cofermentation both glucose and xylose by xylose-fermenting yeasts including native and even engineered strains (Krishnan et al., 1999; Kuyper et al., 2005; Slininger et al., 1987; Zaldivar et al., 2002).

2.2.1.3 Requirement of microaerobic conditions

The performances of xylose-fermenting yeasts are dependent on many factors. Aeration is one of the dominant factors influencing xylose fermentation performance. The different yeasts require different oxygenation conditions for optimal ethanol fermentation. Xylose-fermenting yeasts require low level of oxygen for fermenting xylose. Specifically, the xylose-fermenting yeast, such as *S. stipitis*, requires microaerobic condition for xylose fermentation while glucose-fermenting yeast, such as *S. cerevisiae*, requires anaerobic condition for glucose fermentation. For xylose fermentation, under anaerobic conditions, very low or no ethanol was produced and a high yield of ethanol occurs only under microaerobic conditions. At high OTR, carbon flows preferentially through the tricarboxylic acid (TCA) cycle resulting in greater production of cells

at the expense of ethanol and hence the specific ethanol productivity declined and the yields are low (Laplace et al., 1991). A low OTR permitted preventing the imbalance of NAD+/NADH that occurred in anaerobic/very low OTR conditions which resulting in the production of xylitol. Hence, we need to determine an optimal OTR for the lowest xylitol yields at the highest ethanol yields by maintaining cell viability and NAD+/NADH balance (Delgenes et al., 1989). A metabolic explanation of this is the role of oxygen in cofactor regulation. When oxygen is readily available, NADH produced by the action of XDH is rapidly oxidized to NAD+ by the respiratory chain. This removal of NADH and production NAD+ drives the XDH to produce D-xylulose. Based on the overall fermentative reaction for xylose conversion to ethanol, 3 moles of xylose are required to produce 5 moles of ethanol and carbon dioxide. The theoretical yield of ethanol is based on the following stoichiometry:

$$3C_5H_{10}O_5 \rightarrow 5C_2H_5OH + 5CO_2 \qquad (2.1)$$

This equation assumes the conversion of xylose to xylulose without xylitol accumulation, that xylulose-5-P is converted to fructose-6-P and glyceraldehyde-3-P via PPP without cofactor imbalance, that fructose-6-P and glyceraldehyde-3-P are converted to ethanol via the EMP pathway without losses to acetate or TCA cycle. With this, the theoretical yield is thus 0.51g ethanol/g xylose or 1.67mol ethanol /mol xylose (Chandrakant and Bisaria, 1998).

2.2.1.4 Ethanol inhibition

One of major limiting steps in co-culture process is the low ethanol tolerance of xylose-fermenting organisms, which inhibits their functions of growth and fermentation (de Bari et al., 2004). Ethanol inhibition in xylose-fermenting yeasts has more pronounced effect than that of glucose-fermenting yeasts. This is because, the ethanol inhibition on xylose-fermenting organism occurs at much lower ethanol concentration of ~30g/L for *S. stipitis* while glucose-fermenting

organism of *S. cerevisiae* occurs at 70~100g/L (Casey and Ingledew, 1986). The effects of ethanol tolerance are a combination of different factors such as fermentation conditions. The effects of temperature on ethanol tolerance and thermal death of xylose-fermenting yeast was studied by Lucas and van Uden. The yeasts found to be more tolerant to ethanol at lower temperatures (Lucas and Van Uden, 1985). In order to study the effects of ethanol on metabolic rate of yeast organisms, many studies conducted experiments with adding exogenous ethanol. Both Lucas and van Uden and du Preez et al. cultured cells in the media containing different ethanol concentrations and measured the specific growth rate of yeasts (Preez et al., 1989). The exogenous ethanol introduced into cells showed a less ethanol inhibition compared to the same concentration of ethanol produced endogenously (Hoppe and Hansford, 1982). The effect of ethanol inhibition can be demonstrated better with the specific substrate utilization rate than the specific ethanol production rate, since accumulation of ethanol results in an inhibition effect on the substrate utilization and increased specific xylitol production rate at the expense of the specific ethanol production rate. Also, both effects are enhanced at higher temperatures (Alexander et al., 1989).

2.2.1.5 Co-culture fermentation mechanisms and conditions

There is different fermentation mechanism exists between two different organisms. For instance, *S. cerevisiae* regulates fermentation in response to the presence of glucose, while *S. stipitis* induces fermentative activity in response to oxygen limitation (Jeffries et al., 2007). In addition to mechanism, pH, temperature, initial sugar concentration and composition is another important factor which influences the performance of co-culture fermentation. The selection of above fermentation conditions is dependent on the two selected microorganism strains of the co-culture system. This is because each selected organism will have its own optimal values for above conditions.

2.2.1.6 pH condition

Many researchers, for example, Jeffries (1985) and Alexander et al. (1988), observed that ethanol production is improved at lower pH. These observations support the hypothesis that symport-based sugar uptake systems in yeasts require a transmembrane proton gradient to drive sugar transport. Since cells tend to operate at a slightly a basic internal pH, the transmembrane ΔpH increases when the external pH is reduced. The optimal pH for the single culture of *S. cerevisiae* (pH 5.0), *S. stipitis* (pH 4.5-5.5 range) is around 5.0, but for *E. coli* and *Z. mobilis* are about 7.0. Since most common combination of co-culture organisms are *S. cerevisiae* and *S. stipitis*, the pH of fermentation medium can be controlled at 4.5-5 by adding either sodium hydroxide for increasing pH or hydrogen chloride for decreasing pH (Zaldivar et al., 2001).

2.2.1.7 Temperature condition

The fermentation temperature of current co-culture system is at the range of 28-30^{o}C because the optimal fermentation temperature for the single culture of *S. cerevisiae, S. stipitis, C. shehatae* and *P. tannophilus* is around 30^{o}C (Chen, 2011). However, for xylose-fermenting yeasts, such as *S. stipitis*, most of literatures reported on *S. stipitis* CBS5773, the maximum ethanol tolerance is found at 25^{o}C. Although higher temperature (~30^{o}C) does not have a pronounced effect on xylose utilization performance by *S. stipitis*, the inhibitory effect of ethanol on cell growth increases with increasing temperature so that higher final ethanol concentrations can be achieved by reducing the temperature as ethanol accumulates. According to Delgenes et al. (1988), at 26^{o}C, the inhibitory ethanol concentration to growth was 50.6g/L and to fermentation was 68.5g/L. According to previous findings on the temperature influence on ethanol tolerance, when the temperature was changed from 25 to 30^{o}C, the inhibitory ethanol concentration decreased from 43 to 33 g/L (du Preez et al., 1987). Also, according to Slininger et al. (1990), the

temperature for xylose fermentation by *S. stipitis* NRRL Y-7124 (CBS5773) at 25-26^{o}C maximized ethanol accumulation concentration, minimized residual carbon as xylitol and xylose, and caused little sacrifice to growth rate and fermentation rate. In contrast, most *S. cerevisiae* strains show 30^{o}C as optimum fermentation temperature. However, Torija et al. (2003) showed that fermentation of *S. cerevisiae* at 25^{o}C and at 30^{o}C had no significant differences in fermentation performance since both reached similar maximal cell populations, although the initial fermentation rate was little higher at 30^{o}C than at 25^{o}C, but the ethanol yields between these two fermentation temperatures were not very different. Hence, the ideal temperature for both cell growth and fermentation of co-culture system is set at 25^{o}C which enhances the ethanol tolerance of *S. stipitis*.

2.2.1.8 Initial sugar concentration and composition

For co-fermentation of glucose and xylose in co-culture system, the initial total sugar concentration and composition play an important role in affecting the fermentation performance. Different researchers have chosen different initial sugar concentration and different glucose and xylose composition ratio in their co-culture systems. However, in most of cases, the xylose composition changes from 20-50% since the xylose composition in biomass hydrolysates is close to this range.

2.2.2 Co-culture fermentation mode

The most current co-culture systems are operated in a batch mode, because it is simple and the process is easy to operate. However, the batch mode has some drawbacks. For example, in the mixed sugar medium, the presence of glucose suppresses the xylose fermentation by xylose-fermenting strain in the co-culture system especially at the initial stage. Also, when the high initial glucose concentration is close to completion, the high ethanol concentration (~30g/L) can

inhibit xylose fermentation (Rouhollah et al., 2007). Hence, inefficient conversion of xylose will be resulted.

Unlike batch mode, continuous fermentation mode can avoid the accumulation of ethanol and other inhibiting metabolites (i.e. cellular wastes) in the system by allowing the outflow (Lebeau et al., 1997). In addition, dilution rate can be adjusted to control glucose concentration in the co-culture system to avoid the repression of xylose utilization by glucose. Therefore, fast and simultaneous conversion of glucose and xylose with co-culture system could be achieved by continuous fermentation. However, while glucose-fermenting yeasts grow faster, the cell growth by xylose-fermenting yeasts is relatively slow. Especially, when these xylose-fermenting yeast are co-cultivated with the glucose-fermenting yeast. Hence, the loss of cells or cell washout of xylose-fermenting yeasts associated with slow cell growth via outflow can be problematic in continuous co-culture fermentation. In order to produce ethanol efficiently by fermentation, it is desirable to retain a high concentration of ethanol producing yeasts in a fermentor. To circumvent this problem, cell recycling involving cell separation by membranes and cell immobilization techniques have been studied by others in order to increase volumetric ethanol productivities and yields (Taniguchi et al., 1997a).

Chapter 3. Experimental Protocol and Equipment Development

Co-culture has the potential to simultaneously ferment both glucose and xylose to produce ethanol. Recently, research on using different co-culture processes for lignocellulosic ethanol fermentation has drawn a significant interest (see Table 3.1 from co-culture study), mainly due to their flexibility, tunability and increased resistance to environmental stress. However, up to now, very limited research has been done to investigate the dynamic properties and interactions of co-culture microorganisms due to the lack of effective experimental protocols and equipment. Many researchers have tried different fermentation techniques or schemes to overcome the challenges associated with xylose fermentation in co-culture systems. However, there is still lack of robustness and high-throughput fermentation monitoring techniques for studying the physiology of each organism in complex co-culture system (Huang and Lefsrud, 2014). In our study, we have developed new experimental protocols and equipment to allow the quantification of the dynamic properties of co-culture yeasts and physiological background of each organism to conduct systematically designed fermentative experiments.

3.1 $k_L a$ Measurement for *S. stipitis*

The oxygen transfer rate (OTR) is an important parameter for xylose fermentation by xylose-fermenting yeast *S. stipitis*. This is because xylose fermentation performance depends significantly on the oxygenation level of the culture. High aeration rate results in fast cell growth and acetic acid production, while very low aeration (oxygen-limited) rate often results in xylitol production, both at the expense of reduced ethanol production. Only optimized microaerobic condition promotes ethanol production by maintaining cell viability and NADH balance. Hence,

it is critical to determine the optimal OTR for ethanol production by *S. stipitis*. In order to accurately supply of OTR, it is important to estimate the volumetric mass transfer coefficient $k_L a$ in *S. stipitis*.

3.1.1 Introduction

The OTR is a crucial parameter in aerobic and microaerobic processes, since it is often the rate-limiting factor due to the low solubility of the oxygen in the broth. Therefore, it is an essential parameter that needs to be accurately measured or estimated for the design, operation and scale-up of bioreactors (Garcia-Ochoa and Gomez, 2009). The transfer of the oxygen from the gas bubbles into the cells can be divided into two steps: (1) from the gas phase into the liquid medium phase; (2) from the liquid medium into the cells (or the consumption of oxygen by the cells). The mass transfer rates of oxygen corresponding to these two steps are termed oxygen transfer rate (OTR) and oxygen uptake rate (OUR), respectively. The overall mass balance for the dissolved oxygen (DO) in the well-mixed liquid phase can be written as:

$$\frac{dC_L}{dt} = OTR - OUR \tag{3.1}$$

where C_L denotes the dissolved oxygen concentration in the liquid phase. Based on the two film model (Whitman, 1923) and Henry's law, the net mass transfer of oxygen from the gas bubble to the liquid (i.e., OTR) can be expressed as

$$OTR = k_L a(hC_B - C_L) \tag{3.2}$$

where C_B is the oxygen concentration in the gas phase, h is the Henry's constant for oxygen and $k_L a$ is the volumetric mass transfer coefficient. It has been well recognized that $k_L a$ can be affected by many factors including the fluid properties (e.g., density, diffusivity, and viscosity), the size of the bubbles, the system geometry, and operating conditions (e.g., stirring speed in a stirred tank) (Blanch and Clark, 1996; Bouaifi et al., 2001; Linek et al., 2004; Martin et al., 2008;

Özbek and Gayik, 2001; Wu, 1995). Many different methods to measure $k_L a$ have been published, which can be divided into two groups, chemical method and physical method (Suresh et al., 2009). The chemical methods (Cooper et al., 1944) use chemical reactions to determine the OTR or $k_L a$ and are not applicable for direct measurement of OUR. The physical methods (Baird et al., 1993; Tobajas and Garcia-Calvo, 2000) use gas analyzer, gas chromatography or oxygen probes to measure the gas composition and calculate the OTR and OUR at the same time. Among different methods, the classical dynamic method (Bandyopadhyay and Murphrey, 1967) has been widely used to simultaneously measure $k_L a$ and OUR for different fermentation systems.

$$\frac{dC_L}{dt} = k_L a(hC_B - C_L) - OUR \tag{3.3}$$

The classical dynamic method is a simple and elegant means to measure $k_L a$, which only requires a fast responding DO probe (Rao, 2009). The schematic illustration of the classical dynamic method is given in Figure 3.1(a). By introducing a brief interruption in the oxygen supply to the bioreactor, the overall process can be divided into two steps: degassing and re-gassing. During the degassing process, air is shut off and dissolved oxygen is consumed by cells. By fitting a straight line to the trajectory of the DO concentration, OUR is estimated as the slope of the straight line. During the re-gassing process, air is resumed to bubble through the fermentation broth. By fitting the trajectory of DO concentration to the following equation, $k_L a$ can be estimated. The classical dynamic method was rapidly adopted and became textbook material since its publication (Rao, 2009). In addition, several follow-up articles have been published over the years to improve the original method. In particular, the effect of the probe response time on the accuracy of the $k_L a$ measurement was studied by Heineken, 1971.

3.1.2 Materials and methods

S. stipitis CBS5773 cells were pre-cultured in minimal medium containing (per liter) 20g D-xylose, 1.7g yeast nitrogen base without amino acids or ammonium sulfate and 2.27g urea. Culture medium used in all experiments contained (per liter) 0.5g D-xylose, 1.7g yeast nitrogen base without amino acids or ammonium sulfate and 2.27g urea. All experiments were conducted in a New Brunswick BioFlo110 fermenter (3L) with a working volume of 1.5L under sterile condition. The DO concentrations in the liquid and headspace were monitored with polarographic dissolved oxygen electrodes Inpro6800 (Mettler-Toledo, Columbus, OH). Air or nitrogen gas was used as the gas phase for regassing or absorption and degassing or desorption respectively, in all experiments. The gas flow rate was kept constant at 196mL/min. Experiments were performed with various agitation speeds (250, 350, 450rpm) and biomass concentrations (OD600=0.0, 1.5, 3.0, 4.5, 10.0).

3.1.3 Results and discussion

Despite many successful applications of the dynamic method to measure $k_L a$ for different bioprocesses, we had experienced some limitations during our experiments, which have not been addressed in the past. Some scenarios are described below and illustrated in Figure 3.1(b).

(1) Curving DO trajectory during the degassing step: in our experiments conducted with yeast *Scheffersomyces stipitis*, the trajectory of the DO during the degassing process deviates from a straight line, which directly affects the estimation of OUR.

(2) Slow degassing process at low cell density: during our experiments of medium/high agitation with low cell density, DO decreases very slowly during the degassing step, which limits the range for the re-gassing step (i.e., OD600=0.5 in Figure 3.1(b)). As a result, it is very difficult to

obtain an accurate estimate of k_La due to the small perturbation introduced into the system, that is, the small change in the DO during the regassing step.

(3) Slow re-gassing process at high cell density: under the condition of high cell density with medium/low agitation when air is resumed after degassing step, the DO does not increase noticeably because of the high oxygen consumption rate, which makes the estimation of k_La very difficult (i.e., OD600=7.0 in Figure 3.1(b)).

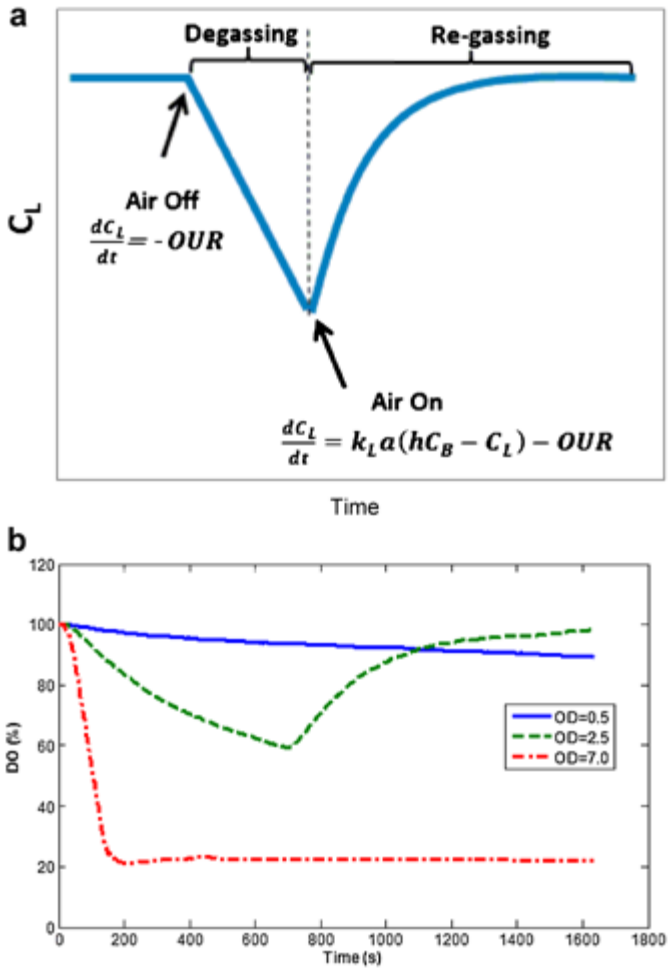

Figure 3.1 (a) Schematic illustration of the classical dynamic method where OUR is estimated by fitting C_L to a straight line during the degassing process and OTR or k_La is estimated by fitting C_L to an exponential curve during the re-gassing process; (b) Cases that the classical dynamic method are less effective in describing the dynamics of mass transfer: obvious curving trajectory during the degassing process (OD_{600}=2.5); slow degassing process at low cell density (OD_{600}=0.5); and slow re-gassing process at high cell density (OD_{600}=7.0). Agitation speed was fixed at 350rpm.

In addition, the mass transfer between the headspace and the liquid phase was not considered in the classical dynamic method, which could have significant impact under certain conditions as illustrated later. In this work, we present an improved dynamic method to address these limitations, which includes both an improved model and an improved procedure. In addition, we use *S. stipitis* as the model system to validate the proposed method, and to investigate the effects of cell concentration and agitation speed on $k_L a$ of the system. To help understand the model development, different mass transfer components involved in an aerated bioreactor are illustrated in Figure 3.2. In the classical dynamic method, only mass transfer between the air bubbles and the liquid broth is considered. But in fact, mass transfer between the headspace and the liquid broth also exists, and sometimes may be dominant. To take this consideration into account, the total mass balance of the dissolved oxygen in a well-mixed liquid phase and headspace can be written as

$$\frac{dC_L}{dt} = k_L a(hC_B - C_L) + k_G a'(hC_H - C_L) - OUR \tag{3.4}$$

$$\frac{dC_H}{dt} = \frac{Q}{V_H}(C_B - C_H) - k_G a'(hC_H - C_L) \tag{3.5}$$

where $k_G a^{'}$ is the volumetric mass transfer coefficient between the headspace and the liquid phase; C_L, C_B, C_H, are the oxygen concentrations in liquid phase, bubbles, and headspace, respectively; Q is the volumetric flow rate of the air or nitrogen entering the headspace, V_H is the headspace volume. Because the measured DO during the experiments is always a relative concentration (i.e., percentage of the calibrated concentration), we convert the model into the relative concentration terms as follows:

$$\frac{dC_{L,m}}{dt} = k_L a\left(C_{B,m} - C_{L,m}\right) + k_G a'\left(C_{H,m} - C_{L,m}\right) - OUR^* \tag{3.6}$$

$$\frac{dC_{H,m}}{dt} = \frac{Q}{V_H}\left(C_{B,m} - C_{H,m}\right) - k_G a' h\left(C_{H,m} - C_{L,m}\right) \quad (3.7)$$

where $OUR^{'}$ = OUR/hC_0; $C_{L,m} = C_L/hC_0$ and $C_{H,m} = C_H/C_0$, are the measured relative DO concentrations in the liquid phase and headspace, respectively, with the DO probe calibrated by the air (or diluted air) fed to the bioreactor (C_0).

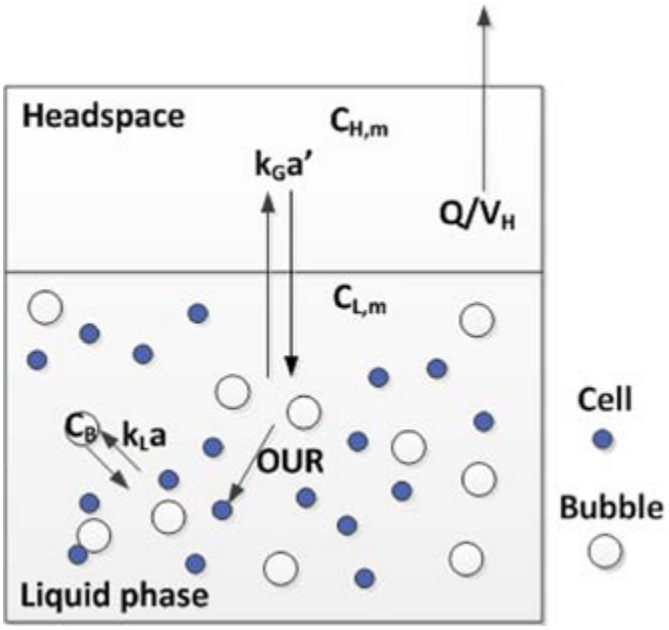

Figure 3.2 Schematic illustration of different mass transfer components involved in an aerated bioreactor.

Compared to the classical dynamic method, the major difference of the modified method is that: during the degassing step, instead of simply shutting off the air supply, we replace air (or diluted air) with nitrogen of the same flow rate, which speeds up the descending process of DO, sometimes significantly; then in the re-gassing step, nitrogen is switched to air (or diluted air) of the same flow rate to bring the DO up. For the improved method, we introduce the following terminology changes. During the "degassing" step, because of the continuous supply of the nitrogen gas instead of complete shutoff of air supply, we rename this step "desorption process," as the gas–liquid mass transfer will result in the desorption of DO into nitrogen bubbles. Corre-

spondingly, for the “re-gassing” step, we rename it “absorption process.” There are several important benefits of the improved procedure. First, it allows a low DO level to be achieved quickly during the desorption process, which not only greatly reduces the risk that the cells could transit into different physiological states during the process, but also allows a larger DO change during the absorption process. As noted earlier, a larger change in DO during the absorption process is desirable, as it can improve the accuracy of the estimated $k_L a$. Second and more importantly, for the case of high cell density where the DO does not increase noticeably during the absorption process, $k_L a$ can be estimated based on the descending DO curve obtained during the desorption process alone. Note that in order to do so, we assume that the air-liquid and nitrogen-liquid interfaces (i.e., A_{air} and A_{N2}) are the same. This is reasonable as O_2 and N_2 have similar physical properties, and about 80% of air is N_2 anyway. In addition, this assumption was supported by our experiments.

It should be noted that the mass transfer between the headspace and the liquid phase was considered in Muller et al. (2012), which also considered the change of C_B. Strictly speaking, C_B keeps decreasing as the bubbles travel through the liquid phase due to the mass transfer. However, because of the short residence time in our experiments and most bioreactors, the amount of the oxygen transferred into the liquid phase is very limited—less than 5% even for the condition of the highest $k_L a$ for our experiments. Therefore, C_B is assumed constant in this work ($C_B = 0$ during the desorption process and $C_B = C_0$ during the absorption process). In addition, we did not consider the probe response time, mainly because the dynamics of the system (with time constant 30–40 min) is much slower than the dynamics of the probe (with time constant about 40 s).

For the modified dynamic procedure described above, during the desorption process, because $C_{B,m} = 0$, Equations (3.6) and (3.7) can be simplified as follows:

$$\frac{dC_{L,m}}{dt} = -k_L a C_{L,m} + k_G a'\left(C_{H,m} - C_{L,m}\right) - OUR^* \tag{3.8}$$

$$\frac{dC_{H,m}}{dt} = -\frac{Q}{V_H} C_{H,m} - k_G a' h\left(C_{H,m} - C_{L,m}\right) \tag{3.9}$$

During the absorption process, because we assume $C_B = C_0$ (or $C_{B,m} = 1$), Equations (3.6) and (3.7) can be simplified as follows:

$$\frac{dC_{L,m}}{dt} = k_L a(1 - C_{L,m}) + k_G a'\left(C_{H,m} - C_{L,m}\right) - OUR^* \tag{3.10}$$

$$\frac{dC_{H,m}}{dt} = \frac{Q}{V_H}(1 - C_{H,m}) - k_G a' h\left(C_{H,m} - C_{L,m}\right) \tag{3.11}$$

It is worth noting that fitting either $C_{L,m}$ or $C_{H,m}$ during the desorption or absorption processes (i.e., any one of the analytical solutions of the Equations (3.8)–(3.11) provided in Supplemental Information) allows us to estimate OUR^*, $k_L a$ and $k_G a'$, simultaneously. Therefore, if both $C_{L,m}$ and $C_{H,m}$ are available over both desorption and absorption processes, we can obtain four sets of independently estimated parameters based on Equations (3.8)–(3.11), and the consistency among them can serve as an indicator of the accuracy of the estimated parameters.

Experiments were conducted to demonstrate the effectiveness of the proposed method, Four cases of different cell density (OD_{600}=1.5, 3.0, 4.5, 10.0) at fixed agitation speed of 450 rpm were examined. Three replicates were conducted for each case. Figure 3.3 shows one case (OD_{600}=4.5) of the measured $C_{L,m}$ and $C_{H,m}$, as well as the predictions generated by the fitted models. Both $C_{L,m}$ and $C_{H,m}$ of the three replicates are very close to each other. To reduce clutter, the measurements and predictions of the replicate 2 were shifted up by 0.2, and the replicate 3 by 0.4. From Figure 3.3 it is observed that the model predictions agree with the measurements very well, which indicates that the models capture the dominant dynamics of the mass transfer pro-

cesses well for both $C_{L,m}$ and $C_{H,m}$, during both desorption and absorption processes. In addition, it indicates that assuming C_B as a constant does not introduce noticeable error to the model. The estimated model parameters are listed in Table 3.1 together with the other three cases. For all four cases, the estimated parameters from the three replicates are almost identical; therefore no standard deviation was provided in the table. It is worth noting that the four estimates of the parameters, obtained independently from $C_{L,m}$ during desorption, $C_{L,m}$ during absorption, $C_{H,m}$ during desorption and $C_{H,m}$ during absorption independently, agree with each other well, which not only confirms that using nitrogen bubbles to estimate the k_La is feasible, but also offers further validation of the accuracy of the estimated k_La. This offers a significant advantage over the classical dynamic method for a couple of reasons. Because the process of fitting solutions of Equations (3.8)–(3.11) with measurements is a nonlinear optimization process, there always exist multiple local solutions. How to pick the correct one is nontrivial due to the nonlinearity of the optimization problem, as the set of parameters that give the smallest fitting error are often not the true parameters. With multiple independent ways to estimate the parameters, such as through $C_{L,m}$ during desorption and absorption, or $C_{H,m}$ and $C_{L,m}$ during desorption, it allows us to find the correct parameters relatively easily, because only the set of true parameters could minimize the fitting error of multiple objective functions. The analytical solutions to the model equations (i.e., Equations (3.8)–(3.11)) and corresponding codes for the curve fitting process can be found in Supplemental Information (published).

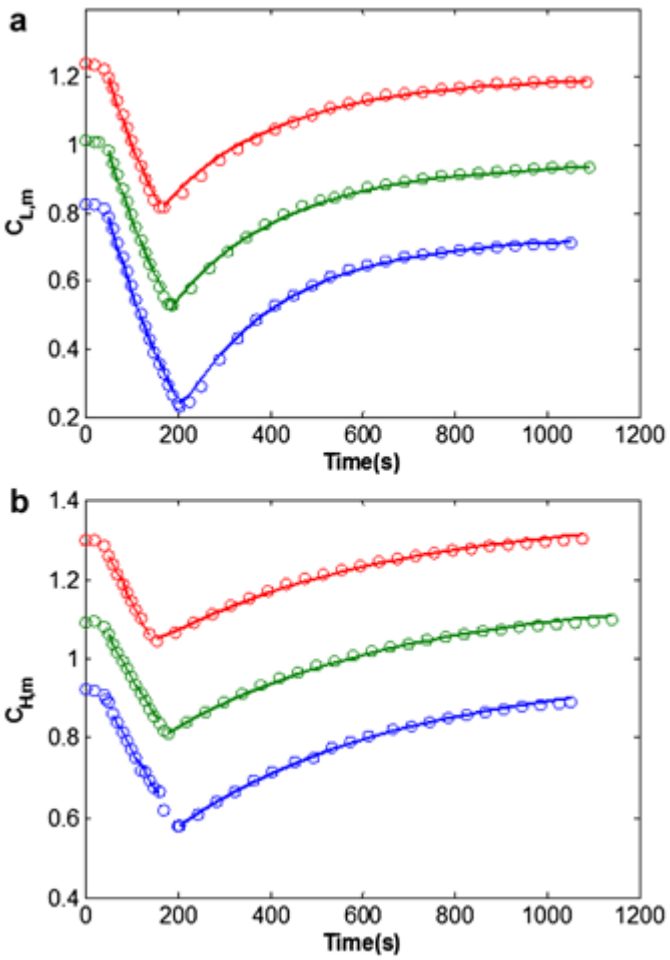

Figure 3.3 Experimental measurements and predictions from the fitted models of three replicates at OD600=4.5 and agitation speed of 450 rpm. (a) Liquid phase; (b) headspace. To reduce clutter, the measurements (green circles) and predictions (green lines) of replicate 2 were shifted up by 0.2, and replicate 3 (red circles and lines) were shifted up by 0.4. Without shifting, the three replicates overlap each other.

Table 3.1 Estimated model parameters of different cases (various OD_{600} at the fixed agitation speed of 450rpm).

Parameter ($10^{-3}s^{-1}$)	450rpm			
	From C_L		From C_H	
	Desorption	Absorption	Desorption	Absorption
OD_{600}=1.5				
k_La	5.55	5.55	5.54	5.55
k_Ga'	9.01	9.01	9.00	9.00
OUR*	7.01	7.01	7.00	7.00
OD_{600}=3.0				
k_La	6.00	6.02	6.02	6.01
k_Ga'	9.25	9.24	9.21	9.25
OUR*	6.31	6.32	6.25	6.70
OD_{600}=4.5				
k_La	4.11	4.12	4.11	4.12
k_Ga'	9.22	9.22	9.20	9.11
OUR*	1.81	1.85	1.87	1.87
OD_{600}=10.0				
k_La	3.64	3.77	3.71	3.85
k_Ga'	1.21	1.11	1.23	1.10
OUR*	1.32	1.42	1.47	1.67

Three replicates of the experiments were conducted to examine the effects of cell density (OD_{600}) and agitation speed (rpm) on k_La and OUR for the system with *S. stipitis*. For cell density, five different OD_{600} were studied, which are 0, 1.5, 3.0, 4.5, and 10.0. For agitation speed, three conditions were studied, which are 250, 350, and 450 rpm. The results are shown in Figure 3.4 where Figure 3.4(a) shows the estimated parameters obtained from the model as a function of agitation speed for OD_{600}=3.0, and Figure 3.4(b) shows the estimated parameters obtained from the model as a function of OD_{600} for the agitation speed of 350rpm. From Figure 3.4(a), it can be seen that both k_La and kGa' increase with increasing agitation speed due to the increase of interfacial area of bubble-liquid and headspace-liquid, with k_La increases much faster than k_Ga'; while OUR* decreases with increasing agitation speed, which can be explained by the physical blocking effect (Ju and Sundararajan, 1995). From Figure 3.4(b), it is observed that k_Ga' is not

affected by the cell density. This is expected because at the same agitation speed, the interfacial area between headspace and liquid phase is not affected by cell density, therefore $k_G a^{'}$ is not affected by cell density. In addition, OUR^{*} increases with cell concentration in a nonlinear fashion, which has been observed somewhere else (Garcia-Ochoa et al., 2010). Finally, with increasing cell density, $k_L a$ first increases and reaches a maximum then subsequently decreases. This phenomenon can be explained by the overall result of several mechanisms. At low cell density, the dominant factor that affects $k_L a$ is the surface renewal and modification of medium by the cells, which results in increased specific gas–liquid interfacial area and $k_L a$ (Ju and Sundararajan, 1995); while at high cell density, cells' blocking effect and absorption of cells to the bubble-liquid interface result in decreased specific interfacial area and less distribution of bubbles, therefore decreased $k_L a$ (Galaction et al., 2004; Martin et al., 2010).

3.1.4 Conclusions

In summary, the improved dynamic method is shown to be simple and effective in obtaining $k_L a$, in a faster and more accurate way than the classical dynamic method. It can utilize the desorption process alone to obtain estimates on $k_L a$, $k_G a$, and OUR. In addition, our experiments on *S. stipitis* confirm that the presence of microorganisms can affect $k_L a$ significantly, with enhanced $k_L a$ at low cell density, and reduced $k_L a$ at high cell density. It is worth noting that dynamic methods (both the classical one and the improved one) estimate OUR based on the mass balance of the liquid space (and head space), while measuring OUR through mass spectrometry monitoring systems adhere to performing a global mass balance. Therefore, depending on what is the rate limiting step (either OUR or OTR), the OUR obtained from the mass spec method could be the same or different from that obtained from the dynamic methods. When OTR is smaller than OUR, how much oxygen the cells can consume is limited by OTR and DO is

closed to 0. Under this condition, OUR obtained from the dynamic method would be large than the OUR obtained from mass spec, and the amount of the oxygen consumed by the cells should be calculated from OTR (i.e., via $k_L a$ and $k_G a^{'}$), instead of the measured OUR. If OTR is larger than OUR, DO will be larger than 0, then the OUR obtained from mass spec monitoring system and the dynamic method would be the same. Although a mass spec monitoring system always obtains the actual amount of oxygen that the cells consumed, it has its own limitations. For example, the instrumentation needs to be highly accurate, since the measurements of the inlet and outlet compositions usually are different only slightly in the case of low OUR, which is quite often. Also the mass spec method requires that the DO be constant in order to attain accurate results, where it was recommended to keep DO from changing ±0.05%. On the other hand, the limitation of the dynamic methods is that the physiochemical change of the media and physiological changes in the cells could be introduced because of the required perturbation.

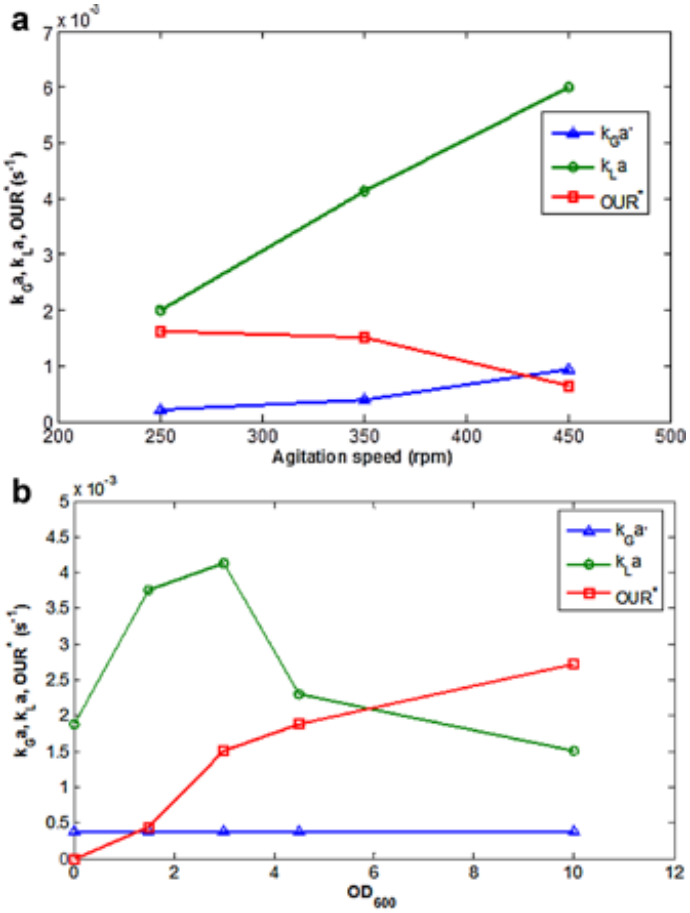

Figure 3.4 Effect of cell density and agitation speed on k_La, k_Ga', and OUR*: (a) effect of agitation speed at OD600=3.0; (b) effect of cell density at agitation speed of 350 rpm.

3.1.5 Precise control of oxygen supply

With the k_La measurement of *S. stipitis*, a precise control of oxygen supply is required in order to study the effects of OURs on xylose fermentation by *S. stipitis*. The efficient conversion of xylose to ethanol by *S. stipitis* is highly influenced by OUR and there exists an optimal OUR. Above the optimal OUR, carbon flows preferentially through the TCA which results in faster cell growth at the expense of ethanol production, while below optimal OUR, the imbalance of cofactors (NAD/NADH, NADP/NADPH) will result in the production of xylitol. Hence, a precise control of oxygen supply is important to maximize the ethanol production. However, a commercial gas mixing component come with the bioreactor does not provide a sufficient control as the

total gas flow rate changes when the ratio between air and nitrogen is adjusted. Hence, in order to achieve accurate and stable oxygen supply, we developed and tested a gas mixing apparatus by adding a buffer tank, which can deliver the desired stable feeding gas as shown in Figure 3.5. To achieve various stable oxygen supply rates, air has to be mixed with nitrogen to achieve desired oxygen compositions by maintaining constant total gas flow rate. Our results confirmed that the developed gas mixing apparatus was able to deliver the desired stable feeding gas which was also confirmed by GC measurements.

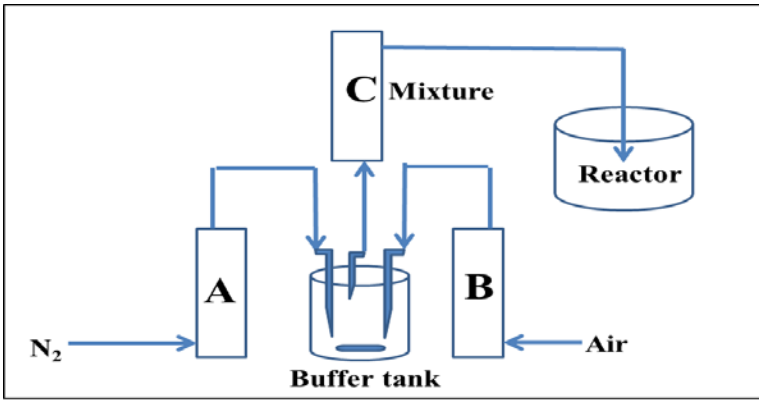

(a)

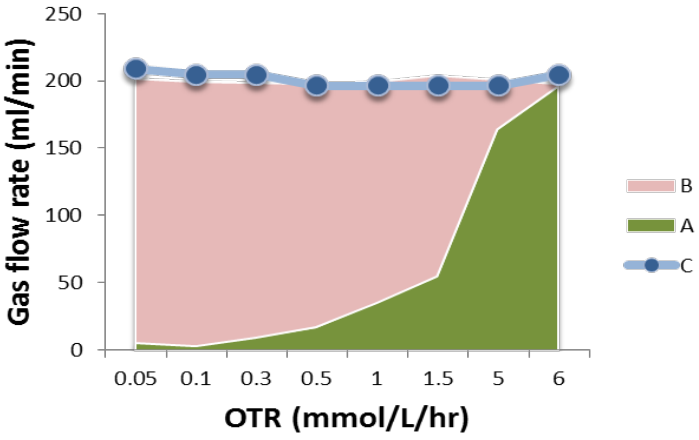

(b)

Figure 3.5 (a) The schematic diagram of gas mixing apparatus for control of oxygen supply; (b) overall flow rate of gas mixture vs. combined gas flow rates of air and nitrogen at different oxygenation levels

3.2 Cell Retention Module

3.2.1 Pseudo-continuous fermentation

In this work, we performed xylose fermentation by *S. stipitis* under a pseudo-continuous operation for both single culture and co-culture experiments. It is characterized by continuous nutrient feeding and continuous cell-free broth withdrawal, which can be implemented through installing a cell retention module (Figure 3.6) to filter out cells from effluent. The pseudo-continuous fermentation which operates with cell retention is not a new idea. It has been used in animal cell cultures called “perfusion” (Butler, 2005). This technique eliminates the washout of cells and culture dilution often occurs within the continuous operation, which severely limits high cell density culture and thus, total productivity. Because *S. stipitis* grows very slowly under oxygen-limiting conditions, “washout” often results under continuous operation.

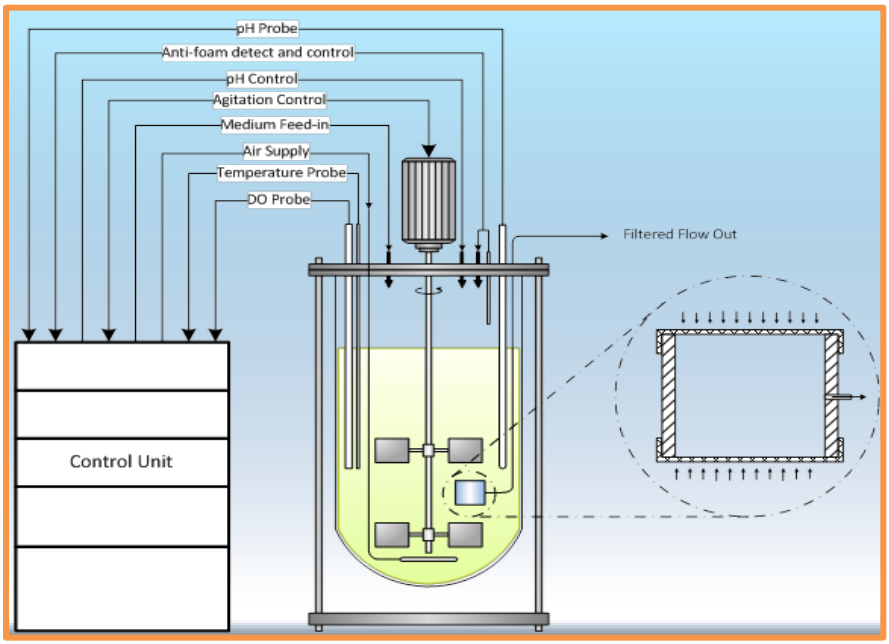

Figure 3.6 The cell retention module installed in a single culture system

The steady-state in our fermentation system can be defined as the state with a constant ethanol production rate under constant biomass production rate. With pseudo-continuous opera-

tion available, the biomass of *S. stipitis* can be controlled by the dual-mode operation, which combines pseudo-continuous operation for biomass accumulation and continuous operation for biomass maintaining or reducing based on dilution rates. One major concern about the pseudo-continuous fermentation is the performance of a cell retention module. The efficient retention of cells within the bioreactor using a cell retention module requires the continuous removal of accumulated cells on the filtration surface due to continuous withdrawal of fermentation broth. If this action is not taken place, the cells become clogged on the filtration surface to decrease and eventually block the outflow rate. To overcome this difficulty, the filtration surface of the module was located right against the propeller (Figure 3.7) to constantly clean through the shear stress generated by agitation, which allowed achieving sustained pseudo-continuous fermentation for more than three months.

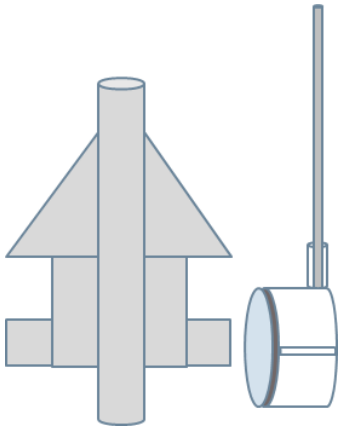

Figure 3.7 The design and position of developed cell retention module for co-culture system

The cell retention within the bioreactor is not only preventing cell washout, but it is also providing an effective way for cells to adapt to the surrounding environment. Microorganisms can adapt to environmental perturbations such as an increase in osmotic pressure, the accumulation of ethanol and carbon dioxide and a decrease in the amount of nutrients. Of these environmental changes, the accumulation of ethanol during cultivation causes the most stress to yeast

cells (Attfield, 1997). Adaptation of cells to environmental changes is achieved by alteration of the intracellular physiological conditions to the surrounding environment (Dinh et al., 2008). The pseudo-continuous operation reaches a pseudo steady-state while environmental pressure is being consistently applied, and gradually increases, which is an ideal case for cell adaptation. The adaptation of yeast under high ethanol concentration is important and leads to survival of the yeast strains that can grow well in high ethanol concentration. More detailed information on ethanol adaptation via pseudo-continuous fermentation can be found in Chapter 5.

3.3 Co-culture Bioreactor Development

One of major technical obstacles in conventional co-culture process is low ethanol yields associated with non-compatible optimal culture conditions between two strains due to the inefficient control of optimal oxygen condition required by each organism. In order to circumvent this problem, we came up with a new equipment to systematically study the co-culture system dynamics. For new equipment, we have developed a two-chambered co-culture bioreactor which enables the confinement of each organism so the effective control of optimal fermentative conditions and independent control and monitoring of each organism are possible. With the developed co-culture bioreactor, we were also able to conduct systematically designed experiments to investigate the dynamic properties of the co-culture system by manipulating different operating parameters, such as OUR, dilution rate, sugar concentration as well as inoculum concentration.

3.3.1 Major limitations in co-culture process

In order to develop an effective co-culture process to achieve simultaneous conversion of glucose and xylose to ethanol, following challenges needed to be addressed.

1) Non-compatible optimal culture conditions (i.e. optimal oxygen transfer rate) between two organisms.

2) Catabolite repression on xylose uptake by glucose: under continuous condition, glucose concentration must be sufficiently low not to repress xylose utilization by the xylose-fermenting yeast.
3) Difficult to monitor/control the biomass development of individual organism.
4) Low ethanol tolerance of xylose-fermenting microorganism.
5) About 80% of existing co-culture research is batch fermentation which limits ethanol productivity and the study of co-culture system systematically.
6) None of the continuous fermentation has achieved the complete consumption of both glucose and xylose, simultaneously.

3.3.2 Proposed co-culture system

A novel two-chambered co-culture bioreactor has been developed to address the identified challenges associated with the conventional co-culture bioreactor system. The schematic diagram and actual set-up of developed bioreactor for co-culture study are shown in Figure 3.8(a). This configured co-culture system enables not only confinement of each strain to each chamber, but also exchange of culture medium and extracellular metabolites between the two chambers through membrane. The two-chambered bioreactor has been constructed by placing a microporous filter membrane (0.45μm pore size, Biodyne plus, Pall Corporation) between two chambers to separate two strains. This configuration enables us to maintain different oxygenation conditions for both strains by adjusting nitrogen and air flow rates into each chamber, independently. The propellers of the agitators are driven by an external magnetic field and the pH and temperature controllers are implemented to control the co-culture system, effectively. In addition to this reactor design, an innovative fermentation scheme, pseudo-continuous fermentation (i.e. continuous fermentation with cell retention), was proposed in the co-culture system.

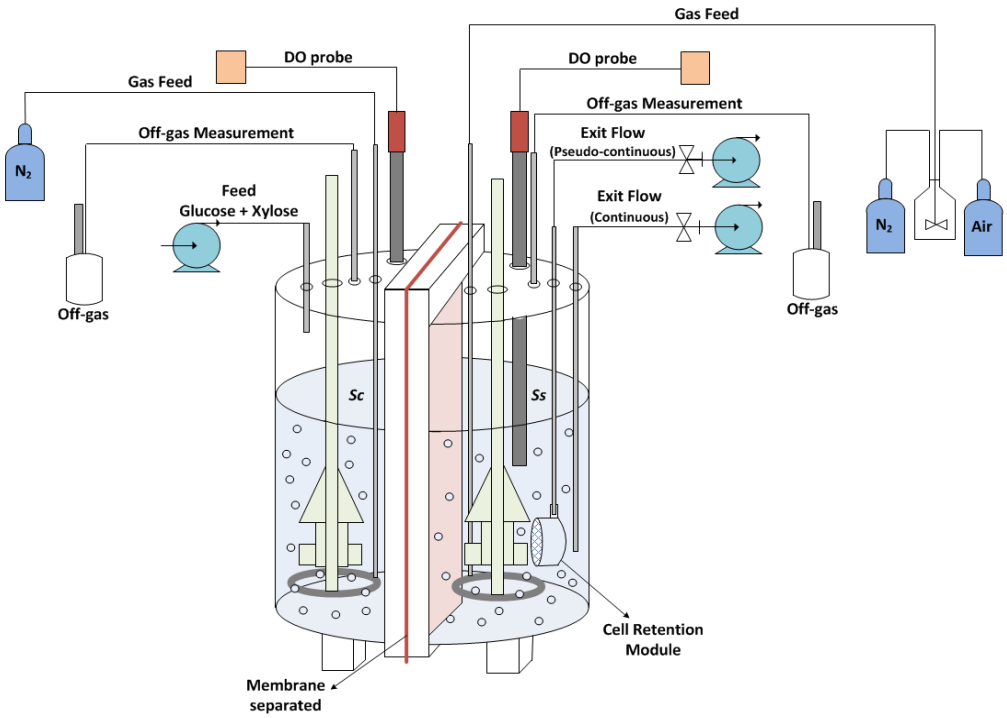

(a)

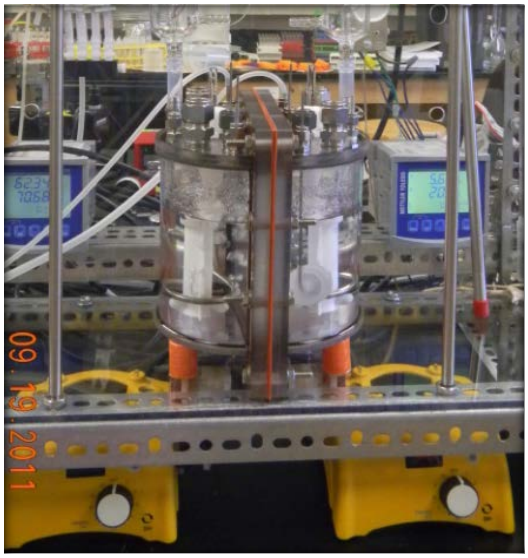

(b)

Figure 3.8 (a) The schematic diagram of co-culture system; (b) Actual set-up of the developed bioreactor for proposed co-culture system

3.3.3 Advantages of novel co-culture bioreactor

There are several benefits associated with our co-culture bioreactor design along with pseudo-continuous fermentation.

1) Membrane-separated two-chamber bioreactor
    - Different oxygen requirements for both stains can be fulfilled by separate control of the gas supply to each chamber.
    - The changes of cell population for both strains can be monitored individually.
    - Continuous removal of cellular wastes and other inhibitors while retaining cells in the reactor.
    - Allow the wide range of feasible operations to study the dynamic properties of co-culture system effectively.
2) Pseudo-continuous fermentation
    - Prevent catabolite repression on *S. stipitis* and enable the complete consumption of glucose and xylose simultaneously. With cell retention, dilution rate can be easily adjusted to maintain the glucose concentration at a very low level to ensure that *S. stipitis* consumes only xylose.
    - Provide an ideal environment for cell adaptation by tolerating cells with high ethanol concentration which improves the ethanol tolerance of both organisms, especially for *S. stipitis*.
    - Prevent frequent cell washout associated with slow growth of *S. stipitis* during fermentation.

3.3.4 Construction of co-culture bioreactor

In the development of the two-chambered co-culture bioreactor, we have tested and modified/improved the different features of the bioreactor to address the following practical aspects of bioreactor operation. These are sterilization, agitation, air distribution, temperature and pH controls, sampling, cell retention module, exhaust gas cooling and etc. The major features of the co-culture bioreactor are summarized as below.

3.3.4.1 Co-culture bioreactor material selection and construction

The bioreactor is originally constructed from transparent PVC material. This material is very easy to work with, but cannot stand for autoclave sterilization conditions which deforms and changes the color of material from transparent to opaque. After this observation, we have switched the plastic material to polycarbonate material, which can stand for the autoclave sterilization conditions since it is a thermoplastic polymer plastic. One major limitation of this material is that the difficulty in gluing different parts of the bioreactor together due to the high chemical resistance characteristics of the polycarbonate material. With extensive research, high temperature epoxy (EPO-TEK) was selected as an adhesive to glue/assemble the different parts of the bioreactor. We have developed the appropriate annealing process (pre- and post-annealing) for polycarbonate and curing process for epoxy and successfully built a two-chambered bioreactor with polycarbonate material as shown in Figure 3.9.

However, the cured epoxy material cannot stand for more than one or two cycles of autoclave process, and then the reactor starts to leak. In the humid environment of autoclave sterilization, the steam (heat and moisture) plays a significant role in diminishing the strength of the bond formed by the epoxy, which resulted in material deterioration. We have modified the design of the bioreactor (adding the trenches of the joint parts) and tested various conditions for

curing time and temperature to better facilitate the epoxy bonding process. However, it could not successfully pass the tests for leakage and autoclave. After extensive research and tests, we have found solvent cement (Weld-On, IPS Corp.), which can provide the strength of joint parts of the bioreactor, effectively. Heating and steam can cause bubbling in the solvent area as the solvent leaves the surface but once the solvent cured completely, the effect could be minimized. Since the solvent cement can only be used for structuring the bioreactor, not for sealing purpose, silicone gel was applied on the top of cured solvent cement to provide the sealing of the bioreactor. With the solvent cement along with silicone gel (Figure 3.10) provided the solution to solve both leakage and sterilization problems. However, the silicone gel cannot stand more than one cycle of autoclave sterilization so the reapplication of silicone gel is required for new experimental run. The process of removing and reapplying silicone gel is not easy and can easily lead to mistakes. With the suggestion from other colleague, we found a sterilizable epoxy (Resbond S5H13, Cotronics Corp.) which can withstand repeated sterilization cycles and can be used for both structuring and sealing (Figure 3.11).

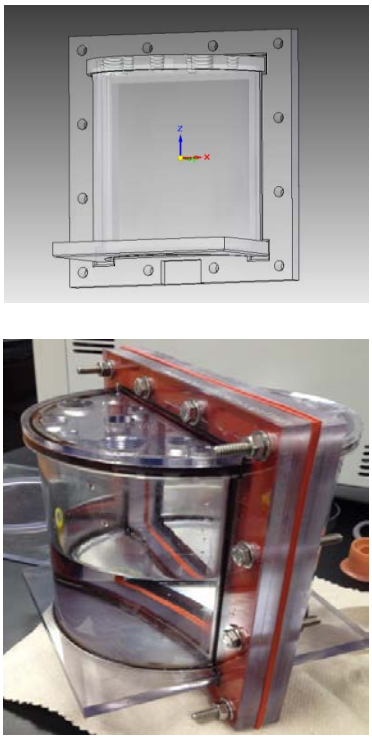

Figure 3.9 The design plot and the assembly of high temperature epoxy glued two-chambered bioreactor

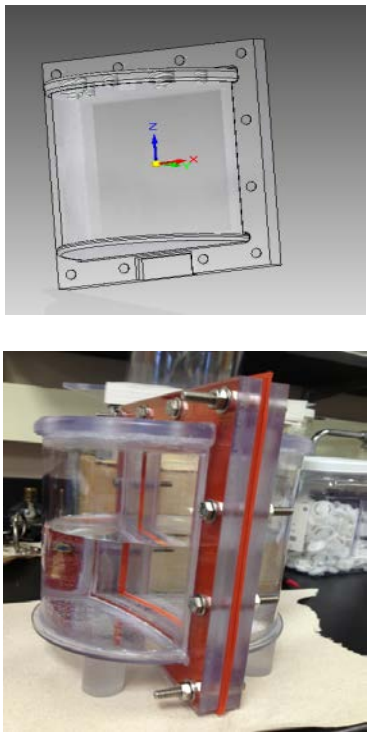

Figure 3.10 The design plot and the assembly of combined solvent cement and silicone gel glued two-chambered bioreactor

Figure 3.11 The assembly of sterilizable epoxy glued two-chambered bioreactor

3.3.4.2 Co-culture bioreactor features

- **Agitation:** initially, the magnetic stirring bar driven by external magnetic field was used to agitate the system. However, this system provides very limited agitation and very limited air distribution as it stays at the bottom of the reactor. To address this problem, we modified the commercial system which uses propeller driven by external magnetic field to fit our purpose. The new agitation system provides effective agitation and air distribution as the propeller plays a significant role in shearing larger bubbles into smaller bubbles to increase the residence time of oxygen mass transfer.
- **Gas distribution/sparger:** gas distributor was modified from air stones to the stainless steel tube which is bent into circular shape with 5 holes drilled on the tube, which provides satisfactory air/nitrogen distribution along with the new agitation system.
- **Sampling:** for easy sampling without introducing any contamination, we developed an in-house made sampling device that is similar to the commercial one, which is made with centrifuge tubes. In this way, we can accurately and directly measure the

sample volume at the time of the sampling. Also it enables easy replacement of the sterile sampling tube for each sampling.

- **Exhaust gas cooling:** cooling system was developed in order to prevent the blockage of the exhaust gas filter. Previously, we have experienced the blockage due to the build-up of the vapors in the filter. To address this difficulty, the exhaust gas port was connected to the condenser along with the cooling water system (water re-circulation system). In addition, the exhaust cooling system prevents the ethanol evaporation as the exhaust gas carries ethanol vapors with it. The exhaust gas flows through a condenser can prevent the ethanol evaporation as the ethanol vapors condense and fall back into the reactor.
- **Off-gas oxygen measurement:** DO probe was installed in off-gas collect bottle to measure the DO of inlet and outlet of off-gas from each chamber.
- **Cell retention module:** previous design of the developed cell retention module (in-house) was difficult to bind membranes to the ends of the rigid plastic tube which caused a leakage due to its tight bindings. In the new design, the cell retention module was built based on the design of commercial filtration system. Modifications were made to reduce the dead space of membrane surface to prevent cell accumulation and by adding a membrane support screen to prevent the breakage of the membrane. Different designs of cell retention modules based on above modifications and different types of membranes were tested with cell broth to observe the performance of module and membrane (Figure 3.12). A vertically positioned cell retention module with facing towards the propeller performed the best and was selected as a final design. The membrane selection was done by testing and comparing different types (i.e. pore size

(0.8μm), thickness, material types) of filter membranes for the outflow rate performance and flow stability over extended period. Supor 800 (Pall Corporation) performed the best among tested membranes due to its superior material type and high water flow rate property.

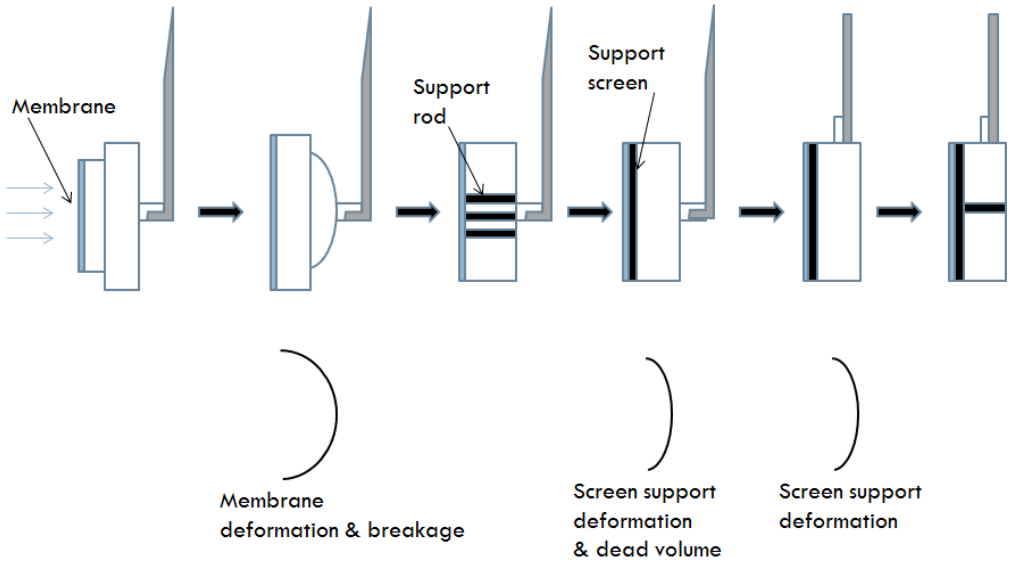

Figure 3.12 The process of development of cell retention module

- **Temperature control:** due to the special design of the co-culture bioreactor, the commercial temperature control system was not fitted for our co-culture system. So, we developed a temperature control system by using the heating bands and a commercial PID controller to control the reactor temperature, uniformly. From the test, it confirms that the reactor temperature can be maintained within ± 1.5 ^{o}C of variation of target temperature.

Chapter 4. Mathematical Modeling Work

4.1 Introduction

Mathematical models of the cellular metabolism have drawn special interest in biotechnology as a tool for understanding the cellular metabolism and physiology. There are two main approaches to mathematical models of biological data based on their structure. Stoichiometric models (metabolic network models) are based on the time invariant characteristics of metabolic networks. Kinetic models are usually based on both stoichiometry and enzyme or microbial kinetics (Gombert and Nielsen, 2000).

However, control and operation of fermentation processes have become a complex task due to the biological nature of the system, its multicomponent character, and the oscillatory behavior of fermentation. The formulation of proper models for the description of biological processes during ethanol production is crucial to optimize the continuous fermentation process to define the optimal cultivation conditions for increasing productivity and conversion of sugars into ethanol. Many studies carried out at laboratory scale for the improvement of bioethanol production processes have been simulated using mathematical models. The unstructured models are frequently used during the control of fermentation processes to describe the dynamic behaviors of the fermentation system.

4.2 Kinetic Model Development

The mathematical models for estimating the dynamic behavior of ethanol production from co-culture system and single culture system are constructed. The parameters of the model were estimated from the experimental data in the medium containing glucose and xylose (co-culture) or xylose alone (single culture) in continuous/pseudo-continuous fermentation. The calculated values form the models corresponded satisfactorily with experimental data, such as cell growth, substrate consumption, ethanol, xylitol, glycerol, and acetic acid productions, especially in the estimation of the specific rates. The developed model allows us to estimate ethanol produced from each strain as well as to investigate the effects of different model parameters on the overall secretion of different products and byproducts. The developed model was validated by independent testing data sets, which shows satisfactory agreement with the experimental data.

4.2.1 Single culture kinetic model

Single culture kinetic model consists of five differential equations which includes cell growth, xylose consumption, ethanol production, xylitol production and acetic acid production. The model equations listed in Table 4.1 represent the dominant kinetic features of *S. stipitis*. The notation and subscripts of model parameters are described in Table 4.2. The single culture kinetic model was developed based on mass balance. The kinetic equations are formulated based on the mass balance of the continuous culture operation as below.

$$In + Product = Out + Accumulation - Consumption \tag{4.1}$$

The cell growth equation in the model, control parameter of operational mode, $OptMod$ was added to accurately estimate the specific growth rate of *S. stipitis,* which can be controlled by continuous or pseudo-continuous operation mode. Hence, in batch or pseudo-continuous operation, $OptMod = 0$ and the equation becomes;

$$\frac{dX_S}{dt} = \mu_S X_S \tag{4.2}$$

For continuous operation, $OptMod = 1$ and the equation becomes;

$$\frac{dX_S}{dt} = \mu_S X_S - \frac{F_{OS} * OptMod}{V} X_S \tag{4.3}$$

For cell growth equation, kinetics of ethanol inhibition and oxygen uptake on cell growth were not included. This is because the ethanol concentration accumulated from *S. stipitis* was not critical level for inhibition and the oxygen uptake rates tested in the experiment were very low. Xylose uptake rate equation can be expressed by combining the amount of xylose fed into the system, $\frac{F_{OS}}{V} Z_{in}$ and the amount of xylose carried out from the system, $\frac{F_{OS}}{V} Z_S$ and amount of xylose accumulated in the system, $v_{ZS} X_s$. The product and byproducts production rates were determined by considering the product carried out by dilution and the accumulation.

Table 4.1 Developed single culture kinetic model

Components	**Equations**
Cell Growth	$\frac{dX_S}{dt} = \mu_S X_S - \frac{F_{OS} * OptMod}{V} X_S$ $\mu_S = \beta(1) + \frac{F_{OS} * OptMod}{V}$ $X_{SO} = exp(\beta(2))$
Xylose	$\frac{dZ_S}{dt} = \frac{F_{OS}}{V}(Z_{in} - Z_S) - v_{ZS} X_S$ $v_{ZS} = \frac{1}{X_S}[\frac{F_{OS}}{V}(Z_{in} - Z_S) - \frac{dZ_S}{dt}]$
Ethanol	$\frac{dE_S}{dt} = -\frac{F_{OS}}{V}(E_S) + v_{ES} X_S$ $v_{ES} = \frac{1}{X_S}[\frac{dE_S}{dt} + \frac{F_{OS}}{V}(E_S)]$
Xylitol	$\frac{dT_S}{dt} = -\frac{F_{OS}}{V}(T_S) + v_{TS} X_S$

	$v_{TS} = \frac{1}{X_S}[\frac{dT_S}{dt} + \frac{F_{OS}}{V}(T_S)]$
Acetic Acid	$\frac{dA_S}{dt} = -\frac{F_{OS}}{V}(A_S) + v_{AS}X_S$ $v_{AS} = \frac{1}{X_S}[\frac{dA_S}{dt} + \frac{F_{OS}}{V}(A_S)]$

Table 4.2 Notation and subscripts of model parameters

Notation	
μ	Specific growth rate (hr^{-1})
$\boldsymbol{X}$	Cell concentration (g/L)
$\boldsymbol{Z}$	Xylose concentration (g/L)
$\boldsymbol{E}$	Ethanol concentration (g/L)
$\boldsymbol{T}$	Xylitol concentration (g/L)
$\boldsymbol{R}$	Glycerol concentration (g/L)
$\boldsymbol{A}$	Acetic acid concentration (g/L)
$\boldsymbol{F}$	Flow rate (L/hr)
$\boldsymbol{D}$	Diffusion coefficient (hr^{-1})
$\boldsymbol{OptMod}$	Operation mode (0: pseudo-continuous, 1: continuous)
$\boldsymbol{\beta}$	Constant
$\boldsymbol{V}$	Total liquid volume (L)
$\boldsymbol{v_Z}$	Specific xylose consumption rate (g/gDCW/hr)
$\boldsymbol{v_E}$	Specific ethanol production rate (g/gDCW/hr)
$\boldsymbol{v_T}$	Specific xylitol production rate (g/gDCW/hr)
$\boldsymbol{v_A}$	Specific acetic acid production rate (g/gDCW/hr)
$\boldsymbol{v_R}$	Specific glycerol production rate (g/gDCW/hr)
Subscripts	
$\boldsymbol{C}$	*S. cerevisiae*
$\boldsymbol{S}$	*S. stipitis*
$\boldsymbol{O}$	Out (outflow)
$\boldsymbol{in}$	In (feed in)
$\boldsymbol{0}$	Initial

4.2.2 Co-culture kinetic model

Co-culture kinetic model (Table 4.3) was developed based on the single culture model with addition of *S. cerevisiae* kinetics and diffusion coefficients. The detailed derivation of co-culture model equations is presented in Appendix A. The diffusion coefficients accounted in this co-culture model describes the diffusion of each metabolite (xylose, ethanol, xylitol, glycerol and

acetic acid) across the membrane. The diffusion coefficients of each metabolite across the membrane at different operational conditions were determined by the experiment. The experiment was carried out using used membrane and new membrane at two different dilution rates with fixed agitation speed and total gas flow rate (same set-up as co-culture experimental run). Feed medium used in this experiment contained different concentrations of metabolites and the concentration of each metabolite was measured from each chamber at every 30min for 10hr. The concentration change profiles of ethanol for both used and new membranes are illustrated in Figure 4.1 and the estimated diffusion coefficients at different dilution rates for used and new membranes are presented in Table 4.4. The equations were formulated based on the mass balance of continuous operation of our developed co-culture system.

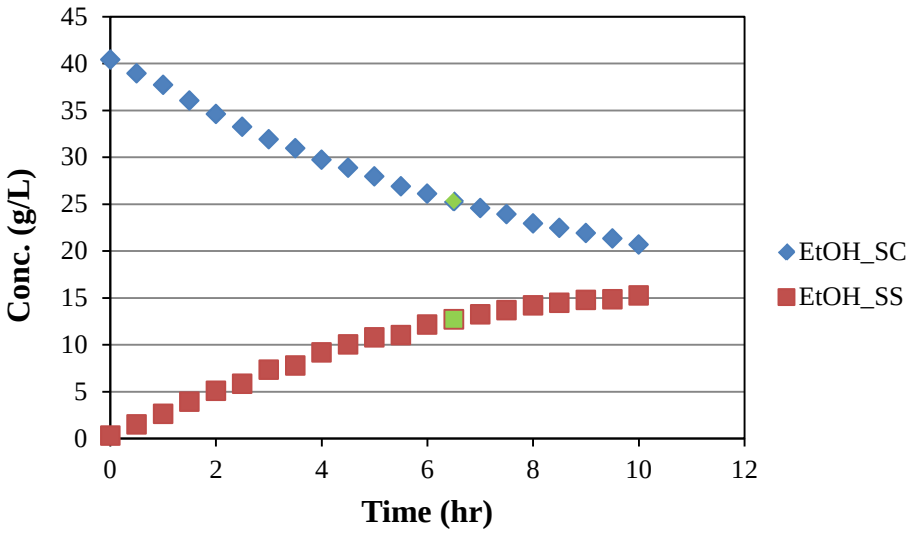

(a)

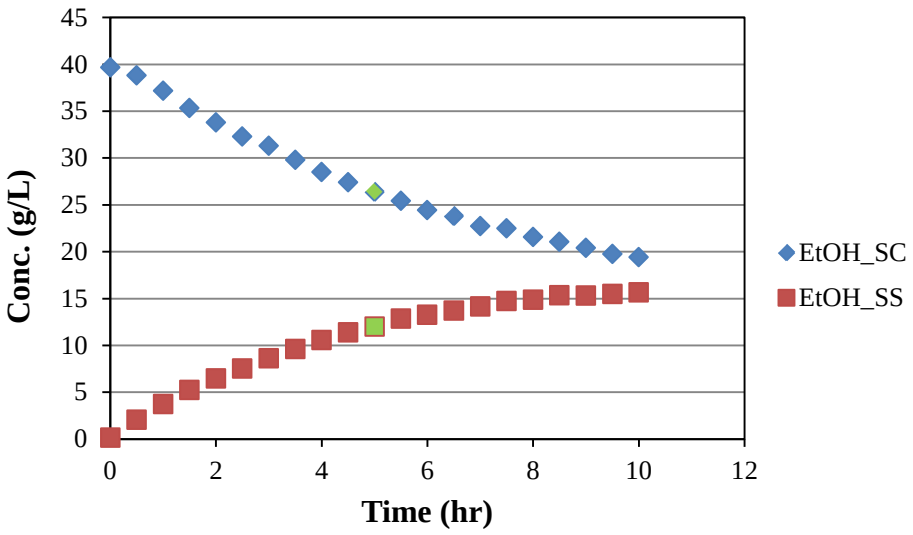

(b)

Figure 4.1The concentration change profile of ethanol across the membrane using (a) used membrane; (b) new membrane

Table 4.3 Developed co-culture kinetic model

Components	**Equations**	
	S. cerevisiae	***S. stipitis***
Cell growth	$\frac{dX_C}{dt} = \mu_C X_C - \frac{F_{OC} * OptMod_C}{V/2} X_C$ $\mu_C = \beta(1) + \frac{F_{oc} * OptMod_C}{V/2}$ $X_{CO} = exp\,(\beta(2))$	$\frac{dX_S}{dt} = \mu_S X_S - \frac{F_{OS} * OptMod_S}{V/2} X_S$ $\mu_S = \beta(1) + \frac{F_{OS} * OptMod_S}{V/2}$ $X_{SO} = exp\,(\beta(2))$
Xylose	$\frac{dZ_C}{dt} = \frac{F_{In}}{V/2}(Z_{In} - Z_C) - v_{ZC}X_C - D_Z\,(Z_C - Z_S)$ $v_{ZC} = \frac{1}{X_C}[\frac{F_{In}}{V/2}(Z_{In} - Z_C) - D_Z(Z_C - Z_S) - \frac{dZ_C}{dt}]$	$\frac{dZ_S}{dt} = \frac{F_{OS}}{V/2}(Z_C - Z_S) - v_{ZS}X_S + D_Z\,(Z_C - Z_S)$ $v_{ZS} = \frac{1}{X_S}[(Z_C - Z_S)(\frac{F_{OS}}{V/2} + D_Z) - \frac{dZ_S}{dt}]$
Ethanol	$\frac{dE_C}{dt} = \frac{F_{In}}{V/2}(-E_C) + v_{EC}X_C - D_E\,(E_C - E_S)$ $v_{EC} = \frac{1}{X_C}[\frac{F_{In}}{V/2}(E_C) + D_E(E_C - E_S) + \frac{dE_C}{dt}$	$\frac{dE_S}{dt} = \frac{F_{OS}}{V/2}(E_C - E_S) + v_{ES}X_S + D_E\,(E_C - E_S)$ $v_{ES} = \frac{1}{X_S}[-(E_C - E_S)(\frac{F_{OS}}{V/2} + D_E) + \frac{dE_S}{dt}]$

Xylitol	$\frac{dE_S}{dt} = \frac{F_{OS}}{V/2}(E_C - E_S) + v_{ES}X_S + D_E\,(E_C - E_S)$ $v_{ES} = \frac{1}{X_S}[-(E_C - E_S)(\frac{F_{OS}}{V/2} + D_E) + \frac{dE_S}{dt}]$	$\frac{dT_S}{dt} = \frac{F_{OS}}{V/2}(T_C - T_S) + v_{TS}X_S + D_T\,(T_C - T_S)$ $v_{TS} = \frac{1}{X_S}[-(T_C - T_S)(\frac{F_{OS}}{V/2} + D_T) + \frac{dT_S}{dt}]$
Glycerol	$\frac{dR_C}{dt} = \frac{F_{In}}{V/2}(-R_C) + v_{RC}X_C - D_R\,(R_C - R_S)$ $v_{RC} = \frac{1}{X_C}[\frac{F_{In}}{V/2}(R_C) + D_R(R_C - R_S) + \frac{dR_C}{dt}]$	$\frac{dR_S}{dt} = \frac{F_{OS}}{V/2}(R_C - R_S) + v_{RS}X_S + D_R\,(R_C - R_S)$ $v_{RS} = \frac{1}{X_S}[-(R_C - R_S)(\frac{F_{OS}}{V/2} + D_R) + \frac{dR_S}{dt}]$
Acetic acid	$\frac{dA_C}{dt} = \frac{F_{In}}{V/2}(-A_C) + v_{AC}X_C - D_A\,(A_C - A_S)$ $v_{AC} = \frac{1}{X_C}[\frac{F_{In}}{V/2}(A_C) + D_A(A_C - A_S) + \frac{dA_C}{dt}]$	$\frac{dA_S}{dt} = \frac{F_{OS}}{V/2}(A_C - A_S) + v_{AS}X_S + D_A\,(A_C - A_S)$ $v_{AS} = \frac{1}{X_S}[-(A_C - A_S)(\frac{F_{OS}}{V/2} + D_A) + \frac{dA_S}{dt}]$

Table 4.4 Estimated diffusion coefficients at different operational conditions

Diffusion coefficient (hr^{-1})	**Used Membrane**		**New Membrane**	
	2rpm	**4rpm**	**2rpm**	**4rpm**
D_E	0.1132	0.1591	0.1130	0.1913
D_A	0.0935	0.1340	0.0951	0.1775
D_R	0.0654	0.0787	0.0719	0.0840
D_Z	0.0588	0.0754	0.0574	0.0971
D_T	0.0588	0.0734	0.0525	0.0981

4.3 Principal Component Analysis (PCA)

The PCA is a multivariate statistical tool to extract knowledge from the high dimensional data generated from the experiment. The analysis of phenotypes on *S. stipitis* by PCA allows the evaluation of cellular processes at greater depth with providing the physiological and biological backgrounds of *S. stipitis*. The PCA analysis is a commonly used for dimension reduction in multivariate analysis method, which extracts the directions corresponding to the largest variations among different variables in a high dimensional data set (Jolliffe, 2002). It also applied in the metabolomics studies to analyze the profiles of metabolites at given conditions (Griffin,

2004). In this study, PCA was applied to *S. stipitis* to extract the key metabolism of how different oxygen uptake and carbon uptake rates would cause metabolism shifts on *S. stipitis*.

4.3.1 Phenotype identification by PCA

PCA can be applied to identify different phenotypes of *S. stipitis* under different OUR conditions. The example of phenotypes identification under different OUR conditions along with phenotype phase plane (PhPP) analysis is demonstrated in Figure 4.2 (Liang et al., 2014). The identified phenotypes can be characterized as in Table 4.5. As shown in Figure 4.2 (a), scores corresponding to the first two PCs are plotted and a total of six phenotypes of metabolism are identified. One phenotype is distinguished from another phenotype when the correlation among fluxes has changed, which is shown on the PCA score plot as two different straight lines, each represents a distinctive correlation among fluxes. Each different phenotype can be characterized to reveal the metabolic products of *S. stipitis* (cell mass, ethanol, xylitol, acetic acid). The biological knowledge embedded in the experimental data can be extracted through the PCA. Under the same phenotype, the variations among different reactions can be completely captured by the loading of a single PC. The result from PhPP (Figure 4.2(b)) also identified six phenotypes.

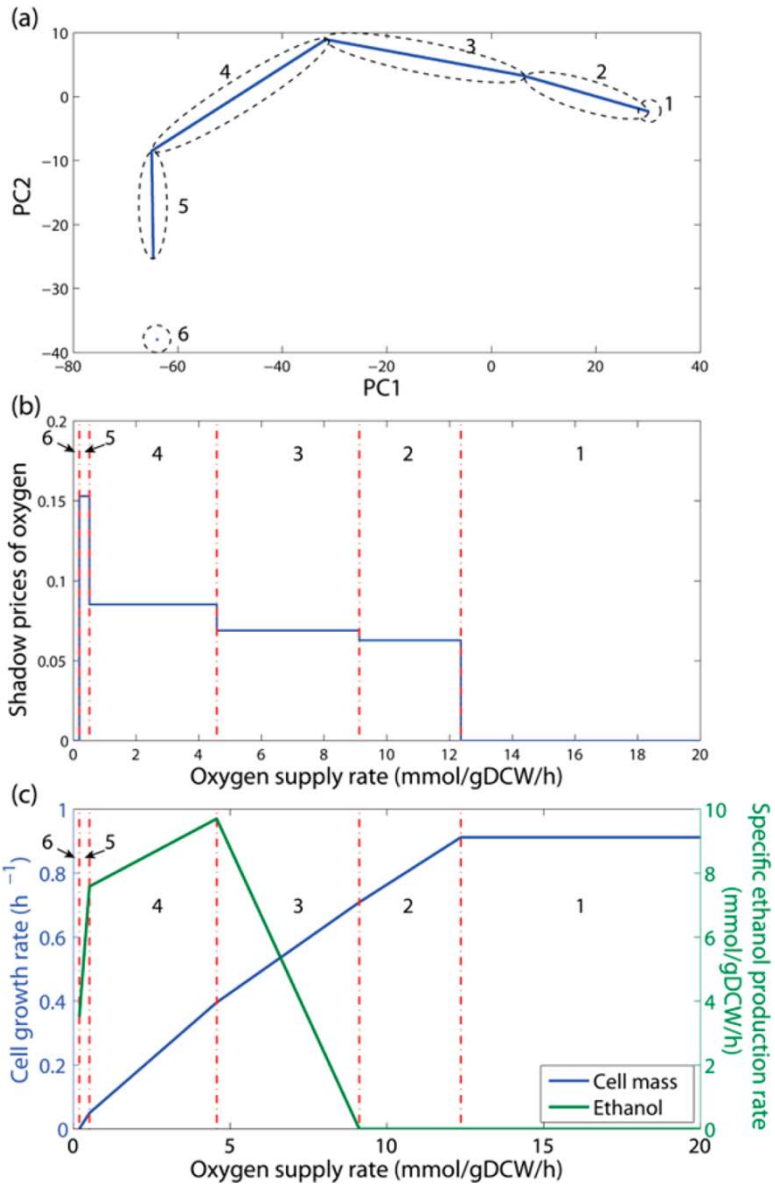

Figure 4.2 Phenotypes identified with PCA when OUR changes within [0,20] mmol/gDCW/hr (a) phenotypes identified by PCA; (b) phenotypes identified by PhPP; (c) model predicted cell growth rates and specific ethanol production rates (Liang et al., 2014)

Table 4.5 Summary of characteristics of identified phenotypes (Liang et al., 2014)

Phenotype	**Growth limitation**	**Metabolic product(s)**	**Main metabolic characteristics**
1	Xylose	Cell mass	Aerobic growth
2	Xylose, Oxygen	Cell mass, acetic acid	Increased acetic acid production
3	Xylose, Oxygen	Cell mass, ethanol, acetic acid	Ethanol production and declined acetic acid production
4	Xylose, Oxygen	Cell mass, ethanol, xylitol	Declined ethanol production and increased xylitol production
5	Oxygen	Cell mass	Declined ethanol and xylitol production
6	-	-	Cannot maintain metabolism (no growth)

Chapter 5. Single Culture Study

5.1 Introduction

Complete substrate utilization of glucose and xylose is one of the prerequisites for rendering lignocellulosic ethanol processes economically competitive. While ethanolic fermentation of hexoses derived from cellulosic biomass, i.e., glucose, mannose and galactose, using baker's yeast *S. cerevisiae* is well established on large scale, the conversion of the pentoses (e.g., xylose and arabinose) to ethanol is still one of the major barriers to industrializing the production of lignocellulosic ethanol. This is because the ethanol production from xylose by native *S. stipitis* requires controlling oxygen supply to maximize ethanol production. High aeration rate results in fast cell growth and acetic acid production, while very low aeration (oxygen-limited) often results in xylitol production, both at the expense of reduced ethanol production. Only optimized microaerobic condition promotes ethanol production by maintaining cell viability and NADH balance. Hence, it is critical to determine the optimal oxygen utilization rate (OUR) for ethanol production by *S. stipitis*.

In order to quantitatively study the effect of OUR on the xylose fermentation performance, we studied the dynamics of *S. stipitis* in response to accurate control of OUR. Several studies have been reported on the optimum oxygenation conditions for ethanol fermentation by *S. stipitis* (Table 5.1). Among these studies, most of the experiments were carried out using batch cultures grown in flasks where the Oxygen Transfer Rate (OTR) and/or Dissolved Oxygen (DO) were not effectively controlled. Different OTR levels have been tested simply by changing volume of media, airflow rate, and agitation speed. However, our research showed that the inaccu-

rate control of OTR/OUR is problematic in these studies. In addition, our research indicated that the optimum OUR alone (i.e., without information on carbon utilization) does not correlate well with ethanol yield. Our research showed that with the same OUR condition tested under controlled chemostat, the ethanol yield changed due to the change of metabolic status or phenotypes of *S. stipitis*. Different phenotypes exist under a single OUR condition, which was verified by Principal Component Analysis (PCA) which enables the extraction of correlations between different cellular physiology with respect to carbon uptake and OUR. This helps us understand and quantify the metabolic mechanism of OUR in continuous fermentation.

Table 5.1 Reported OTR/OUR for xylose fermentation by *S. stipitis*

Literature	**Strain**	**Culture medium**	**OTR/OUR meas. method**	**Operation**	**Optimal OTR/OUR**	**Max. ethanol yield**
(Su et al., 2014)	*S. stipitis* NRRL Y-7124 (CBS5773)	MS medium (modified Slininger et al., 2006) =>	OTR: sulfite-oxidation method, controlled by medium vol. and agitation speed	Batch (flask)	OTR=2.5 to 4.7mmol O_2/L/hr	~0.39
(Slininger et al., 2014)	*S. stipitis* NRRL Y-7124	Complex medium (CCY medium: yeast extract, urea, mineral salts, potassium phosphate buffer)	k_La: method by (Slininger et al., 1991) OTR: Ingold polarographic oxygen electrode, controlled by aeration rate and agitation speed	Batch (fermentor)	k_La=2.4 to 6.0 hr^{-1}	0.34
(Silva et al., 2012)	*S. stipitis* NRRL Y-7124	Nutrient medium (Urea, Yeast extract, $MgSO_4 7H_2O$, xylose)	k_La: method by (Stanbury et al., 2013)	Batch (flask)	k_La=2.3 to 4.9 hr^{-1} (OTR=0.55 to 1.17mmolO_2/L/hr)	~0.29
(Silva et al., 2011)	*S. stipitis* NRRL Y-7124	Complex medium	k_La: static method	Batch (fermentor)	DO=0 for all tested oxygenation levels	N/R
(Silva et al., 2010)	*S. stipitis* NRRL Y-	Rice straw hemicellulosic hy-	V_{flask}/V_{medium} ratio, agitation	Batch (flask)	V_{flask}/V_{medium} ratio=2.5	0.37

	7124	drolysate			@200rpm	
(Unrean and Nguyen, 2012)	*S. stipitis* BCC15191	Minimal medium (YNB, $(NH_4)_2SO_4$, glucose, xylose)	k_La: unsteady state method by (Shuler and Kargi, 2002) OTR: aeration rate (vvm) was controlled by air mix controller	Batch (fermentor)	OTR=1.8 mmol O_2/L/hr (0.1vvm)	0.40
(Yablochkova et al., 2004)	*S. stipitis* Y-2160	Standard nutrient medium containing 2% D-xylose	k_La: colorimetric method with sulfite	Batch (flask)	OTR=5mmol O_2/L/hr	0.25
(Sanchez et al., 2002)	*S. stipitis* ATCC 58376	Complex medium (yeast extract, peptone, glucose, xylose)	k_La: dynamic gassing out method	Batch (Magnetically-stirred fermentor)	k_La=2.9hr^{-1}	0.42 (20G/5X) 0.47 (24G/1X)
(Nigam, 2001)	*S. stipitis* NRRL Y-7124	HSSL (hardwood spent sulfite liquor) medium, Synthetic medium	OTR: sulfite oxidation method, controlled by agitation rate and air sparging velocity	Batch (flask)	OTR=2.0mmol O_2/L/hr	0.41
(Taniguchi, 1997)	*S. stipitis* NRRL Y-7124	Complex medium (CCY medium)	k_La: sulfite oxidation method OTR: Ingold O_2 probe OUR=OTR controlled by agitation speed & cell conc.	Batch (fermentor)	OTR=18.7 mg O_2/L/hr	0.40
(Guebel et al., 1991)	*S. stipitis* NRRL Y-7124	Basal medium (Yeast extract)	OTR: sulfite oxidation method, controlled by ratios of media volume	Batch (flask)	OTR=5mmol O_2/L/hr	0.16
(Laplace et al., 1991)	*S. stipitis* NRRL Y-7124	Medium described by Parekh, 1986	OTR: off-gas analysis by GC	Batch (fermentor)	OTR=1.75 mmol O_2/L/hr	0.43
(Skoog and Hahn-Hägerdal, 1990)	*S. stipitis* CBS6054	Minimal medium (YNB w/ amino acids, K_2HPO_4, KH_2PO_4, xylose)	k_La: Modified sodium sulfite oxidation method	Continuous (fermentor)	Exceeds OTR detection limit (OTR< 1 mmol O_2/L/hr)	0.48
(Dellweg et al., 1989)	*S. stipitis* NRRL Y-7124	Complex medium (Yeast extract, KH_2PO_4, $(NH_4)_2HPO_4$, $MgSO_47H_2O$, D-glucose or D-xylose)	k_La: described by (Rizzi et al., 1989) OTR: controlled by agitation speed	Batch (fermentor)	OUR=3.75 mmol O_2/L/hr	0.39

(Delgenes et al., 1989)	*S. stipitis* NRRL Y-7124	Medium described by Slininger et al., 1982	DOT: monitored by oxygen analyzer with O_2 probe	Batch (fermentor)	OTR=0.7mmol O_2/L/hr	0.42
(Du Preez et al., 1989)	*S. stipitis* CBS7126	Complex medium	DOT: continuous monitor and control by polarographic electrode and digital oxygen meter OTR: control by agitation speed	Fed-batch (fermentor)	DOT=0	~0.35-0.4
(Rizzi et al., 1989)	*S. stipitis* NRRL Y-7124	Complex medium	Difference in % of O_2 and CO_2 between inlet and outlet gases with a paramagnetic oxygen analyzer and an infrared carbon dioxide analyzer	Batch (fermentor)	OTR=3.75 mmol O_2/L/hr	0.39

5.2 Materials and Methods

5.2.1 Microorganism and culture media

Scheffersomyces stipitis CBS 5773 was obtained from ATCC and maintained at 4^{o}C on YPX agar plate containing (per liter) 10g yeast extract, 20g peptone and 20g of xylose. For the culture media, the minimal medium was used for both pre-culture and fermentation which contained 20g xylose for pre-culture or 30g xylose for fermentation, 1.7g yeast nitrogen base without amino acids and ammonium sulfate and 2.27g urea. The xylose concentration of feed medium for continuous fermentation was varied based on the operational conditions.

5.2.2 Cultivation conditions

The pre-culture of *S. stipitis* was carried out in a rotary shaker (250rpm) at 30^{o}C in a 250 mL Erlenmeyer flask which contained 100mL of the pre-culture medium as defined above. The fermentation experiment was carried out in 3L BioFlo 115 fermentor (New Brunswick) with a working volume of 1.5L. The fermentative conditions used in this experiment were as follows.

The temperature was set at 25^{o}C, and pH was controlled to 5.0 with automatic addition of 1.0N NaOH or 1.0N H_2SO_4. The reason of using different temperatures for pre-culture growth and fermentative conditions was due to the difference in optimal temperatures of growth (30^{o}C) and ethanol tolerance (25^{o}C) for *S. stipitis*. Agitation speed was set to 400 rpm, and the total gas flow rate was fixed at 346 mL/min, but the air flow rate was varied based on the operational conditions. Experiment was conducted under excess amounts of xylose at all cultivation conditions.

5.2.3 Control of oxygen supply and monitoring of OUR

Different levels of oxygenation can be achieved by controlling the composition of the feeding gas into the system. Air/oxygen was mixed with nitrogen to achieve desired oxygen composition while maintaining constant total gas flow rate. The conventional feedback control module equipped with many commercial bioreactors is not sufficient to achieve stable OUR as it relies on the DO measurement to determine how much oxygen (air) to be fed into the system. For *S. stipitis*, once the cell density reaches 3gDCW/L, oxygen transfer becomes diffusion limited and the DO measurements closes to detection limits (stays at zero) which makes the conventional DO-based feedback control ineffective.

Hence, in order to achieve stable OUR condition, we used our developed gas-mixing apparatus which can deliver the desired stable oxygen concentration with stable total gas flow rate. The delivered gas composition was confirmed by GC measurements. In order to obtain accurate measurements of OUR, we monitored both the inlet gas and off gas oxygen concentration, and relied on the mass balance of oxygen to calculate OUR, which can be calculated by the difference in % of O_2 between inlet gas and off gas with a polarographic DO electrode from BioFlo 115.

5.2.4 Experimental procedure

5.2.4.1 Initial cell growth and fermentation

The experiment consisted of two stages: cell growth and fermentation. The purpose of cell growth stage was to achieve the desired cell density of *S. stipitis* for fermentation stage, while the fermentation stage allowed us to examine the effect of different OURs and carbon uptake on the fermentation performance. During cell growth stage, after inoculation of pre-cultured *S. stipitis*, cells grow under oxygen-limited condition (batch growth) by purging a mixture of air (141 mL/min) and nitrogen (205 mL/min) gas the fixed total flow rate of 346 mL/min at atmospheric pressure. Such oxygen condition allows relatively fast cell growth while promoted ethanol production, which adapts the cells to higher ethanol concentration for the fermentations stage. The fermentation stage was implemented through either pseudo-continuous (for biomass accumulation) or continuous operation (for biomass maintaining or reduction), depending on the cell growth rate under different operational conditions. The operation time of each mode depended on the cell growth rate, and the detailed estimation of the operation time for each mode can be found in Appendix.

Once the specific OUR of *S. stipitis* became low at ~0.05 due to increase of cell density, continuous operation and increase of aeration rate was achieved. Since specific OUR was directly related to cell density, once cell density increased, OUR decreased significantly. In order to obtain relatively constant OUR while increasing cell density, 3-step change of aeration rates were attained to prevent cells from dramatic change of OUR and the over secretion of acetic acid at high aeration rate. Once desired cell density of *S. stipitis* was reached, the fermentation began at the constant biomass concentration and desired OUR.

5.2.4.2 Control of constant biomass and OUR

It was necessary to maintain constant biomass density under each oxygen condition which allowed us to achieve stable OUR through maintaining stable oxygen supply. With the setup of cell retention module (Figure 5.1) within the bioreactor, dual operation (continuous/pseudo-continuous) mode (Figure 5.2) was implemented in this experiment. Pseudo-continuous operation (Liang et al., 2013) is characterized by continuous nutrient feeding and continuous cell-free broth withdrawal, which can be implemented through installing a cell retention module to filter out cells from effluent. The dual operation mode allows the easy maintenance of constant cell density and stable OUR under much wider oxygen conditions, particularly at lower OUR ranges which often results in wash-out with continuous operation.

Figure 5.1 Cell retention module equipped in the BioFlo 115 for single culture of *S. stipitis*

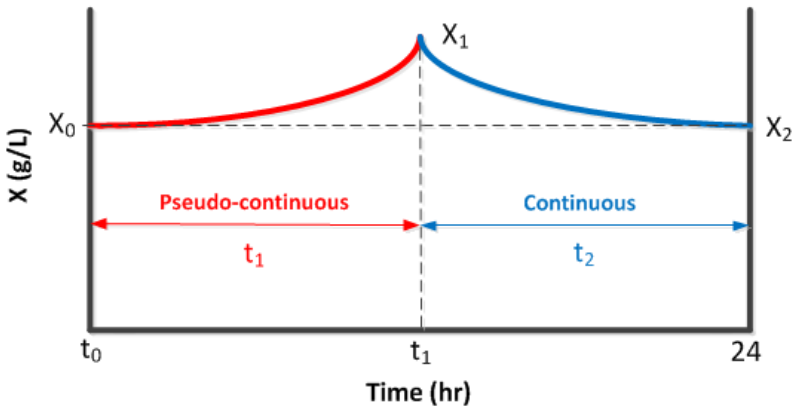

Figure 5.2 Illustration of dual operation mode

5.2.5 Analytical methods

The concentrations of xylose, xylitol, acetic acid, and ethanol were analyzed by Agilent 1200 series high performance liquid chromatography (HPLC) with UV/Vis and refractive index (RI) detector. They were analyzed on an Aminex HPX-87H column (Bio-Rad) at 45^{o}C with 0.05M H_2SO_4 solution as the mobile phase at a flow rate of 0.6mL/min. The run time of each sample was 25min. The concentration of carbon dioxide was measured using a SRI 8610C gas chromatography (GC) with thermal conductivity (TC) detector. They were analyzed on 3' Silica Gel column (column temperature: 105^{o}C) with helium as the carrier gas at 10psia at oven temperature of 80^{o}C. The cell density of each strain was measured turbidometrically at 600 nm. Fermentation broth was diluted according to the cell density using sterile DI water and then the turbidity of solution was measured by a UV/Vis spectrophotometer (Beckman Coulter).

5.2.6 Kinetic model of *S. stipitis*

The kinetic model of *S. stipitis* provides important physiological yeast properties and an important tool for optimizing operational conditions by evaluating model parameters under different OUR conditions. In this work, an unstructured kinetic model was developed to describe the continuous fermentation of xylose on *S. stipitis*. Our model focused on the kinetics of ethanol

production by *S. stipitis* on xylose with a development of a mathematical model considering the effect of OURs and carbon uptake rates. Kinetic parameters were obtained through a system of linear differential equations considering xylose, ethanol, xylitol, acetic acid and total biomass (Table 5.2). Data preprocessing was applied to minimize the data oscillations introduced by measurement error. The control parameter of operational mode change (see cell growth equation) was added to the cell growth equation, which influenced the estimation of cell growth rate.

The model was capable of describing cell, substrate, and ethanol concentrations along with byproducts (xylitol, acetic acid) concentrations during microaerobic fermentation. The model fitted parameters (specific consumption/production rates) were used to analyze the carbon balance and ethanol yields under different OUR conditions. The model equations listed in Table 4.1 represents the kinetic model of *S. stipitis* under continuous/pseudo-continuous fermentation.

5.3 Results and Discussion

5.3.1 Controlled chemostat

In order to quantitatively study the effects of OURs on the cell growth, ethanol production and byproducts secretion, maintaining stable OUR at different levels to achieve chemostat was necessary. This is because, the volumetric mass transfer coefficient ($k_L a$) of oxygen is affected by many factors such as cell density, broth viscosity, etc. (Damiani et al., 2014). Therefore, even if the amount of oxygen delivered to the system is maintained stable with constant total gas flow rate and agitation speed, OTR may still varies over the course of an experiment due to cell density and broth properties changes. The stable OUR was achieved through maintaining constant biomass along with constant oxygen supply. Figure 5.3 shows the data from this experiment where chemostat under different OUR conditions was achieved.

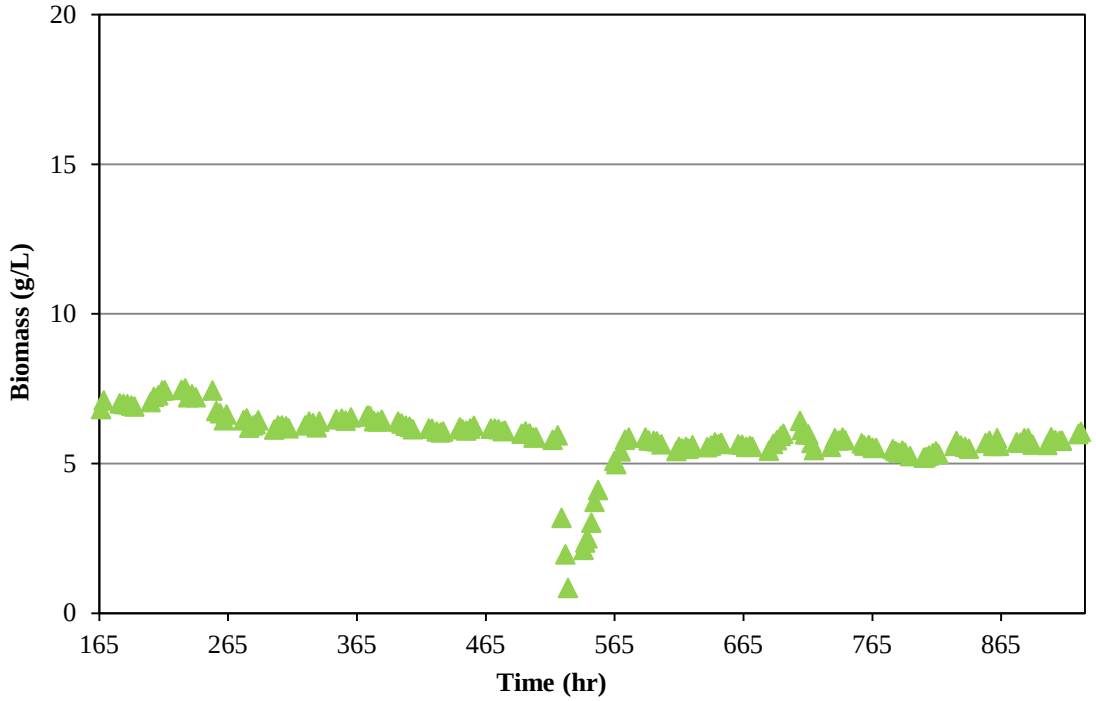

(a)

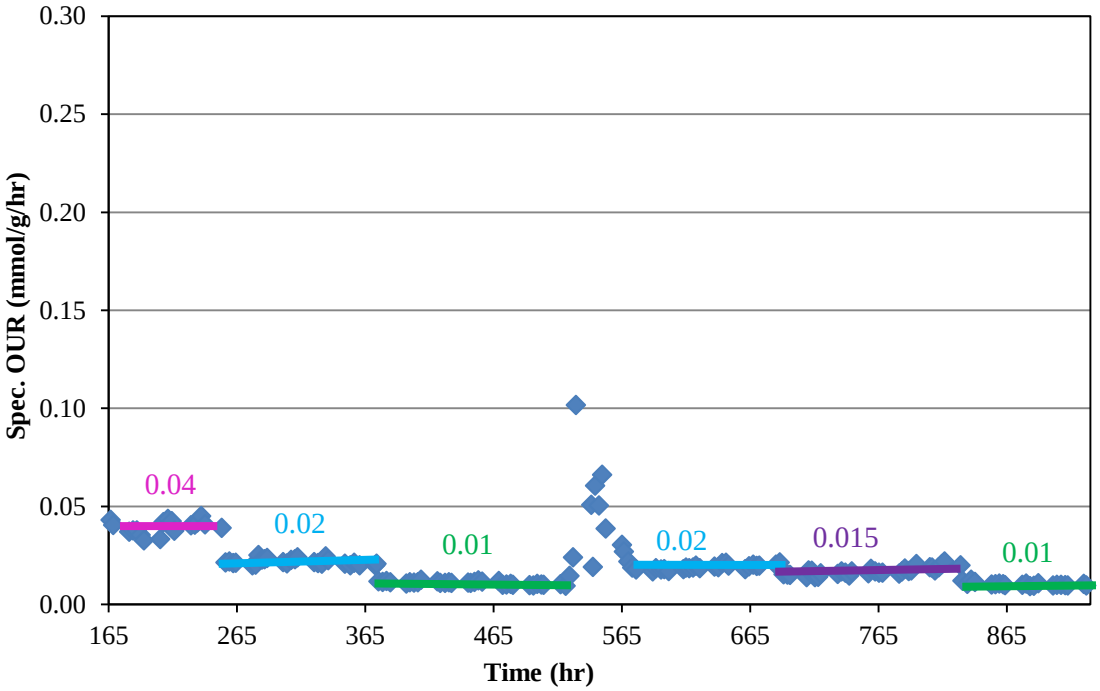

(b)

Figure 5.3 Controlled chemostat under (a) constant cell density; (b) constant OUR

5.3.2 Effects of OURs and carbon uptake on ethanol yields

OUR plays an important role in describing *S. stipitis'* metabolism in the estimation of xylose uptake kinetic parameters, which reveals the key metabolic details of how different oxygen supplies caused metabolism shift, providing efficient utilization of xylose and high ethanol yields (Liang et al., 2014). However, our results indicate that the optimum OUR alone (i.e., without information on carbon utilization) does not correlate well with maximum ethanol yield. At the same/similar OUR conditions tested under controlled chemostat, the ethanol yield changes due to the changes of metabolic status or phenotypes of *S. stipitis*.

Table 5.3 represents the comparison of estimated kinetic parameters under same OURs tested at different metabolic status. Different specific xylose consumption rates (vZs) were observed at the same OUR due to the different vZs at different carbon to oxygen uptake rate ratio (C/O_2), which results in different ethanol yields. Higher ethanol yield (Yes) obtained through higher xylose consumption rate (vZs) along with higher C/O_2 (Figure 5.4). This is because, at different stages of fermentation phase, *S. stipitis* changes their metabolic status or cellular physiological condition along with the time which influences carbon distribution in metabolic pathway of *S. stipitis*. Hence, optimized OUR information alone does not provide the maximum ethanol yield without considering C/O_2.

Table 5.2 Comparison of estimated kinetic parameters at similar OURs

OUR ($mmolO_2$/gDCW/hr)	C/O_2	vZs (mmol/gDCW/hr)	vEs	vAs	vTs	Yes (g/g)	Yas	Yts
0.020	15.3	0.306	0.152	0.022	0.005	0.152	0.028	0.017
0.020	19.3	0.386	0.287	0.023	0.006	0.228	0.024	0.016
0.010	24.1	0.241	0.171	0.004	0.010	0.217	0.006	0.043
0.010	26.3	0.263	0.200	0.006	0.011	0.233	0.010	0.043

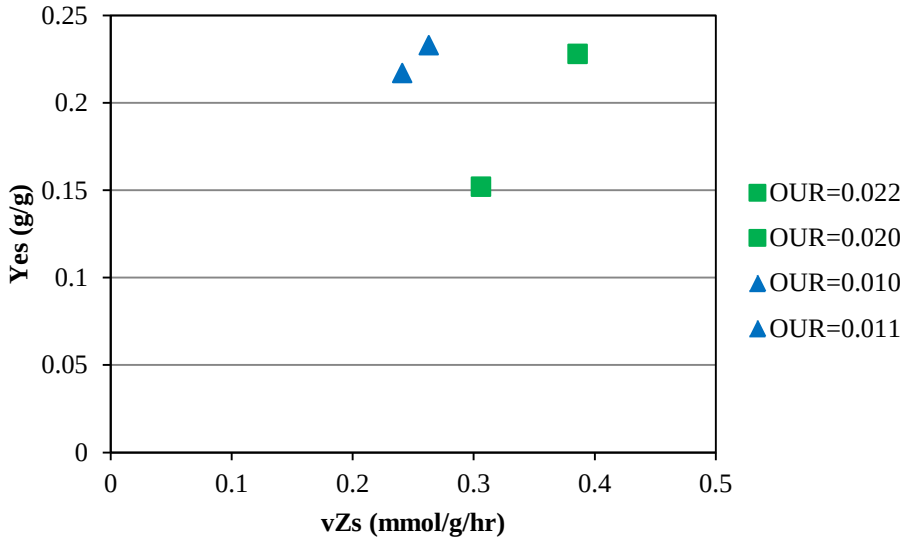

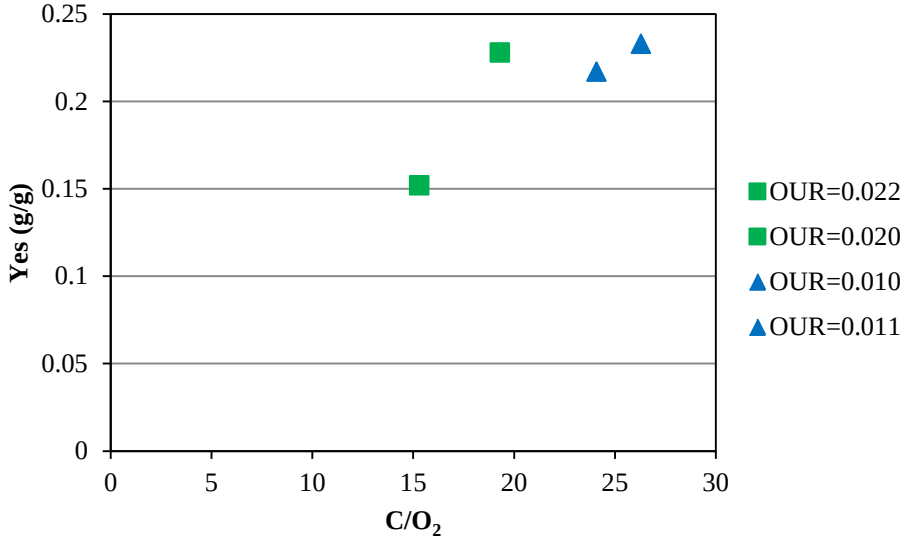

Figure 5.4 Xylose uptake rate (vZs) and C/O_2 on ethanol yields at OURs of ~0.01 and 0.02

5.3.3 Byproducts secretion under different OURs

The effect of OURs on yields of ethanol and byproducts are shown in Figure 5.5. From our study we often observed, when ethanol production decreased along with xylitol, acetic acid accumulation increased with increasing OURs. Su et al. also observed the increase of acetic acid

accumulation with increasing aeration and cell growth. Acetic acid accumulation occurs through the partial oxidation of acetaldehyde when NAD(P)H + H^+ is limited. Increasing aeration increased cell yield and increased the demand for NADPH, which could be balanced by generating more acetic acid. However, xylitol accumulation during fermentation mostly serves as an alternative way to regenerate cofactors such as NAD(P)+ when NAD(P)H + H^+ is in excess (Su et al., 2015).

In our study, at low OUR as shown in Table 5.3, the ethanol yield increased significantly from 0.175 to 0.666 due to the reduction of acetic acid secretion along with high C/O_2 at low OUR. This shows that the acetic acid becomes major byproduct at high OURs, which resulted in a negative impact to ethanol yield.

Table 5.3 Increase of ethanol yield at the reduction of acetic acid accumulation

OUR ($mmolO_2$/gDCW/hr)	C/O_2	vZs (mmol/gDCW/hr)	vEs	vAs	vTs	Yes (g/g)	Yas	Yts
0.040	9.95	0.398	0.069	0.035	0.001	0.054	0.035	0.002
0.019	18.47	0.351	0.234	0.017	0.010	0.204	0.019	0.028

The negative impact of acetic acid also influences the fermentation performance of *S. stipitis* upon initial aeration condition for cell growth. Table 5.4 shows the comparison of two experiments on acetic acid secretions at OUR of ~0.020. The ethanol yield of EXP B was increased by more than twice of EXP A with ~90% reduction of acetic acid yield. The only difference in operational condition of two experiments was the initial aeration condition for cell growth. For EXP B, initial OUR of 0.10~0.15mmol/g/hr was rapidly reduced to 0.05mmol/g/hr upon cell growth, while OUR of 0.15~0.25 mmol/g/hr was maintained at initial cell growth for EXP A. The rapid accumulation of acetic acid at early stage of cell growth in EXP A had a negative effect on ethanol yield and acetic acid inhibition on *S. stipitis*. Hence, it is important to con-

trol or monitor the acetic acid accumulation from the beginning of the experiment by monitoring OUR and carbon uptake (C/O_2).

Acetic acid inhibition on yeast is widely studied (Narendranath et al., 2001; Morita and Silva, 2000; van Zyl et al., 1991). Narendranath et al. shows that a reduction in the rates of substrate consumption and ethanol production occurs when the concentration of acetic acid is increased in the medium. The minimum inhibitory concentration of acetic acid for yeast growth (*S. cerevisiae*) is found to be 0.6% w/v (100mM) and the concentration of 0.05-0.1% w/v begins to stress the yeasts by reducing substrate consumption and ethanol production rates (Narendranath et al., 2001). At optimal pH for yeast fermentation (pH 4.0-5.0), the acetic acid is largely undissociated, which permits diffusion into cell cytoplasm, where it dissociates and causes the intracellular pH to decrease. Due to the decrease of intracellular pH, proton gradient across the membrane cannot be maintained, energy production is uncoupled, and the various nutrients transport is impaired under oxygen-limited conditions (van Zyl et al., 1991). Hence, the presence of acetic acid decreased the rate of xylose utilization. Maiorella et al. reported that the acetic acid interference with yeast metabolism results in an increase in ATP requirement for cell maintenance (Maiorella et al., 1983).

Table 5.4 The impact of acetic acid secretion on fermentation performance of two experiments

EXP	C/O_2	OUR	vZs (mmol/gDCW/hr)	vEs	vAs	vTs	Yes (g/g)	Yas	Yts
A	15.3	0.022	0.306	0.152	0.0216	0.0053	0.152	0.028	0.017
B	32.9	0.023	0.739	0.868	0.0050	0.0079	0.361	0.003	0.011

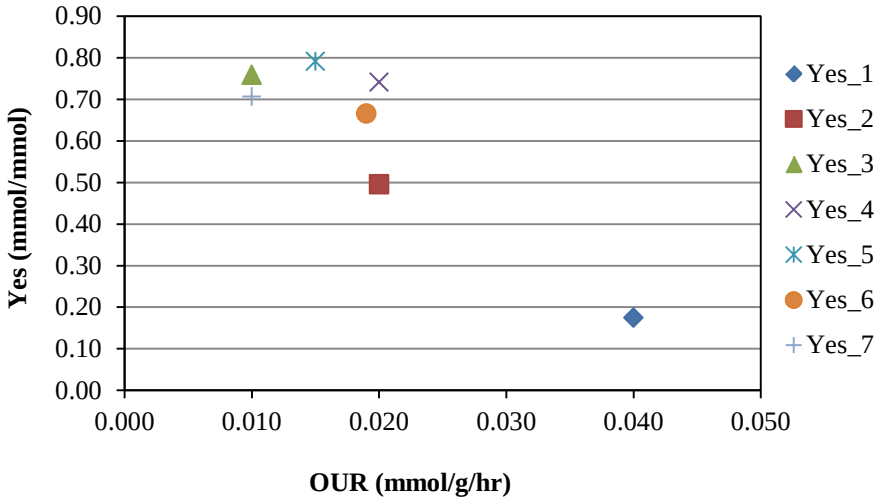
0.90
0.80
0.70
0.60
0.50
0.40
0.30
0.20
0.10
0.00
Yes (mmol/mmol)
0.000
0.010
0.020
0.030
0.040
0.050
OUR (mmol/g/hr)
Yes_1
Yes_2
Yes_3
Yes_4
Yes_5
Yes_6
Yes_7

(a)

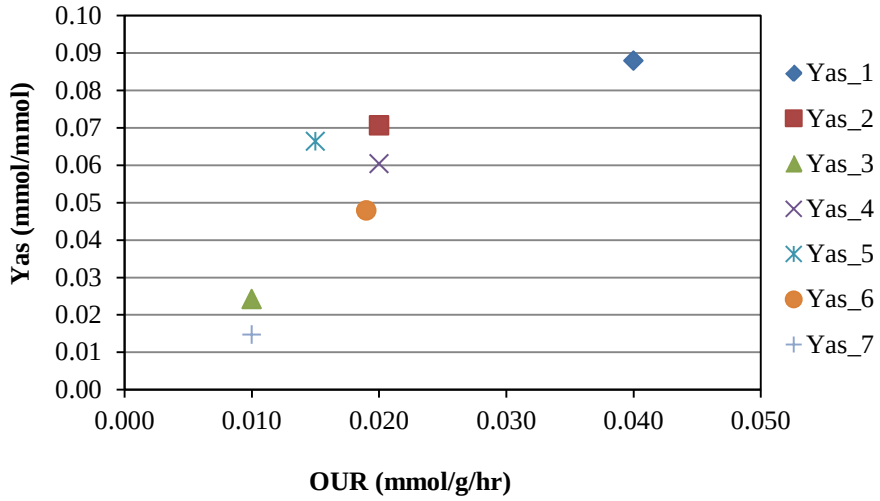
0.10
0.09
0.08
0.07
0.06
0.05
0.04
0.03
0.02
0.01
0.00
Yas (mmol/mmol)
0.000
0.010
0.020
0.030
0.040
0.050
OUR (mmol/g/hr)
Yas_1
Yas_2
Yas_3
Yas_4
Yas_5
Yas_6
Yas_7

(b)

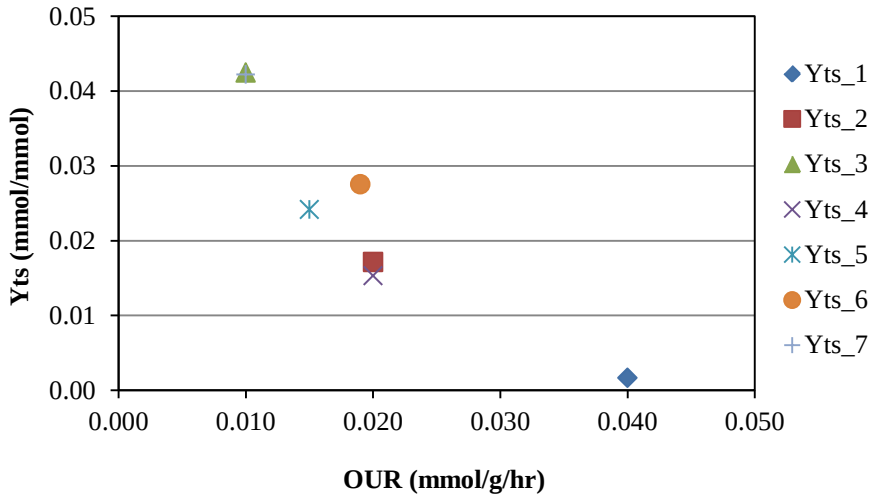

(c)

Figure 5.5 Effects of OURs on yields (a) ethanol; (b) acetic acid; (c) xylitol

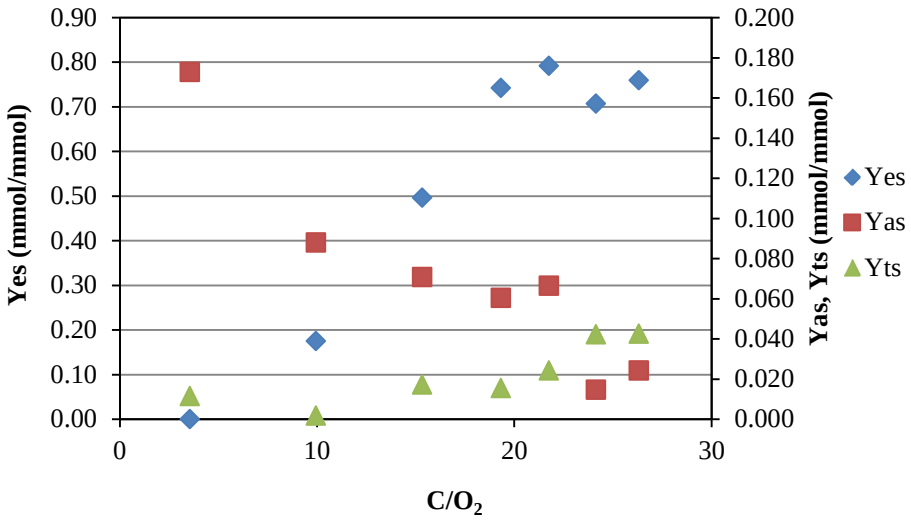

Figure 5.6 Yields of ethanol and byproducts along with C/O_2

5.3.4 Model fitting results along with fitted parameters

Our single culture model describes the dynamics of *S. stipitis* in response to change of OURs. The kinetic model fits the experimental data as shown in Figure 5.7. Kinetic parameters of specific rates of xylose, ethanol, xylitol and acetic acid at each OUR condition were estimated to optimize the next OUR condition to be tested.

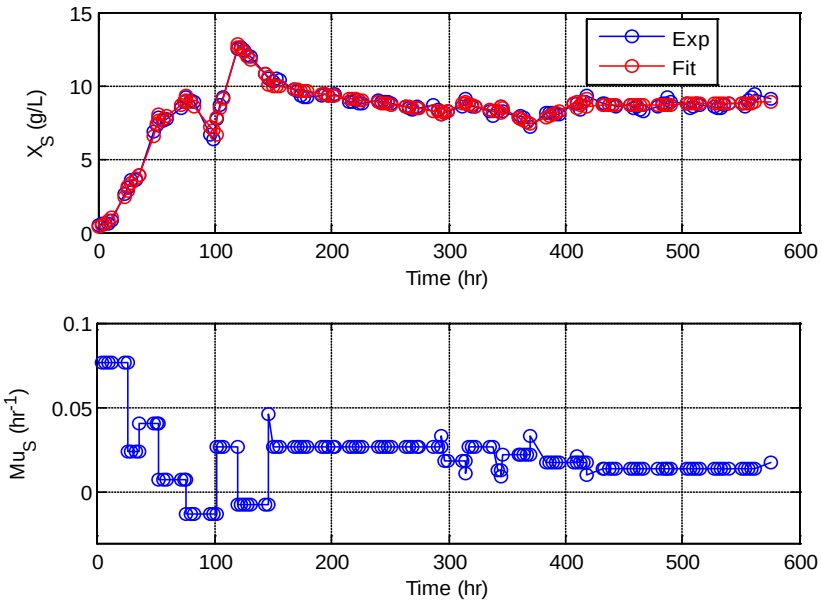

(a)

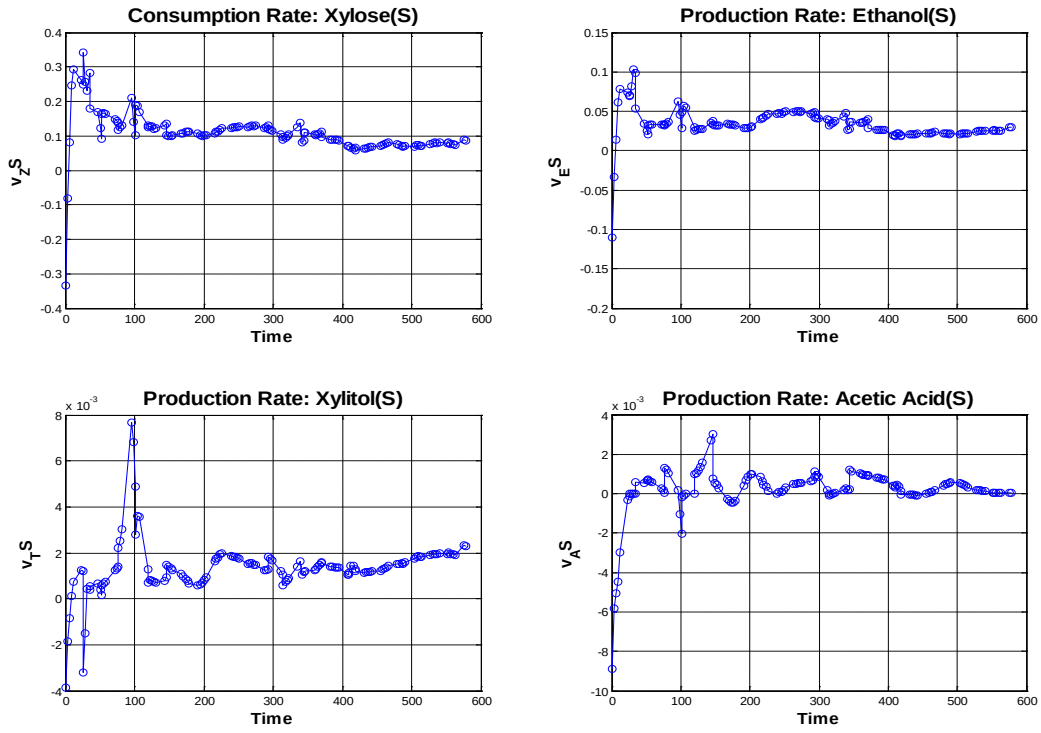

(b)

Figure 5.7 Model fitting results of (a) cell growth; (b) fitted parameters of specific rates (xylose, ethanol, xylitol and acetic acid) along with time

5.3.5 Carbon balance analysis

The amount of carbon (xylose) consumed by *S. stipitis* was accounted for the amount of carbon utilized for the production of ethanol, xylitol, acetic acid, cell mass, and carbon dioxide using model fitted parameters. With the measurement of carbon dioxide from off-gas, we were able to perform carbon mass balance of the xylose fermentation at each time segment. The loss of ethanol and acetic acid by gas stripping was not accounted for in this carbon balance due to the neglected amount. The detailed equations for carbon balance analysis were described in Appendix C and Figure 5.8 shows the error calculated from carbon recovery. The calculated mean percentage errors of carbon balance from both time segments were found to be very small within

±1%. This small carbon balance error confirms that our estimated kinetic parameters from model fitting results can be trustful.

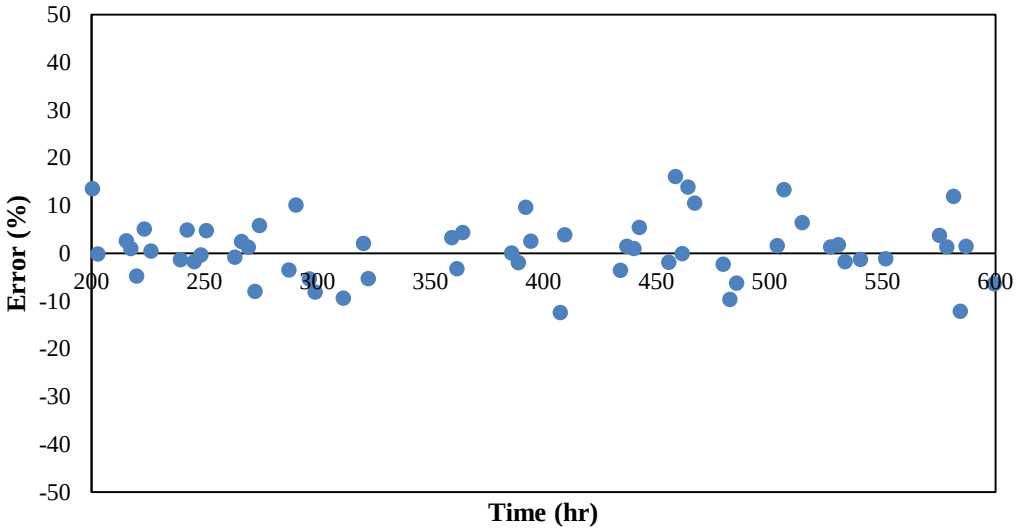

(a)

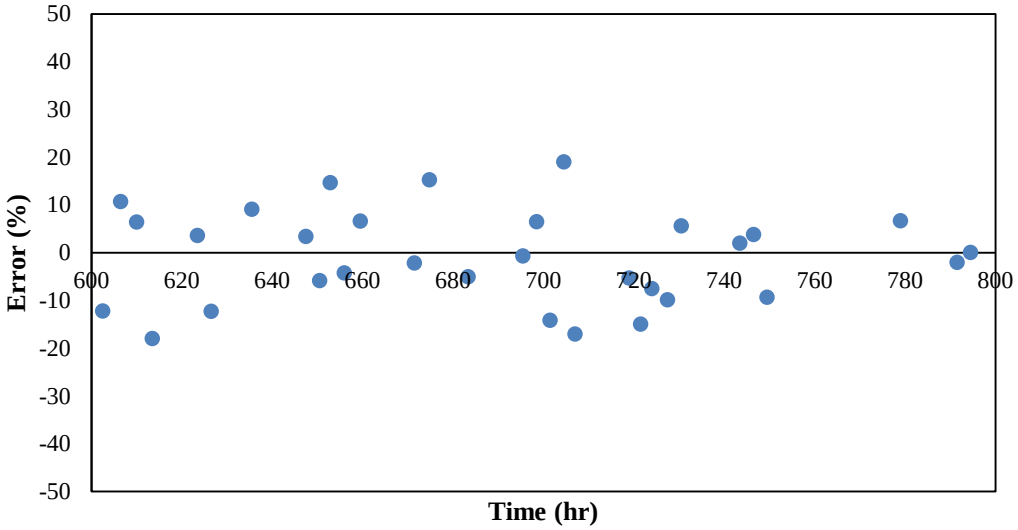

(b)

Figure 5.8 Error calculated from carbon mass balance during (a) 200-600hr; (b) 600-800hr

5.3.6 Analysis of different phenotypes by Principal Component Analysis (PCA)

Many multivariate statistical tools (e.g., principal component analysis [PCA], partial least squats [PLS], Fisher discriminant analysis [FDA], support vector machines [SVM], etc.) can be used to extract information/knowledge from the high dimensional data set generated from the experiment. In this work, PCA was chosen because it serves the purpose of finding how a perturbation propagates through a linear network and extracting the correlations among different fluxes. The PCA can extract the key metabolism of how different oxygen uptake and carbon uptake rates would cause metabolism shifts on *S. stipitis* which analyzes the different phenotypes of *S. stipitis* exist under a single OUR condition at different metabolic status. Different groups of phenotypes were presented in Table 5.5 and Figure 5.9.

Table 5.5 Fitted parameters for different phenotypes of *S. stipitis*

Time (hr)	C/O_2	OUR (mmol/g/hr)	vZs (mmol/g/hr)	vEs	vAs	vTs	Yes (g/g)	Yas	Yts
152.5-296.5	37.4	0.021	0.781	0.896	0.006	0.009	0.350	0.003	0.011
299.0-338.7	32.9	0.023	0.738	0.868	0.005	0.008	0.363	0.002	0.011
341.8-409.5	23.9	0.027	0.637	0.672	0.012	0.009	0.320	0.007	0.014
412.5-455.5	**30.8**	0.014	0.441	0.449	0.001	0.008	**0.313**	0.001	0.019
458.5-587.0	**30.4**	0.017	0.520	0.540	0.004	0.012	**0.318**	0.003	0.024
599.5-606.5	34.7	0.016	0.560	0.649	0.005	0.019	0.356	0.004	0.035

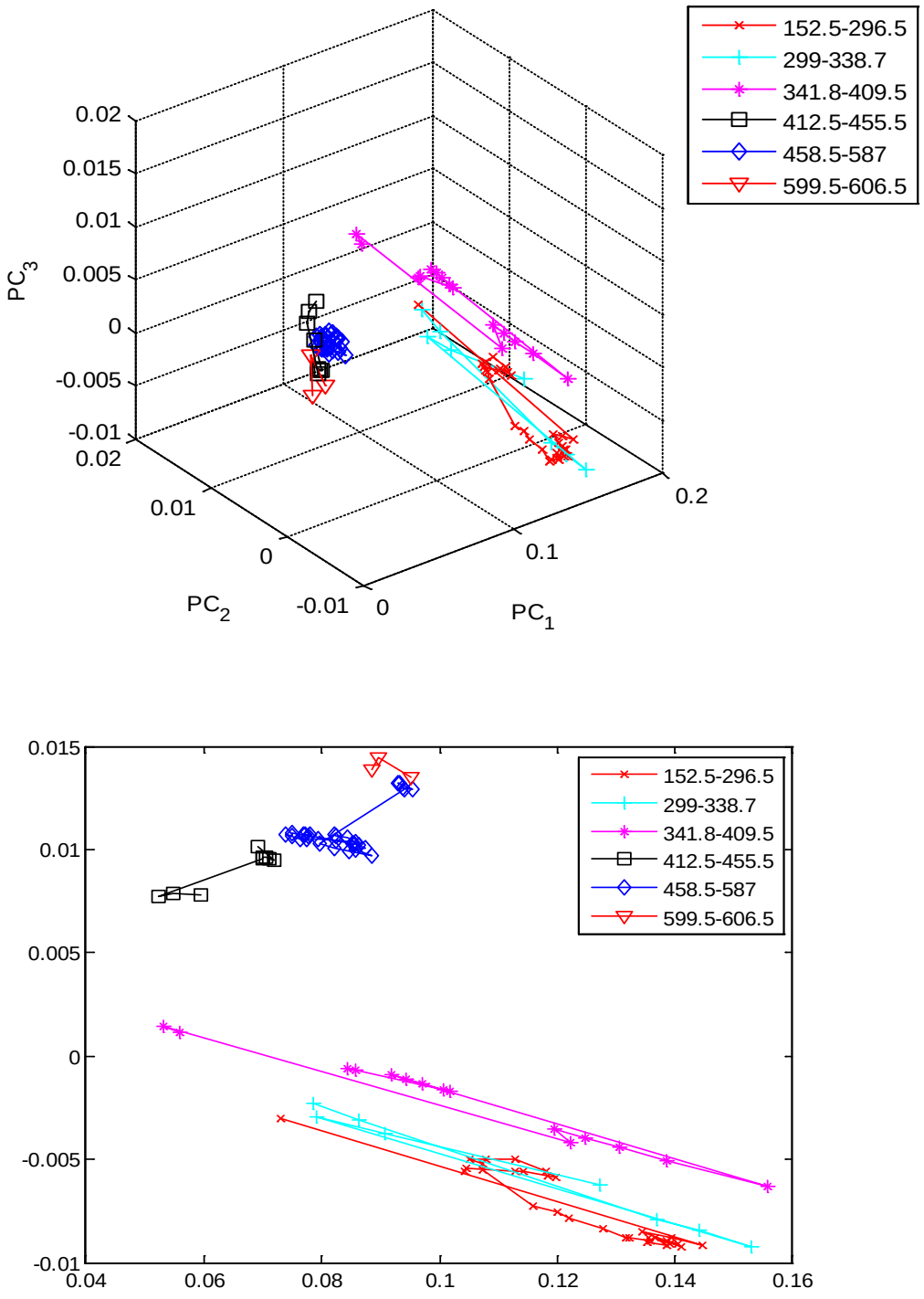

Figure 5.9 Different phenotypes exist under different OURs

5.4 Conclusion

In this study, we were able to quantitatively study the effects of OUR on xylose fermentation by *S. stipitis* under controlled chemostat. The systematic control of chemostat (constant biomass and constant OUR) allows us to study the dynamics of *S. stipitis* in response to both OUR and carbon uptake. We observed under same OUR condition tested at different fermentation stages, the ethanol yield varies due to the change of metabolic status or phenotypes of *S. stipitis*. Hence, optimum OUR alone does not always correlate with the maximum ethanol yield.

Different phenotypes exist under a single OUR condition, which can be verified by PCA as it enables the extraction of correlation between different cellular physiology with respect to OUR and carbon uptake. With different cellular metabolic status, carbon flux distribution changes.

Chapter 6. Co-culture Study

6.1 Introduction

Lignocellulosic biomass is an attractive, sustainable, and abundant carbon source for ethanolic fermentation process. However, the lack of microorganisms which can efficiently ferment all sugars derived from lignocellulosic biomass is one of the key barriers in industrializing lignocellulosic ethanol process. To overcome this barrier, numerous microorganisms have been constructed in the past few decades to ferment the mixture of glucose and xylose, the dominant hexose and pentose from lignocellulosic hydrolysate (Jeffries and Jin, 2004; Kuyper et al., 2005; Ma et al., 2012). As an alternative, co-culture strategy has drawn increased attention for simultaneous conversion of glucose and xylose. Table 6.1 summarizes recent attempts in using co-culture systems for glucose/xylose or lignocellulosic hydrolysate fermentation. Existing results show that co-culture is a promising way to ferment mixed glucose and xylose for ethanol production, especially in reducing fermentation time and improving ethanol productivity. However, existing research mainly examined the ethanol production performance of the co-culture system such as final ethanol yield and productivity, with little or no attempt made to understand the dynamic interactions between the two microbes. In addition, major challenges associated with the co-culture strategy have not been adequately addressed, which include the incompatible oxygen conditions required by two microbes for optimal ethanol production, catabolite repression of xylose utilization when glucose is present, and the low ethanol tolerance of xylose-fermenting microorganisms (Delgenes et al., 1988; Grootjen et al., 1991, 1990; Hanly and Henson, 2011).

In this work, we developed new equipment and approaches to systematically investigate the dynamic properties of a co-culture system of *Saccharomyces cerevisiae* and *Scheffersomyces stipitis*, which also help address some major challenges associated with the co-culture system. The new equipment is a membrane-separated co-culture bioreactor which enables the independent control of the dissolved oxygen (DO) levels in each chamber, and the easy tracking of the biomass of each strain. We also propose a dual continuous/pseudo-continuous operation mode of the bioreactor, which is enabled by an in-house developed cell retention module. The dual-mode operation allows the easy maintenance of constant biomass by adjusting the operation time of each mode.

Table 6.1 Existing work in ethanol production using co-culture systems

Reference	Co-culture strains	Operation mode	Best result (% theoretical yield)
(Gutiérrez-Rivera et al., 2015, 2012)	***S. cerevisiae*** – ***S. stipitis***	batch	88% at 42hr 78% at 200hr
(Chaudhary and Ghosh, 2014)	*Z. mobilis* – ***S. stipitis*** (reactors in series)	continuous	92% for *Z. mobilis* with dilution rate 0.07hr^{-1} 88% for *S. stipitis* with dilution rate 0.048hr^{-1} at 168hr
(Hickert et al., 2013a, 2013b)	***S. cerevisiae*** – *S. arborariae* ***S. cerevisiae*** – *C. shehatae*	batch	94% at 250hr 94% at 250hr
(Singh and Bishnoi, 2012)	***S. cerevisiae*** – ***S. stipitis***	batch	78% at 36hr
(Chandel et al., 2011)	***S. cerevisiae*** – ***S. stipitis***	batch	94% at 84hr
(da Cunha-Pereira et al., 2011)	***S. cerevisiae*** - *S. arborariae*	batch	75% at 150hr
(Li et al., 2011)	***S. cerevisiae*** - ***S. stipitis*** (inactivation of *S. cerevisiae*)	batch	85% at 125hr
(Yadav et al., 2011)	***S. cerevisiae*** – ***S. stipitis***	batch	78% at 36hr
(Fu et al., 2009; Fu and Peiris, 2007)	*Z. mobilis* – ***S. stipitis*** *Z. mobilis* – *P. tannophilis* (successive inoculation)	batch	96% at 40hr 65% at 150 hr
(Okuda et al., 2008)	***S. cerevisiae*** – *E. Coli KO-11*	batch	81% at 47 hr
(Rouhollah et al., 2007)	***S. cerevisiae*** - ***S. stipitis*** *K. marxianus* - ***S. stipitis***	batch	80% at 60 hr 71% at 72 hr
(Lebeau et al., 2007, 1998, 1997)	***S. cerevisiae*** – *C. shehatae* (co-immobilized)	batch continuous batch	95% with dilution rate 0.02 hr^{-1} incomplete consumption of xylose

(Qian et al., 2006)	***S. cerevisiae*** *– P. tannophilis* ***S. cerevisiae*** – house developed recombinant *E. coli*	batch	96% at 72 hr 88% at 72 hr
(De Bari et al., 2004)	***S. cerevisiae - S. Stipitis*** (co-immobilized)	batch	77% at 120 hr
(Kordowska-Wiater and Targoński, 2001)	***S. cerevisiae – S. stipitis*** **(RD)** ***S. cerevisiae – S. stipitis***	batch	76.7% at 96hr 74.4% at 96hr
(Taniguchi, 1997; Taniguchi et al., 1997)	**(RD)** ***S. cerevisiae – S. stipitis***	batch	99% at 40 hr
(J. M. Laplace et al., 1993; Jean M. Laplace et al., 1993)	**(RD)** ***S. cerevisiae – S. stipitis***	continuous	complete xylose and glucose consumption
(Grootjen et al., 1991, 1990)	***S. cerevisiae – S. stipitis*** (immobilized or co-immobilized)	continuous	complete xylose and glucose consumption

6.2 Materials and Methods

6.2.1 Microorganisms and culture media

The strains used in this study were *S. cerevisiae* D5A and *S. stipitis* CBS 5773 which were obtained from Y.Y Lee, Auburn University and ATCC, respectively. The yeast cells were kept frozen at -20^{o}C in stock culture of 20% glycerol and 80% of culture medium containing: 10gL^{-1} yeast extract, 20gL^{-1} peptone and 20gL^{-1} glucose for *S. cerevisiae* or 20gL^{-1} xylose for *S. stipitis*. The cells were also maintained at 4^{o}C on YPD and YPX agar plates for *S. cerevisiae* and *S. stipitis*, respectively. For the culture media, the minimal medium was used for both pre-culture and fermentation which contained 20g D-glucose for *S. cerevisiae* or 20g D-xylose for *S. stipitis*, 1.7g yeast nitrogen base without amino acids or ammonium sulfate and 2.27g urea per liter DI water. The sugar concentrations of feed medium for pseudo-continuous fermentation varied based on the operational conditions.

6.2.2 Reactor design and development

The schematic diagram and actual set-up of the developed membrane-separated bioreactor for co-culture study are shown in Figure 3.8. The body of the bioreactor was constructed using polycarbonate, which consists of two chambers. By placing a microporous filter membrane

(Biodyne Plus, Pall Corporation) between the two chambers, the two strains are separated by the membrane while various metabolites can exchange between the two chambers. The propellers of the agitators are driven by external magnetic fields; pH and temperature are under automatic feedback control (not shown in Figure 3.8a). This two-chamber configuration enables us to monitor and control the biomass development of individual strains during fermentation. It also allows the independent control of different oxygen conditions for each strain by adjusting nitrogen and air gas flow rates to each chamber. In addition, by feeding the substrates into *S. cerevisiae* chamber, glucose can be completely consumed by *S. cerevisiae* before xylose reaches *S. stipitis* chamber. Therefore, the catabolite repression of xylose utilization can be alleviated.

6.2.3 Dual-mode operation

Pseudo-continuous operation is characterized by continuous nutrient feeding and continuous cell-free broth withdrawal, which can be implemented through installing a cell retention module to filter out cells from effluent. The biggest challenge in pseudo-continuous operation is maintaining the stability and effectiveness of cell filtration module. Due to continuous buildup of cells on the filtration surface, commercial filtration modules usually have limited operation time even with back-flash implemented periodically (Taniguchi, 1997). To address this difficulty, we have developed a cell retention module in-house, with the filtration surface located right against the propeller blades. In this way the membrane surface is constantly cleaned through the shear stress generated by agitation, and pseudo-continuous fermentation was sustained for more than three months (Liang et al., 2013).

Pseudo-continuous operation is only needed for *S. stipitis* due to its very slow growth rate under oxygen limited condition, which often results in “wash-out” under continuous operation. With pseudo-continuous mode available, the biomass of *S. stipitis* can be controlled or main-

tained by the dual-mode operation, which combines pseudo-continuous operation (for biomass accumulation) and continuous fermentation (for biomass maintaining or reduction). The operation time of each mode depends on the cell growth rate, and the detailed estimation of the operation time for each mode can be found in Appendix.

6.2.4 Monitoring and independent control of OTR and OUR

The efficient conversion of xylose to ethanol by *S. stipitis* is highly influenced by oxygen utilization rate (OUR). Higher OUR often results in faster cell growth and acetic acid production, while lower OUR often results in xylitol production, both at the expense of reduced ethanol production (du Preez, 1994; Rizzi et al., 1989; Slininger et al., 1991). In order to quantitatively study the effect of OUR on the fermentation performance, accurate control of OUR is necessary. However, there is no direct way to control OUR, and the control of OUR is usually done through the control oxygen transfer rate (OTR) by manipulating the composition of the feeding gas into the system. To achieve the limited oxygen condition for *S. stipitis* chamber, air has to be mixed with nitrogen to achieve desired oxygen composition while maintaining constant total gas flow rate. However, our tests show that the standard gas mixing component equipped with New Brunswick BioFlo 110 cannot deliver the desired stable OTR, as the total gas flow rate changes noticeably when the ratio between air and nitrogen is changed. In order to achieve accurate control of OTR in the co-culture system, we have developed and tested a gas-mixing apparatus. With multiple tests, we confirmed that the developed apparatus was able to deliver desired stable oxygen concentration with stable overall gas flow rate. The delivered gas composition was also confirmed by GC measurements. It has been reported that the volumetric mass transfer coefficient ($k_L a$) of oxygen is affected by many factors such as cell density, broth viscosity, etc. (Damiani et al., 2014). Therefore, even if the total gas flow rate and agitation speed were fixed, $k_L a$ still varies

during the course of an experiment as cell density and broth properties change over time, so does OUR. In order to obtain accurate measurements of OUR, we monitor both the inlet gas and off gas oxygen concentration, and rely on the mass balance of oxygen to calculate OUR.

6.2.5 Experimental procedure

The membrane-separated bioreactor is set up in the way that for each chamber, its effluent can be withdrawn either with or without cell retention, which enables the dual continuous/pseudo-continuous operation. With this setup, totally three operation modes can be implemented in the bioreactor: batch, pseudo-continuous and continuous. During batch operation, there is neither feed-in of substrate medium, nor withdraw of culture broth; during pseudo-continuous operation, there is continuous feed-in of substrate, and continuous withdraw of cell-free broth; during continuous operation, there is continuous feed-in of substrate and withdraw of culture medium. In general, each experiment consists of two stages: cell growth and fermentation. The operating conditions were temperature of 25°C and pH of 5.0. The pH was maintained at 5.0 by automatic addition of 1.0N NaOH.

During cell growth stage: after inoculation, both *S. cerevisiae* and *S. stipitis* grow under oxygen limited-condition by purging a mixture of air (156mL/min) and nitrogen (40mL/min) gas at the fixed total flow rate of 196mL/min at atmospheric pressure. Such oxygen condition allows relatively fast cell growth while promotes ethanol production. The purpose of such condition is to improve cells' ethanol tolerance and condition for the fermentation stage. Cell growth stage can be implemented through either batch operation or pseudo-continuous operation. The purpose of the cell growth stage is to achieve the desired cell density of both strains for fermentation stage.

During fermentation stage: the oxygen condition for the *S. cerevisiae* chamber is maintained at anaerobic by feeding nitrogen gas only, while different oxygen conditions (i.e., different OUR) were tested for *S. stipitis* chamber through manipulating the air to nitrogen ratio of the feeding gas. The fermentation stage can be implemented through either pseudo-continuous or continuous operation, depending on the cell growth rate under different operational conditions. It is desired to maintain constant biomass density under each oxygen condition, hence constant OUR, to study the effect of OUR on ethanol production.

6.2.6 Analytical methods

For the analytical procedures, the concentrations of glucose, xylose, xylitol, glycerol, acetic acid and ethanol were measured using an Agilent 1200 series high performance liquid chromatography (HPLC) with UV/Vis and refractive index (RI) detector. They were analyzed on an Aminex HPX-87H column (Bio-Rad) at 45^{o}C with 0.05M H_2SO_4 solution as the mobile phase at a flow rate of 0.6mL/min. The run time of each sample was 25 min. The concentration of carbon dioxide was measured using a SRI 8610C gas chromatography (GC) with thermal conductivity (TC) detector. They were analyzed on 3' Silica Gel column (column temperature: 105^{o}C) with helium as the carrier gas at 10psia at oven temperature of 80^{o}C. The cell density of each strain was measured turbidometrically at 600nm. Fermentation broth was diluted according to the cell density using sterile DI water and then the turbidity of solution was measured by a UV-VIS spectrophotometer (Beckman Coulter).

6.3 Results and Discussion

6.3.1 Simultaneous complete consumption of glucose and xylose

Among published co-culture studies, incomplete xylose consumption is one of the most common limitations due to the catabolite repression. In this study, since the mixed substrate is

fed into *S. cerevisiae* chamber, this limitation can be alleviated by maintaining very low (basically zero) residual glucose concentration in the *S. cerevisiae* chamber through controlling biomass densities of both strains, glucose concentration in the feed medium, and dilution rate. By consuming all glucose in the *S. cerevisiae* chamber, almost no glucose is present when xylose reaches *S. stipitis* chamber which allows the complete consumption of glucose and xylose simultaneously. In this way, the diauxic kinetics of *S. stipitis* often exhibited in continuous or fed-batch fermentations can be eliminated and complete utilization of both glucose and xylose can be achieved simultaneously under continuous or pseudo-continuous operation as shown in Figure 5.2.

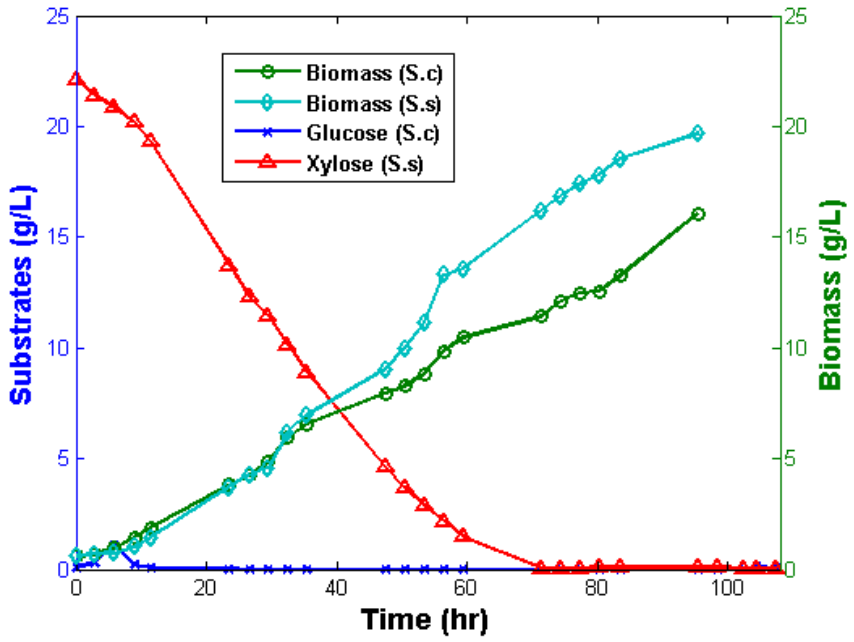

Figure 6.1 Simultaneous consumption of glucose and xylose by *S. cerevisiae* and *S. stipitis*; biomass development of *S. cerevisiae* and *S. stipitis*

6.3.2 Independent monitoring and control of biomass development

With the membrane-separated bioreactor, it is easy to track the cell mass development of each strain during the course of the experiment. Among published co-culture studies, individual biomass of each strain has not been reported, as two strains were mixed together after the inoculation and it was difficult to measure the individual biomass density in the mixture. More importantly, the membrane-separated bioreactor with the pseudo-continuous operation enables the independent control of biomass development of each strain during cell growth stage. Specifically, the cell growth rate of *S. stipitis* was controlled through manipulating OUR in the chamber, as *S. stipitis*' growth rate is highly sensitive to the availability of oxygen. On the other hand, because *S. cerevisiae* is a crab-tree positive strain which can grow anaerobically, OUR is not an effective factor to control cell growth rate. Therefore, the cell grow rate of *S. cerevisiae* was controlled through the availability of substrate (glucose) by manipulating feeding concentration of substrate. In addition, the initial inoculation ratio of the two strains was optimized to enable a more balanced cell growth.

After several runs of trial-and-error, we found the following experimental condition could deliver the desired cell mass development. The initial optical density of both *S. cerevisiae* and *S. stipitis* were 1.0 (OD_{600}) after inoculation, with the initial culture medium in both chambers of the reactor being $20gL^{-1}$ D-xylose with the standard nitrogen base solution. Instead of batch operation, cell growth stage was implemented using pseudo-continuous operation, with the feed-in medium containing $100gL^{-1}$ D-glucose with the standard nitrogen base solution. In this way, we can control the cell growth rate of *S. cerevisiae* though changing substrate feed flow rate, while controlling the cell growth rate of *S. cerevisiae* through the amount of oxygen in the feeding gas. The amount of initial xylose concentration was determined to achieve desired *S. stipitis* biomass

density (about 10 $gDCWL^{-1}$) at the end of the cell growth stage, i.e., when the xylose concentration in *S. stipitis* chamber dropped to below $2gL^{-1}$. During fermentation stage, the feed-in medium switched to a mixture of glucose and xylose with the standard nitrogen base solution. A typical biomass development trajectory for both chambers is shown in Figure 6.1.

6.3.3 Independent control of oxygen requirement

With the membrane separating the two chambers, it is possible to maintain different OUR conditions for the two strains: anaerobic for *S. cerevisiae* while microaerobic for *S. stipitis*. This was done through feed nitrogen only to *S. cerevisiae* chamber while feeding mixture of air and nitrogen to *S. stipitis* chamber. In order to validate the independent control of different OUR conditions in both chambers, we measured the dissolved oxygen in the liquid phase and oxygen content in the offgas using the bioreactor without cells. The experimental results were given in Figure 6.2. Both DO probes that measure the *S. cerevisiae* chamber and *S. stipitis* chamber were calibrated with the feeding gas into *S. stipitis* chamber, so a reading of 100% correspond to the concentration in the feeding mixture to *S. stipitis* chamber. Figure 6.2 clearly showed that different OUR conditions can be achieved: anaerobic in *S. cerevisiae* chamber (0% DO) and microaerobic for *S. stipitis* (100% DO).

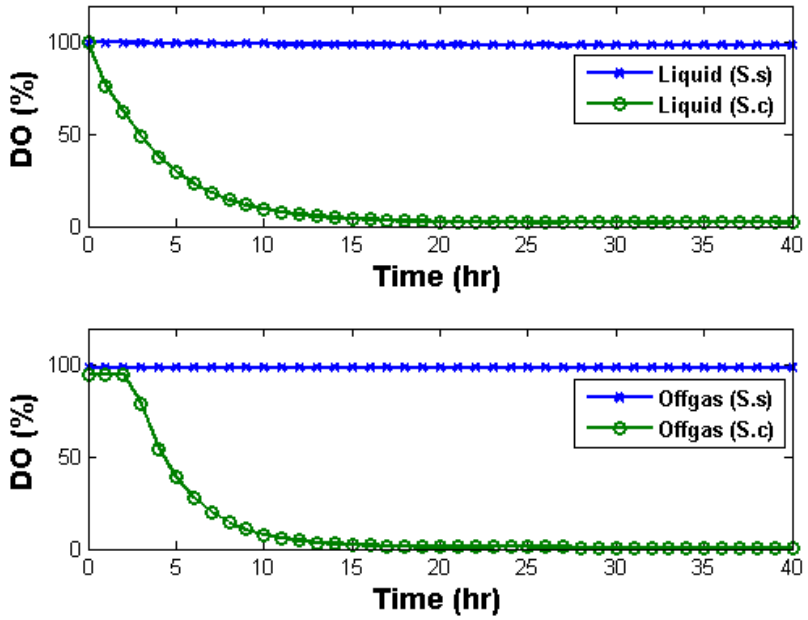

Figure 6.2 Separate control of DO in co-culture system; DO measurement in liquid (top); DO measurement in off-gas (bottom), Feed only N_2 into *S. cerevisiae* and mixture of Air (172mL/min) and N_2 (26mL/min) into *S. stipitis*.

6.3.4 Controlled chemostat under different environmental factors

The purpose of developing the bioreactor and related protocols is to conduct systematic investigations on the co-culture dynamics under chemostat, which allows the quantitative study on the effect of different environmental factors. Among different factors such as population ratio, feeding concentration and dilution rate, OUR is arguably the most important one, as ethanol production by *S. stipitis* is highly sensitive to OUR. It should be noted that in order to maintain constant OUR, maintaining constant biomass is a prerequisite. The conventional feedback control module equipped with many commercial bioreactors is not sufficient for this purpose, which relies on the DO measurement to compute how much oxygen (air) should be fed to the reactor. This is because for S. stipitis chamber, once the biomass density is above 3 $gDCWL^{-1}$, the DO measurements stayed at zero for the rest of the run, as oxygen transfer is diffusion limited when cell density is high. The dual continuous/pseudo-continuous operation allows the easy mainte-

nance of constant cell density and constant OUR under much wider OUR conditions, particularly at lower OUR ranges which often result in wash out with continuous operation. Figure 6.3 shows the data from one run where chemostat under different OUR conditions were achieved.

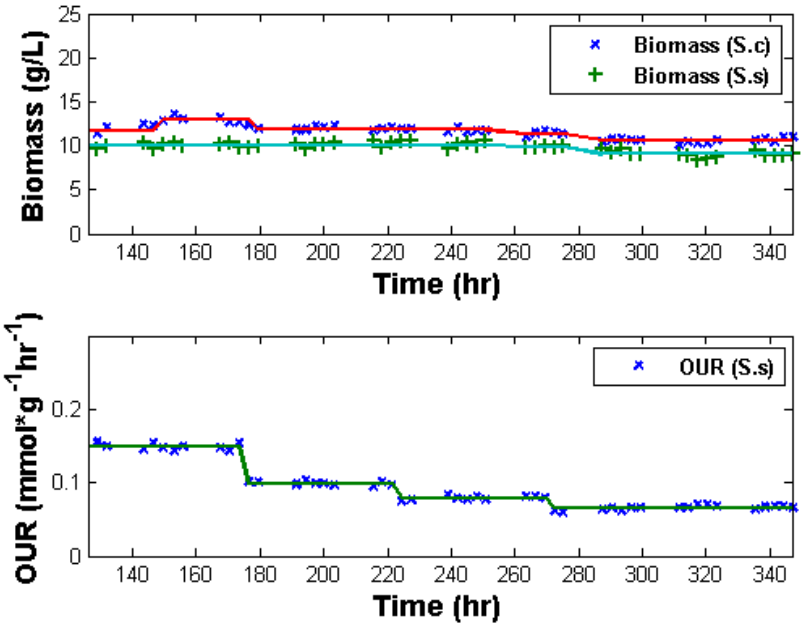

Figure 6.3 Constant biomass of *S. cerevisiae* and *S. stipitis* (top); Constant OUR of *S. stipitis* under controlled chemostat (bottom)

6.3.5 Improvement on ethanol tolerance under pseudo-continuous fermentation

The accumulation of ethanol during cultivation causes stress to yeast cells (Attfield, 1997), which drives the cells to adjust their intracellular physiological conditions to the surrounding environment in order to grow (Dinh et al., 2008). We argue that one added benefit of the pseudo-continuous operation is that it provides an ideal environment for cells to adapt to higher ethanol conditions, as the environmental pressure is being consistently applied and gradually increases. To verify this, we sampled cells from the bioreactor after 2 weeks of experiment, and tested the cells viability after 2 hours ethanol shock with various ethanol concentrations, and compared with that of unadapted cells. The results are given in Figure 6.4, which clearly show that the ethanol tolerance of both *S. cerevisiae* and *S. stipitis*, in terms of cell viability, improved noticeably, particularly at higher ethanol concentration. It was surprising to observe the further improvement on ethanol tolerance of *S. cerevisiae* as it already has much higher ethanol tolerance compared to *S. stipitis*.

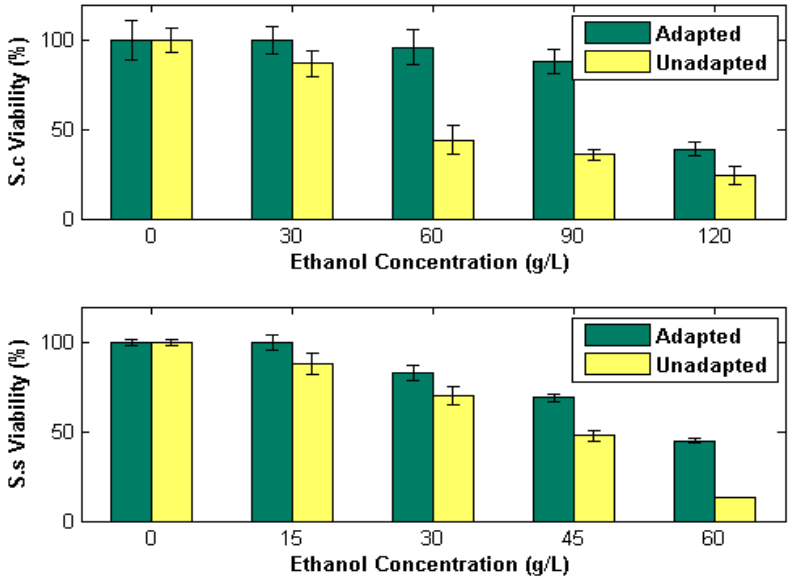

Figure 6.4 Cell viability of adapted and unadapted strains of *S. cerevisiae* under ethanol shock (top); Cell viability of adapted and unadapted strains of *S. stipitis* under ethanol shock (bottom)

6.4 Conclusion

The co-culture system of *S. cerevisiae* and *S. stipitis* has been extensively studied in the last few years to ferment the mixture of glucose and xylose or lignocellulosic hydrolysate. However, most of the results are qualitative due to the difficulties associated with monitoring and control of the co-culture systems. In this work, we developed a membrane-separated bioreactor and associated protocols to facilitate quantitative study of co-culture systems. Through the in-house developed cell retention module and gas mixing apparatus, as well as the dual-mode operation of continuous/pseudo-continuous, we can not only independently monitor and control biomass development of each strain, but also independently control different OUR conditions for each strain. As a result, we were able to obtain chemostat operation of the co-culture system under various conditions, particularly at lower OUR conditions which were not achieved in the past with continuous operation due to cell wash-out.

Chapter 7. Future Work

7.1 Investigation of Dynamic Properties of Co-culture System with PCA

Further systematic study on co-culture experiment will be conducted to identify the optimal co-culture conditions using a developed co-culture bioreactor and modeling approaches (kinetic modeling and PCA). We will systematically study the effects of OURs and carbon uptake for *S. stipitis* to maximize the xylose fermentation in co-culture system using PCA as a tool. In addition, the dynamic interactions and behaviors of the paired strains of *S. cerevisiae* and *S. stipitis* in the co-culture system will be investigated under different environmental factors of OURs (for *S. stipitis*) and dilution rates along with mixed sugar concentrations in the feed.

Appendices

Appendix A: derivations of co-culture kinetic model equations

Biomass

S. cerevisiae

$$\frac{dX_C}{dt} = \mu_C X_C - \frac{F_{OC}\ OptMod_C}{V/2}\ X_C$$

$$\frac{dX_C}{dt} = X_C\ (\mu_C - \frac{F_{OC}\ OptMod_C}{V/2})$$

$$\int_{X_{C0}}^{X_C} \frac{1}{X_C} dX_C = \int_{t_0}^{t} dt\ (\mu_C - \frac{F_{OC}\ OptMod_C}{V/2})$$

$$lnX_C - lnX_{C0} = (t - t_0)(\mu_C - \frac{F_{OC}\ OptMod_C}{V/2})$$

$$lnX_C = t\left(\mu_C - \frac{F_{OC}\ OptMod_C}{V/2}\right) + lnX_{C0}$$

$$C = \mu_C - \frac{F_{OC}\ OptMod_C}{V/2}$$

$$lnX_C = Ct + lnX_{C0}$$

$$Y = X\ [\ {}^{C}_{lnX_{C0}}]$$

$$X = [t \quad 1]$$

$$\beta(1) = C = \mu_C - \frac{F_{OC}\ OptMod_C}{V/2}$$

$$\mu_C = \beta(1) + \frac{F_{OC}\ OptMod_C}{V/2}$$

$$\beta(2) = lnX_{C0}$$

$$X_{CO} = \exp(\beta(2))$$

S. stipitis

$$\frac{dX_S}{dt} = \mu_S X_S - \frac{F_{OS}\ OptMod_S}{V/2}\ X_S$$

$$\mu_S = \beta(1) + \frac{F_{OS}\ OptMod_S}{V/2}$$

$$X_{S0} = \exp(\beta(2))$$

Xylose

S. cerevisiae

$$\frac{dZ_C}{dt} = \frac{F_{In}}{V/2}(Z_{In} - Z_C) - v_{ZC}X_C - D_Z\ (Z_C - Z_S)$$

$$v_{ZC} = \frac{1}{X_C}[\frac{F_{In}}{V/2}(Z_{In} - Z_C) - D_Z(Z_C - Z_S) - \frac{dZ_C}{dt}]$$

S. stipitis

$$\frac{dZ_S}{dt} = \frac{F_{OS}}{V/2}(Z_C - Z_S) - v_{ZS}X_S + D_Z\ (Z_C - Z_S)$$

$$v_{ZS} = \frac{1}{X_S}[(Z_C - Z_S)(\frac{F_{OS}}{V/2} + D_Z) - \frac{dZ_S}{dt}]$$

Ethanol

S. cerevisiae

$$\frac{dE_C}{dt} = \frac{F_{In}}{V/2}(-E_C) + v_{EC}X_C - D_E\ (E_C - E_S)$$

$$v_{EC} = \frac{1}{X_C}[\frac{F_{In}}{V/2}(E_C) + D_E(E_C - E_S) + \frac{dE_C}{dt}]$$

S. stipitis

$$\frac{dE_S}{dt} = \frac{F_{OS}}{V/2}(E_C - E_S) + v_{ES}X_S + D_E\ (E_C - E_S)$$

$$v_{ES} = \frac{1}{X_S}[-(E_C - E_S)(\frac{F_{OS}}{V/2} + D_E) + \frac{dE_S}{dt}]$$

Xylitol

S. cerevisiae

$$\frac{dT_C}{dt} = \frac{F_{In}}{V/2}(-T_C) + v_{TC}X_C - D_T\ (T_C - T_S)$$

$$v_{TC} = \frac{1}{X_C}[\frac{F_{In}}{V/2}(T_C) + D_T(T_C - T_S) + \frac{dT_C}{dt}]$$

S. stipitis

$$\frac{dT_S}{dt} = \frac{F_{OS}}{V/2}(T_C - T_S) + v_{TS}X_S + D_T\ (T_C - T_S)$$

$$v_{TS} = \frac{1}{X_S}[-(T_C - T_S)(\frac{F_{OS}}{V/2} + D_T) + \frac{dT_S}{dt}]$$

Glycerol

S. cerevisiae

$$\frac{dR_C}{dt} = \frac{F_{In}}{V/2}(-R_C) + v_{RC}X_C - D_R\ (R_C - R_S)$$

$$v_{RC} = \frac{1}{X_C}[\frac{F_{In}}{V/2}(R_C) + D_R(R_C - R_S) + \frac{dR_C}{dt}]$$

S. stipitis

$$\frac{dR_S}{dt} = \frac{F_{OS}}{V/2}(R_C - R_S) + v_{RS}X_S + D_R\ (R_C - R_S)$$

$$v_{RS} = \frac{1}{X_S}[-(R_C - R_S)(\frac{F_{OS}}{V/2} + D_R) + \frac{dR_S}{dt}]$$

Acetic Acid

S. cerevisiae

$$\frac{dA_C}{dt} = \frac{F_{In}}{V/2}(-A_C) + v_{AC}X_C - D_A\,(A_C - A_S)$$

$$v_{AC} = \frac{1}{X_C}[\frac{F_{In}}{V/2}(A_C) + D_A(A_C - A_S) + \frac{dA_C}{dt}]$$

S. stipitis

$$\frac{dA_S}{dt} = \frac{F_{OS}}{V/2}(A_C - A_S) + v_{AS}X_S + D_A\,(A_C - A_S)$$

$$v_{AS} = \frac{1}{X_S}[-(A_C - A_S)(\frac{F_{OS}}{V/2} + D_A) + \frac{dA_S}{dt}]$$

Appendix B: calculation of continuous/pseudo-continuous operational duration

Biomass development for pseudo-continuous operation

$$\frac{dX}{dt} = \mu X$$

Biomass development for continuous operation

$$\frac{dX}{dt} = (\mu - \frac{F}{V})X$$

Calculation for operation duration

$$X_1 = X_0 e^{\mu t_1}$$

$$X_2 = X_1 e^{(\mu - \frac{F}{V})(t - t_1)}$$

$$X_2 = X_0$$

$$t_2 = t - t_1$$

$$X_0 = X_0\ e^{\mu t_1 + (\mu - \frac{F}{V})t_2}$$

$$\mu t_1 + \left(\mu - \frac{F}{V}\right)t_2 = 0$$

$$\frac{t_1}{t_2} = \frac{(\frac{F}{V} - \mu)}{\mu}$$

$$\frac{t_1}{t_2} = \frac{(D - \mu)}{\mu}$$

$$t_1 = Pseudo - continuous\ operation\ time\ (hr)$$

$$t_2 = Continuous\ operation\ time\ (hr)$$

$$t = Total\ time\ (24hr)$$

$$\mu = Cell\ growth\ rate\ (hr^{-1})$$

$$F = Flow\ rate\ (L/hr)$$

$$V = Volmue\ (L)$$

$$D = Dilution\ rate\ (hr^{-1})$$

$$X_0 = Initial\ biomass\ concentration\ at\ t_0\ (g/L)$$

$$X_1 = Biomass\ concentration\ at\ t_1 (g/L)$$

$$X_2 = Biomass\ concentration\ at\ t_2 (g/L)$$

Appendix C: Carbon balance analysis for co-culture system

Overall mass balance is

$$\Delta m_{acc} = \Delta m_{in} - \Delta m_{out} - \Delta m_{consum} + \Delta m_{prod}$$

For glucose or xylose consumption, mass balance is

$$\Delta m_{consum} = \Delta m_{in} - \Delta m_{out} - \Delta m_{acc}$$

$$\Delta m_{in} = F_{in} \times C_{in} \times (t_2 - t_1)$$

$$\Delta m_{acc} = 1/2 V_{t_1} \times [(C_2 - C_1)_{sc} + (C_2 - C_1)_{ss}]$$

$$\Delta m_{out} = \int_{t_1}^{t_2} F_{out} C_t dt = F \int_{t_1}^{t_2} C_t dt = \frac{F_{out}}{2}(C_1 t_2 + C_2 t_2 - C_1 t_1 - C_2 t_1)$$

Component	Empirical Formula	Molecular Weight (g/mol)
Glucose	$C_6H_{12}O_6$	180.16
Xylose	$C_5H_{10}O_5$	150.13
Xylitol	$C_5H_{12}O_5$	152.15
Glycerol	$C_3H_8O_3$	92.09
Acetic Acid	$C_2H_4O_2$	60.05
Ethanol	C_2H_6O	46.07
Carbon Dioxide	CO_2	44.01
S. cerevisiae	$CH_{1.66}N_{0.13}O_{0.4}$	23.5
	$CH_{1.75}N_{0.15}O_{0.5}$	23.9
	$CH_{1.64}N_{0.16}O_{0.52}P_{0.01}S_{0.005}$	26.9
S. stipitis	$C_4H_{7.05}N_{0.56}O_{2.20}$	98

$$\Delta m_{consum} = F_{in} \times C_{in} \times (t_2 - t_1) - F\left[t_2\left(\frac{1}{2}C_2 + \frac{1}{2}C_1\right) - t_1\left(\frac{1}{2}C_2 + \frac{1}{2}C_1\right)\right]_{out} - 1/2V_{t_1}$$
$$\times [(C_2 - C_1)_{sc} + (C_2 - C_1)_{ss}]$$

For ethanol or other byproducts, mass balance is

$$\Delta m_{prod} = \Delta m_{out} + \Delta m_{acc}$$

$$\Delta m_{prod} = F_{out}\left[t_2\left(\frac{1}{2}C_2 + \frac{1}{2}C_1\right) - t_1\left(\frac{1}{2}C_2 + \frac{1}{2}C_1\right)\right]_{out} + 1/2V_{t_1}[(C_2 - C_1)_{sc} + (C_2 - C_1)_{ss}]$$

Carbon mass balance is

$$\Delta m_{carbon\ cons} = \Delta m_G(0.3996) + \Delta m_Z(0.3997)$$

$$\Delta m_{carbon\ prod} = \Delta m_E(0.5209) + \Delta m_{Zylt}(0.3943) + \Delta m_{Gly}(0.3909) + \Delta m_{AA}(0.3997) + \Delta m_{CO_2}(0.2727) + \Delta m_{sc}(0.5106) + \Delta m_{ss}(0.4898)$$

Appendix C: Carbon balance analysis for single culture system

Overall mass balance is

$$\Delta m_{acc} = \Delta m_{in} - \Delta m_{out} - \Delta m_{cons} + \Delta m_{prod}$$

For xylose consumption, mass balance is

$$\Delta m_{cons} = \Delta m_{in} - \Delta m_{out} - \Delta m_{acc}$$

$$\Delta m_{in} = F_{in} \times C_{in} \times (t_2 - t_1)$$
$$\Delta m_{acc} = V_{t_1} \times [(C_2 - C_1)_{ss}]$$
$$\Delta m_{out} = \int_{t_1}^{t_2} F_{out} C_t dt = F \int_{t_1}^{t_2} C_t dt = \frac{F_{out}}{2}(C_1 t_2 + C_2 t_2 - C_1 t_1 - C_2 t_1)$$

$$\Delta m_{cons} = F_{in} \times C_{in} \times (t_2 - t_1) - F_{out}\left[t_2\left(\frac{1}{2}C_2 + \frac{1}{2}C_1\right) - t_1\left(\frac{1}{2}C_2 + \frac{1}{2}C_1\right)\right]_{out} - V_{t_1}$$
$$\times [(C_2 - C_1)_{ss}]$$

For ethanol or other byproducts, mass balance is

$$\Delta m_{prod} = \Delta m_{out} + \Delta m_{acc}$$

$$\Delta m_{prod} = F_{out}\left[t_2\left(\frac{1}{2}C_2 + \frac{1}{2}C_1\right) - t_1\left(\frac{1}{2}C_2 + \frac{1}{2}C_1\right)\right]_{out} + V_{t_1}[(C_2 - C_1)_{ss}]$$

Carbon mass balance is

$$\Delta m_{carbon\ cons} = \Delta m_Z(0.3997)$$

$$\Delta m_{carbon\ prod} = \Delta m_E(0.5209) + \Delta m_{Zylt}(0.3943) + \Delta m_{AA}(0.3997) + \Delta m_{CO_2}(0.2727)$$
$$+ \Delta m_{ss}(0.4898)$$

Bibliography

Alexander, M. A., Chapman, T. W., Jeffries, T. W., 1988. Continuous xylose fermentation by Candida shehatae in a two-stage reactor. Appl Biochem Biotechnol, 17, pp.221-229.

Agbogbo, F. K., Coward-Kelly, G., Torry-Smith, M., Wenger, K., Jeffries, T. W., 2007. The effect of initial cell concentration on xylose fermentation by Pichia stipitis. Appl Biochem Biotechnol, pp.136-140.

Agbogbo, F. K., Coward-Kelly, G., 2008. Cellulosic ethanol production using the naturally occurring xylose-fermenting yeast, Pichia stipitis. Biotechnol Lett, 30, pp.1515-1524.

Alexander, M. A., Chapman, T. W., Jeffries, T. W., 1989. Continuous-culture responses of Candida shehatae to shifts in temperature and aeration : implications for ethanol inhibition. Appl Environ Microbiol, 55, pp.9–12.

Almeida, J. R. M., Modig, T., Petersson, A., Hahn-Hagerdal, B., Liden, G., Gorwa-Grauslund, M. F., 2007. Mini-Review: Increased tolerance and conversion of inhibitors in lignocellulosic hydrolysates by Saccharomyces cerevisiae. J Chem Technol Biotechnol, 82, pp.340-349.

Alper, H., Stepha-nopoulos, G., 2009. Engineering for biofuels: exploiting innate microbial capacity or importing biosynthetic potential. Nature Reviews Microbiology, 7, pp.715-723.

Attfield, P. V., 1997. Stress tolerance: The key to effective strains of industrial baker's yeast. Nat Biotechnol, 15, pp.1351-1357.

Baird, M. H. I., Rama, N. V., Shen, Z. J., 1993. Oxygen absorption in a baffled tank agitated by delta paddle impeller. Can J Chem Eng, 71, pp.195–201.

Bandyopadhyay, B., Murphrey, A. E., 1967. Dynamic measurement of the volumetric oxygen transfer coefficient in fermentation systems. Biotechnol Bioeng. 15, PP.533-544.

Bartholomew, W. H., Karow, E. O., Sfat, M. R., 1950. Oxygen transfer and agitation in submerged fermentations: mass transfer of oxygen in submerged fermentation of Streptomyces griseus. Industry Engineering Chemistry. pp.1801-1809.

Beck, M. J., Johnson, R. D., Baker, C. S., 1990. Ethanol production from glucose/xylose mixes by incorporating microbes in selected fermentation schemes. Appl Biochem Biotechnol, 24, pp.415-424.

Berg, C., 2004. World ethanol production. The distillery and bioethanol network. (http://www.distill.com/worldethanolproduction.htm).

Bicho, P. A., Runnals, P. L., Cunningham, J. D., Lee, Hung., 1988. Induction of xylose reductase and xylitol dehydrogenase activities in Pachysolen tannophilus and Pichia stipitis on mixed sugars. Applied and Environmental Microbiology, 54, pp.50-54.

Blanch, H. W., Clark, D. S., 1996. Biochemical Engineering, Marcel Dekker Inc.

Bouaifi, M,, Hebrard, G,, Bastoul, D., Roustan, M., 2001. A comparative study of gas hold-up, bubble size, interfacial area and mass transfer coefficients in stirred gas–liquid reactors and bubble columns. Chem Eng Proc, 40, pp.97–111.

Bruinenberg, P. M., Bot, P. H. M., Dijken, J. P., Scheffers, W. A., 1983. The role of redox balances in the anaerobic fermentation of xylose by yeasts. Appl Microbiol Biotechnol, 18, pp.287-292.

Bull, S. R., Riley, C. J., Tyson, K. S., Costella, R., 1992. Total fuel cycle and emission analysis of biomass to ethanol. In: Energy from biomass and wastes vol. XVI (Klass DL ed.) Institute of gas technology, Chicago, IL. pp.1-14.

Butler, M., 2005. Animal cell cultures: recent achievements and perspectives in the production of biopharmaceuticals, App. Microbiol. Biotechnol., 68, pp.283-291.

Casey, J. P., Ingledew, W. M. M., 1986. Ethanol tolerance in yeasts. Critical Reviews in Microbiology, 13, pp.219–280.

Cartwright, C. P., Juroszek, J. R., Beaven, M. J., Ruby, F. M. S., De Morais, S. M. F., and Rose, A. H., 1986. Ethanol dissipates the proton motive force across the plasma membrane of Saccharomyces cerevisiae, J Gen Microbiol, 132, pp.369-377.

Ciesarova, Z., Domeny, Z., Smogrovicova, D., Pakova, J., Sturdik, E., 1998. Comparison of ethanol tolerance of free and immobilized Saccharomyces uvarum yeasts. Folia Microbiol, 43, pp.55-58.

Chandel, A. K., Chan, E. S., Ravinder, R., Narasu, M. L., Rao, L. V., and Ravindra, P., 2007. Economics and environmental impact of bioethanol production technologies: an appraisal. Molecular Biology, 2, pp.14-32.

Chandel, A. K., Singh, O. V., Narasu, M. L., Rao, L. V., 2011. Bioconversion of Saccharum spontaneum (wild sugarcane) hemicellulosic hydrolysate into ethanol by mono and co-cultures of Pichia stipitis NCIM3498 and thermotolerant Saccharomyces cerevisiae-VS 3. New Biotechnol, 28, pp.593–599.

Chandrakant, P., Bisaria, V.S., 1998. Simultaneous bioconversion of cellulose and hemicellulose to ethanol. Critical Reviews in Biotechnol, 18, pp.295-331.

Chaudhary, G., Ghosh, S., 2014. Two-reactor, continuous culture fermentation for fuel ethanol production from lignocellulosic acid hydrolysate using Zymomonas mobilis and Scheffersomyces stipitis. RSC Adv, 4, pp.36412-36418.

Chen, Y., 2011. Development and application of co-culture for ethanol production by co-fermentation of glucose and xylose: a systematic review. J Ind Microbiol Biotechnol, 38, pp.581-597.

Cherubini, F., 2010. The Biorefinery concept: Using biomass instead of oil for producing energy and chemicals. Energy Conversion and Management, 51, pp.1412-1421.

Choi, G. W., Kim. H. W. K. Y-R., Chung, B. W., 2008. Ethanol production by Zymomonas mobilis CHZ2501 from industrial starch feedstocks. Biotechnol Bioproc Eng, 13, pp.765-771.

Chu B. C. H., Lee, H., 2007. Genetic improvement of Saccharomyces cerevisiae for xylose fermentation. Biotechnol Adv, 25, pp.425-441.

Ciesarova, Z., Domeny, Z., Smogrovicova, D., Pakova, J., Sturdik, E., 1998. Comparison of ethanol tolerance of free and immobilized Saccharomyces uvarum yeasts. Folia Microbiol, 43, pp.55-58.

Cooper C. M,. Fernstorm G. A., Miller S. A., 1944. Performance of agitated gas–liquid contactors. Ind Eng Chem, 6, pp.504–509.

Da Cunha-Pereira, F., Hickert, L. R., Sehnem, N. T., de Souza-Cruz, P. B., Rosa, C. A., Ayub, M. A. Z., 2011. Conversion of sugars present in rice hull hydrolysates into ethanol by Spathaspora arborariae, Saccharomyces cerevisiae, and their co-fermentations. Bioresour. Technol, 102, pp.4218–4225.

Damiani, A. L., Kim, M. H., Wang, J., 2014. An improved dynamic method to measure kLa in bioreactors. Biotechnol Bioeng, 111, pp.2120–2125.

D'Amore. T., Panchal, C. J., Russell, I., Stewart, G. G., 1990. A study of ethanol tolerance in yeast, Crit Rev Biotechnol, 9. pp. 287-304.

de Bari, I., Cuna, D., Nanna, F., Braccio, G., 2004. Ethanol production in immobilized-cell bioreactors from mixed sugar syrups and enzymatic hydrolysates of steam exploded biomass. Appl Biochem Biotechnol, 114, pp.539–557.

Delgenes J. P., Moletta, R., Navarro, J. M., 1988. Ethanol tolerance of Pichia stipitis Y-7124 grown on a D-xylose, D-glucose and L-arabinose mixture. J Ferm Technol, 66, pp.417-422.

Delgenes J. P., Moletta, R., Navarro, J. M., 1989. Fermentation of D-xylose, D-glucose, L-arabinose mixture by Pichia stipitis: Effect of the oxygen transfer rate on fermentation performance. Biotechnol Bioenergy, 34, pp.398–402.

Delgenes J. P., Laplace, J. M., Moletta, R., Navarro, J. M., 1996. Comparative study of separated fermentations and cofermentation processes to produce ethanol from hardwood derived hydrolysates. Biomass Bioenergy, 11, pp.353–360.

Desimone, M. F., Degrossi, J., D'Aquino, M., Diaz, L. E., 2002. Ethanol tolerance in free and sol-gel immobilized Saccharomyces cerevisiae. Biotechnol Lett, 24, pp.1557-1559.

Dien. B. S., Jung, H. J. G., Vogel, K. P., Clasler, M. D., Lamb, J. A. F. S., Iten, L., Mitchell, R. B., Sarath, G., 2006. Chemical composition and response to dilute acid pretreatment and enzymatic saccharification of alfalfa, reed canarygrass and switchgrass. Biomass and Bioenergy, 30, pp.880-891.

Dihn, T. N., Nagahisa, K., Hirasawa, T., Chikara, F., Hiroshi, S., 2008. Adaptation of Saccharomyces cerevisiae cells to high ethanol concentration and changes in fatty acid composition of membrane and cell size. PLoS ONE, 3, e2623, pp.1-7.

Du Preez J. C., 1994. Process parameters and environmental-factors affecting D-xylose fermentation by yeasts. Enzyme Microb Technol,16, pp.944–956.

Eiteman, M. A., Lee, S. A., Altman, R., Altman, E., 2008. A co-fermentation strategy to consume sugar mixture effectively. J Bio Eng, 2, pp.1-8.

Eiteman, M. A., Lee, S. A., Altman, R., Altman, E., 2009. A substrate-selective co-fermentation strategy with Escherichia coli produces lactate by simultaneously consuming xylose and glucose. Biotechnol Bioeng, 102, pp.822-827.

Eken-Saraçoğlu, N., Arslan, Y., 2000. Comparison of different pretreatments in ethanol fermentation using corn cob hemicellulosic hydrolysate with Pichia stipitis and Candida shehatae. Biotechnology Letters, 22, pp.855-858.

Energy Information Administration (EIA). 2011. Annual Energy Review 2010. Report No. DOE/EIA-0384(2010) pp. 37, (http://www.eia.gov/totalenergy/data/annual/pdf/aer.pdf)

Florens, L., Carozza, M. J., Swanson, S. K., Fournier, M., Coleman, M. K., et.al., (2006) Analyzing Chromatin Remodeling Complexes using Shotgun Proteomics and Normalized Spectral Abundance Factors. Methods, 40, pp.303-311.

Fu, N., Peiris, P., 2007. Co-fermentation of a mixture of glucose and xylose to ethanol by Zymomonas mobilis and Pachysolen tannophilus. World J Microbiol Biotechnol, 24, pp.1091–1097.

Fu, N., Peiris, P., Markham, J., Bavor, J., 2009. A novel co-culture process with Zymomonas mobilis and Pichia stipitis for efficient ethanol production on glucose/xylose mixtures. Enzy Microb Technol, 45, pp.210–217.

Galaction, A. I, Cascaval, D., Oniscu, C., Turnea, M., 2004. Prediction of oxygen mass transfer coefficients in stirred bioreactors for bacteria, yeasts and fungus broths. Biochemical Engineering Journal, 20, pp.85-94.

Garcia-Ochoa, F., Gomez, E., 2005. Prediction of gas-liquid mass transfer coefficient in sparged stirred tank bioreactors. Biotechnol Bioeng. 92, pp.761-772.

Garcia-Ochoa, F., Gomez, E., 2009. Bioreactor scale-up and oxygen transfer rate in microbial processes: An overview. Biotechnol Adv. 27, pp.153-176.

Garcia-Ochoa, F., Gomez, E., 2010. Oxygen uptake rate in microbial process: An overview. Biochemical Engineering Journal, 49, pp.289-307.

Ghose, T. K., Bisaria, V. S., 1979. Studies on mechanism of enzymatic hydrolysis of cellulosic substances. Biotechnol Bioeng, 21, pp.131-146.

Griffin, J. L., 2004. Metabolic profiles to define the genome: Can we hear the phenotypes? Philos Trans R. Soc, 359, pp.857-871.

Grootjen, D. R. J., Meijlink, L. H. H. M., Van der Lans, R. G. J. M., Luyben, K. C. A., 1990. Cofermentation of glucose and xylose with immobilized Pichia stipitis and Saccharomyces cerevisiae. Enzym Microb Technol, 12, pp.860–864.

Grootjen, D. R. J, Meijlink, L. H. H. M., Vleesenbeek, R., van der Lans, R. G. J. M., Luyben, K. C. A. M., 1991a. Cofermentation of glucose and xylose with immobilized Pichia stipitis in combination with Saccharomyces cerevisiae. Enzyme Microb Technol, 13, pp.530–536.

Grootjen, D. R. J, Jansen, M. L., van der Lans, R. G. J. M., Luyben, K. C. A. M., 1991b. Reactors in series for the complete conversion of glucose/xylose mixtures by Pichia stipitis and Saccharomyces cerevisiae. Enzyme Microb Technol, 13, pp.828–833.

Gutiérrez-Rivera, B., Waliszewski-Kubiak, K., Carvajal-Zarrabal, O., Aguilar-Uscanga, M. G., 2012. Conversion efficiency of glucose/xylose mixtures for ethanol production using Saccharomyces cerevisiae ITV01 and Pichia stipitis NRRL Y-7124. J Chem Technol Biotechnol, 87, pp.263–270.

Gutiérrez-Rivera, B., Ortiz-Muñiz, B., Gómez-Rodríguez, J., Cárdenas-Cágal, A., González, J. M. D., Aguilar-Uscanga, M. G., 2015. Bioethanol production from hydrolyzed sugarcane bagasse supplemented with molasses “B” in a mixed yeast culture. Renew Energy, 74, pp.399–405.

Hahn-Hagerdal. B., Karhumaa, K., Jeppsson, M., Gorwa-Grauslund, M. F., 2007. Metabolic engineering for pentose utilization in Saccharomyces cerevisiae. Adv Biochem Eng/Biotechnol, 108, pp.147-177.

Hahn-Hägerdal. B, Karhumaa, K., Fonseca, C., Spencer-Martins, I., Gorwa-Grauslund, M.F.,2007. Towards industrial pentose-fermenting yeast strains. Appl Microbiol Biotechnol, 74, pp. 937–953.

Hanly, T. J., Henson, M. A., 2011. Dynamic flux balance modeling of microbial co-cultures for efficient batch fermentation of glucose and xylose mixtures. Biotechnol. Bioeng, 108, pp.376–385.

Heineken F. G., 1971. Oxygen mass transfer and oxygen respiration rate measurements utilizing fast response oxygen electrodes. Biotechnol Bioeng, 84, pp.351–358.

Hickert, L. R., Cunha-Pereira, F. da, Souza-Cruz, P. B. de, Rosa, C. A., Ayub, M. A. Z., 2013a. Ethanogenic fermentation of co-cultures of Candida shehatae HM 52.2 and Saccharomyces cerevisiae ICV D254 in synthetic medium and rice hull hydrolysate. Bioresour Technol, 131, pp.508–514.

Hickert, L. R., de Souza-Cruz, P. B., Rosa, C. A., Ayub, M. A. Z., 2013b. Simultaneous saccharification and co-fermentation of un-detoxified rice hull hydrolysate by Saccharomyces cerevisiae ICV D254 and Spathaspora arborariae NRRL Y-48658 for the production of ethanol and xylitol. Bioresour Technol,143, pp.112–116.

Hoppe, G. K., Hansford, G. S., 1982. Ethanol inhibition of continuous anaerobic yeast growth. Biotechnology Letters, 4, pp.39–44.

Huang E., Lefsrud M., 2014. Fermentation Monitoring of a Co-culture Process with Saccharomyces cerevisiae and Scheffersomyces stipitis Using Shotgun Proteomics. J Bioprocess Biotech, 144, pp.1-7.

Ingram, L. O., 1986. Microbial tolerance to alcohols: Roles of the cell membrane. Tibtech, pp.40-44.

Jeffries, T. W., 1983. Utilization of xylose by bacteria, yeasts and fungi. Advances in Biochemical Engineering Biotechnology, 27, pp.1-32.

Jefferies, T. W., Fady, J. H, Lightfoot, E. N., 1985. Effect of glucose supplements on the fermentation of xylose by Pachysolen tannophilus. Biotechnol Bioeng, 27, pp.171-176.

Jefferies, T. W., Jin, Y. S., 2004. Metabolic engineering for improved fermentation of pentoses by yeasts. Appl Microbiol Biotechnol, 63, pp.495-509.

Jefferies, T. W., 2006. Engineering yeasts for xylose metabolism. Curr Opin Biotechnol, 17, pp.320-326.

Jefferies, T. W. et al, 2007. Genome sequence of the lignocellulosic-bioconverting and xylose-fermenting yeast Pichia stipitis. Nature Biotechnol, 25, pp.319-326.

Jimenez, J. and van Uden, N., 1985. Use of extracellular acidification for the rapid testing of ethanol tolerance in yeasts. Appl Environ Microbiol, 53, pp.1196-1198.

Jin, Y. S., Laplaza, J. M., Jeffries, T. W., 2004. Saccharomyces cerevisiae engineered for xylose metabolism exhibits a respiratory response. Appl Env Microbiol, 70, pp.6816-6825.

Jolliffe, I. T., Principal component analysis, 2nd ed.; Springer, 2002, pp.487-487.

Jones, R. P., Greenfield, P. F., 1987. Ethanol and the fluidity of the yeast plasma membrane. Yeast, 3, pp.223-232.

Jirku, V., 1999. Whole cell immobilization as a means of enhancing ethanol tolerance, J Ind Microbiol Biotechnol, 22, pp.147-151.

Ju, L. K., Sundararajan, A., 1995. The effects of cells on oxygen transfer in bioreactors. Bioprocess Engineering. 13, pp.271-278.

Keshwani, D. R., Cheng, J. J., 2009. Switchgrass for bioethanol and other value-added applications: A Review. Bioresource Technology, 100, pp.1515-1523.

Kheshgi, H. S., Prince, R. C., Marland, G., 2000. The potential of biomass fuels in the context of global climate change: Focus on transportation fuels. Annual Rev. Energy Environ, 25, pp.199-244.

Kilian, S. G., can Uden, N., 1988. Transport of xylose and glucose in the xylose-fermenting yeast Pichia stipitis. Appl Microbiol Biotechnol, 27, pp.545-548.

Kim, J. S., Park, S. C., Kim, J. W., Park, J. C., Park, S. M., Lee J. S., 2010. Production of bioethanol from lignocellulose: Status and perspectives in Korea. Bioresour Technol, 101, pp.4801-4805.

Kim, S., Dale, E. B., 2004. Global potential bioethanol production from wasted crops and crop residues. Biomass Bioenergy, 26, pp.361-375.

Kordowska-Wiater, M., Targoński, Z., 2001. Ethanol production on the media containing glucose and xylose by coculture of Pichia stipitis CCY 39501 and respiratory deficient mutant of Saccharomyces cerevisiae V30. Electron. J. Pol. Agric. Univ, 4.

Kordowska-wiater, M., Targonski, Z., 2002. Ethanol fermentation on glucose/xylose mixture by co-cultivation of restricted glucose catabolite repressed mutants of Pichia stipitis with respiratory deficient mutants of Saccharomyces cerevisiae. Acta Microbiol Pol, 51, pp.345–352.

Krisch, J., Szajani, B., 1997. Ethanol and acetic acid tolerance in free and immobilized cells of Saccharomyces cerevisiae and Acetobacter aceti. Biotechnol Lett, 19, pp.525-528.

Kuyper, M., Toirkens, M. J., Diderich, J. A., Winkler, A. A., Dijken, J. P., Pronk J. K., 2005. Evolutionary engineering of mixed-sugar utilization by a xylose-fermenting Saccharomyces cerevisiae strain. FEMS Yeast Res, 5, pp.925-934.

Lange, J. P., 2007. Lignocellulose conversion: an introduction to chemistry, process and economics. Biofuels, Bioproducts and Biorefining, 1, pp.39-48.

Laplace, J. M., Delgenes, J. P., Moletta, R., Navarro, J. M., 1991. Combined alcoholic fermentation of D-xylose and D-glucose by four selected microbial strains: Process considerations in relation to ethanol tolerance. Biotechnol Lett, 13, pp.445-450.

Laplace, J. M., Delgenes, J. P., Moletta, R., Navarro, J. M.., 1993a. Cofermentation of glucose and xylose to ethanol by a respiratory-deficient mutant of Saccharomyces cerevisiae cocultivated with a xylose-fermenting yeast. J Ferment Bioeng, 75, pp.207–212.

Laplace, J. M., Delgenes, J. P., Moletta, R., Navarro, J. M., 1993b. Ethanol production from glucose and xylose by separated and co-culture processes using high cell density systems. Process Biochem, 28, pp.519–525.

Laplace, J. M., Delgenes, J. P., Moletta, R., Navarro, J. M., 1993c. Effects of culture conditions on the co-fermentation of a glucose and xylose mixture to ethanol by a mutant of Saccharomyces diastaticus associated with Pichia stipitis. Appl Microbiol Biotechnol, 39, pp.760–763.

Leao, C., van Uden, N., 1984. Effects of ethanol and other alkanols on passive proton influx in the yeast Saccharomyces cerevisiae. Biochem Biophys Acta, 774, pp.43-48.

Leao, C., van Uden, N., 1985. Effects of ethanol and other alkanols on the temperature relations of glucose transport and fermentation in Saccharomyces cerevisiae. Appl Microbiol Biotechnol, 22, pp.359-363.

Lebeau, T., Jouenne, T., Junter, G. A., 1997. Simultaneous fermentation of glucose and xylose by pure and mixed cultures of Saccharomyces cerevisiae and Candida shehatae immobilized in a two-chambered bioreactor. Enzyme Microb Technol, 21, pp.265–272.

Lebeau, T., Jouenne, T., Junter, G. A., 1998. Continuous alcoholic fermentation of glucose/xylose mixtures by co-immobilized Saccharomyces cerevisiae and Candida shehatae. Appl Microbiol Biotechnol, 50, pp.309–313.

Lee, C. W., Chang, H. N., 1987. Kinetics of ethanol fermentations in membrane cell recycle fermenters. Biotechnol Bioeng, 29, pp.1105-1112.

Lee, J. S., Parameswaran, B., Lee, J. P., Park, S. C., 2008. Recent developments of key technologies on cellulosic ethanol production. J. Scientific and Industrial Research , 67, pp.865-973.

Leschine, S. B., Canale Parola, E., 1984. Ethanol production form cellulose by a coculture of Zymomonas mobilis and a clostridium. Curr Microbiol, 11, pp.129-136.

Li, Y., Park, J., Shiroma, R., Tokuyasu, K., 2011. Bioethanol production from rice straw by a sequential use of Saccharomyces cerevisiae and Pichia stipitis with heat inactivation of Saccharomyces cerevisiae cells prior to xylose fermentation. J. Biosci. Bioeng. 111, pp.682–686.

Liang, M., Kim, M.H., He, Q.P., Wang, J., 2013. Impact of pseudo-continuous fermentation on the ethanol tolerance of Scheffersomyces stipitis. J. Biosci. Bioeng. 116, pp.319–326.

Liang, M., Damiani A., He, Q.P., Wang, J., 2014. Elucidating xylose metabolism of Schefferso-myces stipitis for lignocellulosic ethanol production. ACS Sustainable Chem. Eng, 2, pp.38–48.

Lin, Y., Tanaka, S., 2006. Ethanol fermentation from biomass resources: current state and prospects. Appl Microbiol Biotechnol, 69, pp.627-642.

Linek V, Kordac M, Fujasova M, Moucha T., 2004. Gas–liquid mass transfer coefficient in stirred tanks interpreted through models of idealized eddy structure of turbulence in the bubble vicinity. Chem Eng Proc, 43, pp.1511–1517.

Lucas, C, Van Uden, N., 1985. The temperature profiles of growth, thermal death and ethanol tolerance of the xylose-fermenting yeas Candida shehatae. J. Basic Microbiol., 25, pp.547–550.

Lynd L. R., 1996. Overview and evaluation of fuel ethanol production from cellulosic biomass: technology, economics, the environment, and policy. Annu Rev Energy Environ, 21, pp.403–465.

Lynd, L. R., Van Zyl, W. H., Mcbride, J. E., Laser, M., 2005. Consolidated bioprocessing of cellulosic biomass: an update. Current opinion in biotechnology, 16, pp.577-583.

Ma, M., Liu, Z. L., Moon, J., 2012. Genetic engineering of inhibitor-tolerant Saccharomyces cerevisiae for improved xylose utilization in ethanol production. BioEnergy Res, 5, pp.459–469.

Marris, E., 2006. Sugar cane and ethanol: drink the best and drive the rest. Nature, 444, pp.670-672.

Maiorella, B., Blanch, H. W., Wilke C. R., 1983. By-product inhibition effects on ethanolic fe mentation by Saccharomyces cerevisiae. Biotech Bioeng, 25, pp.103-121.

Martin M., Montes F. J., Galan M. A., 2008. Bubbling process in stirred tank reactors II: Agitator effect on the mass transfer rates. Chem Eng Sci, 63, pp.3223–3234.

Martin M., Montes F. J., Galan M. A., 2010. Mass transfer rates from bubbles in stirred tanks operating with viscous fluids. Chem Eng Sci, 65, pp.3814-3824.

McMillan, J. D., 1993. Xylose fermentation to ethanol: a Review. NREL/TP-421-4944.

Mielenz J. R., 2001. Ethanol production from biomass: technology and commercialization status. Current Opinion in Microbiology, 4, pp.324-329.

Monique H., Faaij A., van den Broek R., Berndes G., Gielen D., Turkenburg W., 2003. Exploration of the ranges of the global potential of biomass for energy. Biomass Bioenergy, 25, pp.119–133.

Muller, S., Murray, D. B., Machne, R., 2012. A new dynamic model for highly efficient mass transfer in aerated bioreactors and consequences for kLa identification. Biotech Bioeng, 109, pp.2997-3006.

Nakamura, Y., Sawada, T., Inoue, E., 2001. Mathematical model for ethanol production from mixed sugars by Pichia stipitis. J Chem Technol Biotechnol, 76, pp.251-260.

Narendranath, N. V., Thomas, K. C., Ingledew, W. M., 2001. Effects of acetic acid and lactic acid on the growth of Saccharomyces cerevisiae in a minimal medium. J Ind. Microb. Biotechnol. 26, pp.171-177.

Nigam J. N., 2002. Bioconversion of water-hyacinth (Eichhornia crassipes) hemicellulose acid hydrolysate to motor fuel ethanol by xylose-fermenting yeast. J Biotechnol, 87, pp.17-27.

Ohgren, K., Bura, R.., Saddler, J., Zacchi, G., 2007. Effect of hemicellulose and lignin removal on enzymatic hydrolysis of steam pretreated corn stover. Bioresource technology, 98, pp.2503-10.

Ohta, K., Beall, D. S., Mejia, J. P., Shanmugam, K. T., Ingram, L. O., 1991. Genetic improvement of Escherichia coli for ethanol production: chromosomal integration of Zymomonas mobilis genes encoding pyruvate decarboxylase and alcohol dehydrogenase II, Appl Environ Microbiol, 57, pp.893-900.

Okuda, N., Ninomiya, K., Katakura, Y., Shioya, S., 2008. Strategies for reducing supplemental medium cost in bioethanol production from waste house wood hydrolysate by ethanologenic Escherichia coli: inoculum size increase and coculture with Saccharomyces cerevisiae. J Biosci Bioeng, 105, pp.90–6.

Olsson, L., Hahn-Hagerdal, B., 1996. Fermentation of lignocellulosic hydrolysates for ethanol production. Enzyme Microb Technol, 18, pp.312-331.

Özbek, B, Gayik, S., 2001. The studies on the oxygen mass transfer coefficient in a bioreactor. Proc Biochem, 36, pp.729–741.

Perlack R. D. et al., 2005. Biomass as a Feedstock for a Bioenergy and Bioproducts Industry: The Technical Feasibility of a Billion-Ton Annual Supply, Oak Ridge National Laboratory. (http://www1.eere.energy.gov/biomass/pdfs/final_billionton_vision_report2.pdf)

Polman, K., 1994. Review and analysis of renewable feedstocks for the production of commodity chemicals. Applied Biochem Biotechnol, 46, pp.709-722.

Preez, J. C., Driessel, B. van., Prior, B. A., 1989. Applied Microbiology Biotechnology Ethanol tolerance of Pichia stipitis and Candida shehatae strains in fed-batch cultures at controlled low dissolved oxygen levels. Applied Microbiology and Biotechnology, pp.53–58.

Qian M., Tian S., Li X., Zhang J., Pan Y., Yang X., 2006. Ethanol production from dilute-acid softwood hydrolysate by co-culture. Appl Biochem Biotechnol, 134, pp.273–283.

Ragauskas, A. J., Williams, C. K., Davison, B. H., Britovsek, G., Cairney, J., Eckert, C. A., Frederick, W. J., Hallett, J. P., Leak, D. J., Liotta, C. L., Mielenz, J. R., Murphy, R., Templer, R., Tschaplinski, T., 2006. The path forward for biofuels and biomaterials. Science (New York, N.Y.), 311, pp.484-489.

Rao G., 2009. Vintage paper: Dynamic measurement of the volumetric oxygen transfer coefficient in fermentation systems. Biotechnol Bioeng, 104, pp.841–852.

Reis M. A. M., Serafim L. S., Lemos P. C., Ramos A. M., Aguiar F. R., et.al., 2003. Production of Polyhydroxyalkanoates by Mixed Microbial Cultures. Bioprocess Biosyst Eng, 25, pp.377-385.

Rizzi M., Klein C., Schulze C., Buithanh N. A., Dellweg H., 1989. Xylose fermentation by yeasts. 5. Use of ATP balances for modeling oxygen-limited growth and fermentation of yeast Pichia stipitis with xylose as carbon sources. Biotechnol Bioeng, 34, pp.509–514.

Rodrguez J., Kleerebezem R, Lema J. M., Van Loosdrecht M., 2006. Modeling Product Formation in Anaerobic Mixed Culture Fermentations. Biotechnol Bioeng, 93, pp.592-606.

Rogers P, Lee K, Skotnicki M, Tribe D. 1982. Ethanol production by Zymomonas mobilis A. Fiechter (Ed.), Microbial reactions, advances in biochemical engineering/biotechnology, 23:37–84.

Rouhollah, H., Iraj, N., Giti, E., Sorah, A., 2007. Mixed sugar fermentation by Pichia stipitis, Saccharomyces cerevisiae, and an isolated xylose-fermenting Kluyveromyces marxianus and their cocultures. African J Biotechnol, 6, pp.1110-1114.

Saha, B. C., Iten, L. B., Cotta, M. A., Wu, Y. V., 2005. Dilute acid pretreatment, enzymatic saccharification and fermentation of wheat straw to ethanol. Proc Biochem , 40, pp.3693-3700

Saha, B. C., 2003. Hemicellulose bioconversion. J. Ind Microbiol Biotechnol, 30, pp.279-291.

Sassner, P., Galbe, M., Zacchi, G., 2008. Techno-economic evaluation of bioethanol production from three different lignocellulosic materials. Biomass and Bioeng, 32, pp.422-430.

Sedlak, M., Ho, N. W. Y., 2004. Production of ethanol from cellulosic biomass hydrolysates using genetically engineered Saccharomyces yeast capable of cofermenting glucose and xylose. Appl Biochem Biotechnol, 114, pp.403-416.

Service, R. F., 2007. Cellulosic ethanol. Biofuel researchers prepare to reap a new harvest. Science (New York, N.Y.), 315, pp.1488-1491.

Shama, G., 1988. Developments in bioreactors for fuel ethanol production. Proc Biochem, 23, pp.13 8-145.

Silva, J. P. A., Mussatto S. I., Roberto, I. C., Teixeira J. A., 2012. Fermentation medium and oxygen transfer conditions that maximize the xylose conversion to ethanol by Pichia stipitis. Renewable Energy, 37, pp.259-265.

Singh, A., Bishnoi, N. R., 2012. Enzymatic hydrolysis optimization of microwave alkali pretreated wheat straw and ethanol production by yeast. Bioresour Technol, 108, pp.94–101.

Skoog, K., Hahn-Hagerdal, B., 1990. Effect of oxygenation on xylose fermentation by Pichia stipitis. Appl and Environ Microbiol, 56, pp.3389-3394.

Slininger, P. J., Branstrator, J. E., Lomont, J. M., Dien, B. S., Okos, M. R., Ladisch, M. R., Bothast, R. J., 1990. Stoichiometry and kinetics of xylose fermentation by Pichia stipitis. Annuals of the New York Academy of Sciences, 589, pp.25-40.

Slininger P. J., Branstrator L. E., Bothast R. J., Okos M. R., Ladisch M. R., 1991. Growth, death, and oxygen-uptake kinetics of Pichia stipitis on xylose. Biotechnol Bioeng, 37, pp.973–980.

Slininger, P. J., Dien, B. S., Lomont, J. M., Bothast, R. J., Ladisch, M. R., 2014. Evaluation of a kinetic model for computer simulation of growth and fermentation by Scheffersomyces (Pichia) stipitis Fed D-xylose. Biotechnol Bioeng, 111, pp.1532-1540.

Stephanopoulos, G., 2007. Challenges in Engineering Microbes for Biofuels Production. Science, 315, pp.801-804.

Su, Y., Willis, L. B., Jeffries, T. W., 2015, Effects of aeration on growth, ethanol and polyol accumulation by Spathaspora passalidarum NRRL Y-27907 and Scheffersomyces stipitis NRRL Y-7124. Biotechnol Bioeng, 112, pp.457-469.

Suresh S., Srivastava V. S., Mishra I. M., 2009. Techniques for oxygen transfer measurement in bioreactors: A review. J Chem Technol Biotechnol, 84, pp.1091–1103.

Sun, Y., Cheng, J., 2002, Hydrolysis of lignocellulosic materials for ethanol production: a review Biores Technol, 83, pp.1-11

Tampier, M., Smith, D., Bibeau, E., Beauchemin, P. A., 2004. Identifying environmentally preferable uses for biomass resources. (http://www.cec.org/filedPDF/ECONOMY/Biomass-Stage-I_II_en.pdf)

Taniguchi M, Itaya T, Tohma T, Fujii M., 1997a. Ethanol production from a mixture of glucose and xylose by a novel co-culture system with two fermentors and two microfiltration modules. J Ferment Bioeng, 84, pp.59–64.

Taniguchi M, Tohma T, Itaya T, Fujii M., 1997b. Ethanol production from a mixture of glucose and xylose by co-culture of Pichia stipitis and a respiratory-deficient mutant of Saccharomyces cerevisiae. J Ferment Bioeng, 83, pp.364–370.

Taniguchi, M., Tanaka, T., 2004. Clarification of interactions among microorganisms and development of co-culture system for production. Adv Biochem Eng Biotechnol, 90, pp.35–62.

Thomas, D. D., Rose, A. H., 1979. Inhibitory effect of ethanol on growth and solute accumulation by Saccharomyces cerevisiae as affected by plasma-membrane lipid composition. Arch Microbiol, 122, pp.49-55.

Tobajas M, Garcia-Calvo E., 2000. Comparison of experimental methods for determination of the volumetric mass transfer coefficient in fermentation processes. Heat Mass Transfer 36, pp.201–207.

Tohyama M, Patarinska T., Qiang Z, Shimizu K., 2002. Modeling of the mixed culture and periodic control for PHB production. Biochem Eng J,10, pp.157-173.

Toivola, A., Yarrow, D., Van-den-bosch, E., Van-dijken. J. P., Sheffers, W. A., 1984, Alcoholic fermentation of D-xylose by yeasts. Appl Microb Biotechnol, 47, pp.1221-1223.

Tomas-Pejo, E., Oliva, J. M., Ballesteros, M., Olsson, L., 2008. Comparison of SHF and SSF processes from steam-exploded wheat straw for ethanol production by xylose-fermenting and robust glucose-fermenting Saccharomyces cerevisiae strains. Biotechnology and bioengineering, 100, pp.1122-1131.

Toon, S. T., Philippidis, G. P., Ho, N. W., Chen, Z., Brainard, A., Lumpkin, R. E., Riley, C. J., 1997. Enhanced cofermentation of glucose and xylose by recombinant Saccharomyces yeast strains in batch and continuous operating modes. Applied Biochem Biotechnol, 65, pp.243-255.

Torija, M. J., Rozes, N., Poblet, M., et al., 2003. Effects of fermentation temperature on the strain population of Saccharomyces cerevisiae. International J of Food Microbiol, 80, pp.47-53.

Unrean P., Nguyen, N. H. A., 2012. Metabolic pathway analysis of Scheffersomyces (Pichia) stipitis: effect of oxygen availability on ethanol synthesis and flux distributions. Appl Microbiol Biotechnol, 94, pp.1387-1398.

USDOE 2006a. Biomass Feedstock Composition and Property Database.

USDOE 2006b. Breaking the biological barriers to cellulosic ethanol a joint research agenda : a research roadmap resulting from the Biomass to Biofuels Workshop.

Van Zyl, C., Prior, B. A., Kilian, S. G., Kock, J. L. F., 1989. D-xylose utilization by Saccharomyces cerevisiae. J Gen Microbiol, 135, pp.2791-2798.

Van Zyl, C., Prior, B. A., du Preez, J. C., 1991. Acetic acid inhibition of D-xylose fermentation by Pichia stipitis. Enzyme Microb Technol, 13, pp.82-86.

Watanabe, T., Watanabe, I., Yamamoto, M., Ando, A., Nakamura, T., 2011. A UV-induced mutant of Pichia stipitis with increased ethanol production from xylose and selection of a spontaneous mutant with increased ethanol tolerance. Bioresour Technol, 102, pp.1844-1848.

Whitman W. G., 1923. Preliminary experimental confirmation of the two-film theory of gas absorption. Chem Metal Eng, 29, pp.146–149.

Wise, D. L., 1969. Increased oxygen mass transfer rates from single bubbles in microbial systems at low Reynolds number. Biotechnol and Bioeng, 6, pp.647-681.

Wu H. 1995. An issue on applications of a disk turbine for gas–liquid mass transfer. Chem Eng Sci, 50, pp.2801–2811.

Wyman C. E., 1994. Ethanol from lignocellulosic biomass – technology, economics, and opportunities. Bioresour Technol, 50, pp.3–16.

Wyman C. E., 1999. Biomass ethanol: technical progress, opportunities, and commercial challenges. Ann Rev Energy Environ, 24, pp.189-226.

Wyman C. E., 2003. Potential synergies and challenges in refining cellulosic biomass to fuels, chemicals, and power. Biotechnol Prog, 19, pp.254-262.

Yadav, K. S., Naseeruddin, S., Prashanthi, G. S., Sateesh, L., Rao, L. V., 2011. Bioethanol fermentation of concentrated rice straw hydrolysate using co-culture of Saccharomyces cerevisiae and Pichia stipitis. Bioresour. Technol, 102, pp.6473–6478.

Zaldivar, J., Nielsen, J., Olsson, L., 2001. Fuel ethanol production from lignocellulose: a challenge for metabolic engineering and process integration. Appl Microbiol Biotechnol, 56, pp.17-34.

Zaldivar, J., Nielsen, J., Olsson, L., 2002. Fermentation performance and intracellular metabolite patterns in laboratory and industrial xylose-fermenting Saccharomyces cerevisiae. Appl Microbiol Biotechnol, 59, pp.436-442.

Zhang, M., Eddy, C., Deanda, K., Finkelstein, M, Picataggio, S., 1995. Metabolic engineering of a pentose metabolism pathway in ethanologenic Zymomonas mobilis, Science,267, pp. 240-243.

Zhou, B., Martin, G. J. O., Pamment, N. B., 2008. Increased phenotypic stability and ethanol tolerance of recombinant Escherichia coli KO11 when immobilized in continuous fluidized bed culture. Biotechnology and Bioengineering, 100, pp.627-633.